Properties of Layer-by-Layer Single-cell Encapsulation and the Potential Applications in Transplantation Therapy for Neurologic Disorders

by

Wenyan Li

A Thesis submitted to the Faculty of Graduate Studies of

The University of Manitoba

in partial fulfillment of the requirements of the degree of

DOCTOR OF PHILOSOPHY

Department of Human Anatomy & Cell Science
University of Manitoba
Winnipeg

Abstract

Layer-by-layer (LbL) self-assembly is a rapidly developing biomaterial technique for fabricating multilayered structure on substrates. In this project, we report the encapsulation of single neural stem cells (NSCs) using the LbL self-assembly technique with polyelectrolytes gelatin and alginate. The encapsulation did not affect the viability, proliferation and differentiation of the encapsulated NSCs. When insulin-like growth factor-1 (IGF-1) was loaded on the coating material alginate, its release from alginate into the medium presented in a time- and pH-dependent way. As expected, the released IGF-1 significantly enhanced the proliferation of the encapsulated NSCs, demonstrating a drug-carrier function of the LbL single-cell nanocoating.

Permeability of the LbL encapsulation is critically important for its versatile applications. It was determined on PC12 cells encapsulated with gelatin and hyaluronic acid (HA). Under optimal conditions, permeability of LbL membrane against FITC-dextran (FD) increased along with the decrement of the molecular weight of FD. Higher concentrations of the coating materials and higher numbers of coating layers would yield decreased permeability to FD. In addition, maintaining a physiological pH was also important to keep the integrity of the LbL encapsulation system. Encapsulation with 0.5% of the materials for 8-layer was proven to effectively inhibit the interaction of tumor necrosis factor-α (TNF-α) with its receptor in the first 3 days and robustly alleviated cell apoptosis induced by TNF-α.

Since the encapsulation structure creates a favorable microenvironment for cells to survive and function, it holds significant potential for cell transplantation therapies for neurologic disorders such as stroke, and spinal cord injury.

Acknowledgements

I wish to express my sincere appreciation to the Department of Human Anatomy & Cell Science, University of Manitoba for offering me the opportunity to pursue my graduate studies here. The past six years of studying abroad are tough, but very rewarding, which laid the foundation for my future career in research of neuroscience and biomaterials. Importantly, I feel grateful to China Scholarship Council (CSC), Canadian Stroke Network (CSN) and Canadian Institutes of Health Research (CIHR) for providing sufficient financial support to my life and research work.

This thesis would have never been finished without the guidance and instructions by Dr. Jiming Kong. Since the first day I enrolled in the program, he began to offer me tremendous help. Whenever I met any obstacles in my courses and research project, he was always there for giving me inspiring advices and practical approaches. Dr. Kong is a great mentor not only in my study, but also in my life. He helped me to get a better knowledge of how to survive in this country, how to think like a real scientist, how to communicate with other people and how to be a good person. Also, I would like to express my deep appreciation to Dr. Malcolm Xing who provided great help in my project. He guided me to know about biomaterial science about which I never knew before. At the same time, the advisory committee provided great help for my study. I feel grateful to Dr. Maria Vrontakis, Dr. Hassan Marzban and Dr. Michael Namaka, for their valuable suggestions to my coursework and my experiments since

the first year. I would never finish my study program without their encouragement, kindness and professional help.

Meanwhile, other professors from the Department of Human Anatomy and Cell Science helped me either. I would give my appreciation to the Department Head, Dr. Thomas Klonisch for establishing the advanced research platform and keeping the atmosphere of academic thinking in the department. I also wish to thank Dr. Hugo Bergen, Dr. Sabine Hombach-Klonisch, Dr. Saeid Ghavami, Dr. Sari Hannila and Dr. Jason Peeler for their help not only in experiments, but also in the teaching work of Human Anatomy. They helped me to enhance my all-round skills in both research and teaching.

In our lab, I feel so lucky to have so many supportive colleagues. Dr. Teng Guan is a great lab manager, providing devoted help to all the lab members and everything in lab. There are also many visiting students and scholars coming and leaving in these five years. I have learned different things from them, and also learned how to cooperate with people.

Last but not the least, I would thank my families and friends who gave huge out-lab support. Although my parents are living far from me, they strongly supported me so that I could always feel warm and was able to fully focus on my study. My friends in Winnipeg are also very supportive. We accompanied each other in the leisure time and they made our life not boring anymore. Most importantly, I would thank my wife Xiaosha Zhang. She is also a PhD student and need to go through this tough road. We

helped each other in both daily life and study, so I would never make it to complete the program without her.

I wish to dedicate this thesis to

my families, for all your love,

encouragement and support.

Table of Contents

List of Figures

List of Tables

List of Abbreviations

A. niger	*Aspergillus niger*
ActD	Actinomycin D
AD	Alzheimer’s disease
AFM	atomic force microscope
ALS	amyotrophic lateral sclerosis
ANOVA	analysis of variance
AuNPs	gold nanoparticles
AWBP	artery wall binding peptide
B. subtilis	*Bacillus subtilis*
bFGF	fibroblast growth factor-2
BMP-2	bone morphogenetic protein-2
BSA	bovine serum albumin
BrdU	bromodeoxyuridine
CAG	cytosine-adenine-guanine
CDs	cyclodextrins
CNS	central nervous system
Co-IP	co-immunoprecipitation
DISC	death-domain-containing proteins
DMSO	dimethyl sulfoxide
DPBS	Dulbecco's phosphate-buffered saline
DPCs	dermal papilla cells
E. coli	*Escherichia coli*
EDA	ethylenediamine
EDC	1-ethyl-3-(3-dimethylaminopropyl) carbodiimide
EGF	epidermal growth factor
FACS	fluorescence-activated cell sorting
FD	FITC-dextran
FDA	US Food and Drug Administration
FITC	fluorescein 5(6)-isothiocyanate
GAPDH	glyceraldehyde 3-phosphate dehydrogenase
GDNF	glial cell-derived neurotrophic factor
GFAP	glial fibrillary acidic protein
GPER1	G-protein coupled estrogen receptor 1

HA	hyaluronic acid
HBSS	Hank’s balanced salt solution
HD	Huntington’s Disease
HMMR	hyaluronan mediated motility receptor
HRP	horseradish peroxidase
HTCC	N-((2-Hydroxy-3-trimethylammonium) propyl) chitosan chloride
i.c.v.	intracerebroventricular
i.v.	intravenous
IAPs	inhibitor of apoptosis proteins
ICAM-1	intercellular adhesion molecule-1
IEP	isoelectric point
IGF-1	insulin-like growth factor-1
iPSCs	induced-pluripotent stem cells
LbL	layer-by-layer
MHC	major histocompatibility complexes
MNPs	magnetic nanoparticles
MS	multiple sclerosis
MSCs	mesenchymal stem cells
MTT	3-(4,5-Dimethylthiazol-2-yl)-2,5-diphenyltetrazolium bromide
MWNTs	multiwalled carbon nanotubes
NGF	nerve growth factor
NMDAR	N-methyl-D-aspartate receptor
NSCs	neural stem cells
OB	olfactory bulb
PAH	poly (allylamine hydrochloride)
PAMAM	poly (amido amine)
PAMPs	pathogen-associated molecular pattern molecules
PAR	protease-activated receptor
PD	Parkinson’s Disease
PDDA	poly (dimethyldiallylammonium chloride)
PDL	poly-D-lysine
PDMAEMA	poly (2-dimethylamino ethylmethacrylate)
PEI	polyethylenimine
PEG	polyethylene glycol
PLA	proximity ligation assay
PLL	poly-L-lysine
PNS	periphery nervous system
PSS	poly (styrene sulfonate) sodium salt
qPCR	quantitative real-time polymerase chain reaction

RIP1	receptor-interacting protein 1
RIPA	radio immunoprecipitation assay
S. cerevisiae	*Saccharomyces cerevisiae*
SDS-PAGE	sodium dodecyl sulfate-polyacrylamide gel electrophoresis
SEM	scanning electron microscopy
SGZ	subgranular zone
SMAD	small mothers against decapentaplegic
SN	substantia nigra
SVZ	subventricular zone
T. asperellum	*Trichoderma asperellum*
TBST	Triton X-100 in DPBS
TEM	transmission electron microscopy
TNF-α	tumor necrosis factor-α
TNF-R1	tumor necrosis factor-receptor 1
TRADD	TNFR-associated death domain protein
TRAFs	TNF receptor-associated factors
VCAM-1	vascular cell adhesion molecule 1

Chapter 1. Introduction

1.1 LbL Single-cell Encapsulation

1.1.1 An Overview of Encapsulation Strategies on Cells

Cell encapsulation, which establishes material films on cells, belongs to cell surface engineering. According to the number of cells encapsulated, there are cell mass encapsulation and single-cell encapsulation. In cell mass encapsulation, the coating procedure is performed on cell groups. As such, effects on single cells are often difficult to be investigated[1, 2]. Therefore, single-cell encapsulation has attracted more and more attention since it was introduced because the influence on each cells can be homogenized[3, 4].

Single-cell encapsulation was introduced early in 2000 and is developing rapidly in recent years[5]. Scattered and modifiable 3D models on bacteria, fungi and mammalian cells with different materials have been reported for various purposes[6-8]. Furthermore, novel applications such as cell therapy, cell biosensor and biocatalyst have been realized in the past decade[4, 9-11]. The single-cell encapsulation combines technologies in biomaterial, physics, chemistry and biology, exerting broad potentials in the future.

1.1.2 History of LbL Single-cell Encapsulation

In 1992, Decher *et al*. introduced the method of LbL self-assembly, which is based on the electrostatic adsorption of polycations and polyanions[12]. Since then, this

technique has been rapidly developed in fields such as material science, chemistry and biomedicine[13-16].

The first cell encapsulation was reported by Möhwald *et al*. in 2000. Since the surface of cells is negatively charged, they applied poly (allylamine hydrochloride) (PAH) as the polycation and poly (styrene sulfonate) sodium salt (PSS) as the polyanion to encapsulate the fixed human erythrocytes[17]. Other materials were also applied in encapsulating fixed *Escherichia coli* (*E. coli*). These encapsulation models were characterized in multiple ways, proving the feasibility of the methodology[6]. The single-cell encapsulation technique was soon applied on live cells. For example, Mirkin and colleagues encapsulated live fungi such as *Aspergillus niger (A. niger)* with gold nanoparticles (AuNPs)[18]. However in these studies, cells are just regarded as the core to accomplish the encapsulation model, of which the emphasis is on material features instead of the cellular functions[19, 20]. Also, some of the materials are toxic to the relatively fragile mammalian cells.

Lvov *et al.* began to focus on functional status of cells after encapsulation and completed the first encapsulation work on mammalian cells. They coated platelet with poly (dimethyl diallylammonium chloride) (PDDA) and PSS. Aggregation and secretion are found to be influenced when conditions of coating changed[8]. The same method was applied on *Bacillus subtilis* (*B. subtilis*), showing the roughness and viscidity on the surface[21]. Furthermore, Diaspro *et al*. noticed that encapsulation with PAH and PSS can be tuned to influence the growth of *Saccharomyces cerevisiae* (*S. cerevisiae*)[22]. These pioneering studies indicate that the LbL single-cell

encapsulation is able to maintain the normal functions of encapsulated cells such as viability and proliferation, establishing the foundation of current applications.

Versatile applications of LbL encapsulation appeared in 2009 when Tabrizian and Winnik enabled human erythrocytes to be exempted from immune attack by coating cells with protective layer and camouflage layer[23]. This technique was further applied to determine the kinetics of germination in *B. subtilis*, and to observe the influence on the uptake of nutrients in the extracellular matrix[24]. Techniques such as bio-inspired silica coating was applied in LbL single-cell encapsulation as well[25]. Lin and Li *et al*. applied the materials as the reservoirs for regulators, enhancing multiple functions of neural stem cells (NSCs) and dermal papilla cells (DPCs)[26, 27]. Mooney *et al*. managed to transplant marrow stromal cells which were encapsulated by tunable gel into mice and facilitated the insensitivity of cells towards exogenous cytokines[28]. Notably, some of the methods and materials are not biocompatible to mammalian cells. Compared to bacteria and fungi, polycations used in LbL technique are usually synthetic polymers, causing toxicity to most mammalian cells due to the easily-generated pores on the cell membrane[29]. Therefore, biocompatibility of the applications is a priority in studies on mammalian cells.

1.1.3 Biomaterials Applied in LbL Single-cell Encapsulation

Polyelectrolytes, including polycations and polyanions, are the fundamental constitutes in the LbL research. Polyanions have been utilized in many fields such as drug delivery and peptide synthesis[30, 31]. Polycations can combine with negatively

charged protein and nucleic acid through the electrostatic adsorption. They are also reputed for the characteristics like anti-inflammation, anti-tumor and anti-oxidation[32, 33]. The differences among the various types of polyelectrolytes reside in their side chains, hydrogen bonds, electrostatic adsorption, potential, amine groups and nucleophilicity. According to different degrees of their biocompatibility, some of them are used mostly in non-mammalian cells encapsulating and some in mammalian cells encapsulating.

1.1.3.1 Polycations Applied in Non-mammalian Cells Encapsulating

Cytotoxicity of the biomaterials is largely caused by polycations which devastate cell membrane. Therefore some polycations, especially the synthetic polycations, are more appropriate for non-mammalian cells which have protective cell wall. Application of synthetic polymers is supposed to be homogenous since their manufacturing is strictly standardized and the polymer products are extremely consistent. Therefore, the reaction with functional groups of biomolecules will be more controllable and predictable[34].

1.1.3.1.1 Polyethylenimine (PEI)

PEI is the most extensively used synthetic polycation. There are primary, secondary and tertiary amino groups inside the molecular structure. Its structure can be either linear or branched with diverse molecular weight. Linear PEI is obtained through the hydrolysis of 2-ethyl-2-oxazoline polymerization and it is solid at room temperature. Oppositely, branched PEI which is fabricated by polymerization of aziridine in acidic condition is viscous under room temperature. Owing to the plenty of active amine

groups PEI contains, it can be modified feasibly to obtain diverse functions. In the transfection research, PEI with higher molecular weight and higher degree of branching forms steady co-polymers with DNA. Linear PEI with the same molecular weight is not able to bind efficiently. Nonetheless, considerable cytotoxicity and non-degradability of PEI tremendously hinder its application in medicine[35].

The cytotoxicity of PEI can be effectively lowered by amine modification. For example, cystamine derivatives with disulphide bond were crosslinked with primary amine on PEI[36]. Additionally, acylation and acetylation of PEI also lead to alleviated cytotoxicity[37]. However, these procedures are technically challenging. It is easier to modify primary amines with optimum amount of trimethylene carbonate. Toxicity of PEI can be significantly reduced by conjugation of merely one trimethylene carbonate molecule[38].

Unmodified PEI is also known to be nondegradable. Reportedly, adding short cleavable chains of PEI to the long chains will produce cleavable PEI derivatives that are degradable and less toxic. There is also a report showing the modification with disulfide bond crosslinked on PEI backbone[36]. Another attempt is to apply reactive ester bond in order to endow PEI with degradability[39].

Due to the potent cationic feature, PEI was rarely applied in cell encapsulation, even for non-mammalian cells. Kozlovskaya *et al*. encapsulated yeast cells with PEI as the first layer. To lower the positive charges, they diluted PEI in the buffer with the pH of 7.0 so that cellular functions were not significantly affected. They addressed that the encapsulation structure was able to be stabilized on cell surface for 6 days and

the permeability of multilayers allowed nutrients to get access[40].

1.1.3.1.2 PAH

PAH is obtained via the reaction of hydrochloric acid with poly(allylamine phosphate), which is produced from the polymerization of allylamine phosphate at the presence of 2,2'-azo-bis-2-amidinopropane dihydrochloride. PAH molecules containing plenty of hydrogen bonds are highly hydrophilic, but not soluble in organic solutions[41].

The favorable solubility and the weak positive charges enable PAH to be applied in cell encapsulation. For example, in 2005, PAH was applied to encapsulate yeasts, demonstrating the protective effect against shear force and ability of cutoff based on molecular weight[42]. Further, PAH and PSS layers were found to be deposited on the yeast cell surface together with nanotubes to stabilize the encapsulation structure[43].

1.1.3.1.3 PDDA

PDDA is the homopolymer of diallyl dimethyl ammonium chloride which is synthesized from reaction of allyl chloride and dimethylamine. Polymerization is processed under the catalysis by peroxide and its molecular weight varies[44]. It possesses high cationic density which makes it a potent polyelectrolyte in cell encapsulation. Encapsulation of *Allochromatium vinosum* was performed using PDDA and PSS. They verified that the encapsulation would not inhibit bacteria's metabolism[45]. However, like most synthetic polycations, it exhibits distinct cytotoxicity to mammalian cells.

1.1.3.2 Polycations Applied in Mammalian Cells Encapsulating

Since the very beginning of encapsulation on mammalian cells, biocompatibility has become a priority of choosing polycations. Owing to the biocompatibility, biodegradability, and low immunogenicity, natural polycations and a few synthetic polycations are viewed as adequate materials for encapsulation on mammalian cells[46, 47]. Further, most of them also have reactive sites which enable different types of chemical modifications[48]. Without doubt, most of these mammalian cell-favored materials can also be applied on non-mammalian cells.

1.1.3.2.1 Gelatin

Gelatin which is derived from collagen belongs to natural polyelectrolytes. Due to its ideal biodegradability and biocompatibility, it is widely used in medicine and pharmacology. Gelatin is constituted by 18 amino acids with varied charges. Lysine and arginine residuals in the structure endow gelatin with positive charges. There are two types of gelatin according to the ways of extraction. Type A gelatin is produced by acidic degradation, having an isoelectric point (IEP) at 7.0-9.0. Oppositely, type B gelatin is obtained by basic degradation with an IEP at 4.7-5.4, because the amino groups in asparagine and glutamine are hydrolyzed into negatively charged carboxyl groups thus lowering the IEP. Therefore, these two treatments yield gelatin with opposite characteristics. US Food and Drug Administration (FDA) has already confirmed its safety in food additive so that it is able to be extensively studied in material science[49, 50]. In most occasions, type A gelatin is more frequently studied due to its ability to react with negatively charged substances, including the cell

membrane. NSCs and DPCs have been reported to be encapsulated with gelatin, with no apparent adverse effects observed[26, 27]. It is confirmed to be an inert and safe polycation, adequate for mammalian cell encapsulation.

Since gelatin is a weak polycation, cationization is sometimes needed. It can be achieved via two processes. When pH of environment is lower than IEP, the amine groups of gelatin become protonated. The other way is to crosslink ethylenediamine (EDA) and spermine with the mediation of EDC on gelatin to increase its composition of amine groups. As such, the modified gelatin will gain more positive charges which are required in some applications[50, 51].

1.1.3.2.2 Cationic Cellulose

This special natural polycation has been used for therapeutic purposes since its derivatives are acknowledged to be hydrophilic, biodegradable and anti-bacteria. It contains a linear structure composed of β-1, 4-D-glucan molecules existing widely in the nature[52].

Cationic cellulose could be achieved via etherification of glycidyl ammonium or alkylene epoxides. Although there are many studies involving cationic cellulose, production of stable derivatives is still a challenge. The main reason is the insolubility in aqueous and organic solutions, resulted from the strong hydrogen bonds within their molecules[53]. Some people esterified cellulose under the alkaline environment to endow it with amphiphilicity[54]. This new derivative is considered as an ideal carrier for insoluble drugs.

Aside from cationic cellulose, cellulose can also be modified with hydroxypropyl

or hydroxyethyl. Hydroxypropyl cellulose is a biocompatible material that has received FDA approval. It is added with poly(2-dimethylamino ethylmethacrylate) (PDMAEMA) chains to generate comb-shaped polymers, which exhibit outstanding features for carrying gene products[55]. Polyethylene glycol (PEG) substitution is performed to produce cationic polyquaternium derivatives, such as polyquaternium-4-cellulose, belonging to hydroxyethyl cellulose which also improve the gene transportation[56].

Cellulose has already been utilized in the encapsulation of epithelial cells for cell therapies. It is addressed to inhibit the immune response on the grafted cells by the host[57]. However, the safety of its application is still under debate. Some studies found that only mere influence was observed on the proliferation of encapsulated cells[58]. Some groups verified that strong inflammation will be elicited after the encapsulated cells are transplanted[59]. Clinical practice will be better performed only when the basic features of the cellulose are thoroughly clarified.

1.1.3.2.3 Poly(amido amine) (PAMAM)

Among various types of synthetic polycations, PAMAM is a peculiar one with ideal characteristics—it is degradable, biocompatible and of low cytotoxicity. Its synthesis is achieved by Michael-type polyaddition of amino groups with bis-acrylamides and amino groups arranged alongside the backbone. PAMAM itself is a highly functionalized polymer of which the side chains can be flexibly substituted. Generally, linear form is a powerful gene deliverer owing to its naturally high capacity in binding DNA[60].

In some occasions, PAMAM can be modified to be more reductive for improving the drug delivery. These derivatives comprise acetals or ketals alongside the backbone and they will be hydrolyzed under acidic condition[61]. The hydrolyzed oligoamine groups can be coupled with cystamine bisacrylamide that contains disulfide bonds via Michael-type reaction[62]. Even the primary amine monomer is reacted with cystamine bisacrylamide to synthesize PAMAM derivatives. Taking advantages of these disulfide bonds, PAMAM can be modified to be more biocompatible, stronger in buffering and efficient in transfection[63, 64].

Besides the potency in DNA binding, PAMAM has been well-recognized to be used in mammalian cell encapsulation. Islets are coated with phosphine-modified PAMAM in a covalent way, without interruption of cellular functions since the decreased cations further mitigate the cytotoxicity of the material[65]. This encapsulation complex is also suggested to endow immunoprotection for the grafts.

1.1.3.2.4 Chitosan

As a natural polycation, chitosan has randomly distributed N-acetylglucosamine and D-glucosamine which are varied in ratio, alignment and chain length. It is also known as a polybase with a pKa from 6.0-6.5, which endows chitosan with pH reactivity. Since this pKa approximates to be weak acidity or neutrality, it demonstrated great potential in the biological research[66].

In the conditions of which the pH is lower than pKa, chitosan will obtain high charge density, exerting the feature to be cationic. When pH is neutral, charge density on chitosan will be lower, decreasing its cytotoxicity. However, chitosan becomes

unstable and tends to aggregate because of the lower solubility under the neutral pH. On the other hand, acetylation and molecular weight can be altered to influence the charge density, affecting the transfection efficiency[67]. Chitosan is able to interact with polyanions due to these features, so that it is often used to combine with negatively charged biomacromolecules and even cell membrane. One of the main obstacles of chitosan in the bio-therapy area is from the low solubility in neutral conditions. Another is that the drug will be released rapidly from the chitosan substrate since chitosan swells to a high degree in water[68].

To overcome these disadvantages, chitosan has been modified chemically. Each glucoside in chitosan molecule has one amine group and two hydroxyl groups to be reacted. Modification of the cation can be processed by alkalinization of the amino group, or by adding side chains to the backbone. All those modifications will not yield to changes of the major characteristics, but introduce new features, such as protecting amine groups to improve the transfection[69]. Chitosan alkalinization leads to controllable cation features and will not affect the dependence of pH at the same time. Additionally, its solubility in aqueous solution with wider pH fluctuations can also be improved. The adhesiveness of chitosan changes along with the degree of alkalinization, making the derivatives suitable for delivering gene products. Reaction between chitosan and methyiiodide under alkaline condition is a direct way of alkalinization[70]. Among different forms of alkalinized chitosan, N, N, N-trimethyl chitosan chloride is a broadly used one[71]. Other types of modification are also widely reported. For example, Jia *et al*. synthesized the quaternary ammonium salts of

chitosan which are anti-bacteria[72]. Crosslinking with folic acid enables chitosan to transport 5-aminolevulinic acid to human colorectal cancer cells. This crosslinking can be catalyzed with 1-ethyl-3-(3-dimethylaminopropyl) carbodiimide (EDC) with varying starting ratios[73]. Another chitosan derivative is from the modification by octadecyl-quaternized lysine, which is applied to produce lipidosomes for carrying paclitaxel that is originally insoluble. N-((2-Hydroxy-3-trimethylammonium) propyl) chitosan chloride (HTCC) is fabricated via reaction with glycidyl-trimethyl-ammonium chloride[74]. The good solubility and permeability promote their efficiency in neutral conditions. Permeability is realized by the reaction of negatively charged site on tight junctions with the positively charged HTCC; the junctions will open to facilitate drug transportation. By adding poly-L-lysine (PLL) to chitosan, the latter will possess higher density of cations. This derivative has stronger affinity to negatively charged biomolecules with lower cytotoxicity and higher transfection efficiency than PEI does[75].

Chitosan is often used in the encapsulation of diverse types of cells such as MSCs and PC12 cells[76, 77]. Although it is soluble only under acidic conditions and not stable mechanically, chitosan and alginate are proven to encapsulate islets for transplantation into diabetic animal models[78]. Some studies apply N-acetylated chitosan to enhance its solubility and stability in the cell encapsulation, however, the biocompatibility becomes an obstacle[79]. Therefore, utilization of chitosan and its derivatives needs cautiousness.

1.1.3.2.5 Poly-L-lysine (PLL)

As a cationic polycation, PLL composed of homopolymer contains vast primary amine groups. They can conveniently combine with negatively charged biomolecules following protonation, by the force of electrostatic adsorption. During the fabrication, one lysine monomer is protected by a primary amine group, and then it is converted into a cyclic lysine anhydride. After the ring-open reaction of this cyclic anhydride by the initiator, PLL is produced. In this context, molecular weight of PLL can be easily manipulated by adjusting the ratio of lysine monomer and initiator[80].

PLL has always been applied in polyelectrolyte complex formation since it is fabricated. Under the neutral conditions, primary amino groups on PLL are partially protonated. This gives PLL the ability to buffer from pH 5.7 to pH 7.7. PLL with a high molecular weight is supposed to be cytotoxic and it has the tendency of forming aggregations. With the reduction of molecular weight, the complex with PLL becomes unsteady[81]. The fact indicates that the amount of primary amino groups counts in the polyplexes production.

To overcome the limitations, branched derivatives have been developed. PEG was added to PLL to establish co-polymer with advanced buffering capacity and decrease the deposition[82]. Bioactive peptide can be conjugated with the PEG-PLL polymer. One example is that the artery wall binding peptide (AWBP) is linked with PEG-PLL through the reaction of cysteine on AWBP with the vinyl sulfone groups on the co-polymer. The efficiency in transfection becomes significantly enhanced compared with the efficiency of PLL or even PEG-PLL[83]. Biological tissue-targeting delivery

of drugs can be achieved via the modification of PLL polymers. For example, lactic acid conjugation exerts the ability of hepatic tissue targeting. Doxorubicin is able to be delivered and released by this modified co-polymer. Leukemia cells can also be targeted via the reaction of JL1 antigen on the co-polymer[84-86].

An advantage of the application of PLL dendrimer is the relatively lower cytotoxicity. Denkewalter *et al*. designs the bidirectional asymmetric core that is coupled by l-lysine monomer and benzhydrylamine[87]. Followed by acid-induced deprotonation, the activated lysine derivative will form the PLL dendrimer which is of the early generation. Thereafter, almost all the PLL dendrimers are synthesized on this basis. For example, induction of lysine, succinimyldipropyldiamine and arginine into PLL yields derivatives to be less toxic as well as higher positive charges[88, 89].

PLL is acknowledged as a powerful polycation for mammalian cell encapsulation. Veerabadran *et al*. performed single-cell encapsulation on MSCs with PLL and HA. They address that the thickness of the multilayers can be 6.0-9.0 nm and the morphology and cell survival are maintained for 7 days[90]. Wilson *et al*. modified PLL with PEG to further reduce its cytotoxicity. The PEG-PLL copolymer is demonstrated to encapsulate the islets of which the functions are not interfered. The encapsulated grafts exhibit significant therapeutic benefits for the murine model[91].

1.1.3.3 Polyanions Applied in Cells Encapsulating

Compared to polycations, most polyanions are much less cytotoxic so that people have a broader scope for selection. The commonly used polyanions are described in below.

1.1.3.3.1 Alginate

Alginate is extracted from algae. It is constituted by 1,4′-linked β-D-mannuronic acid and α-L-guluronic acid residues in varied sequences as the structure of linear polysaccharide[92]. Different composition of the residues is determined by the source of algae. High ratio of guluronic residues leads to more solid structure since they have higher affinity to bivalent cations. On the contrary, a high ratio of D-mannuronic residue results in soft gels[93]. Therefore, with a wide range of selection, they can meet different requirements.

In order to fabricate capsules, bivalent ions like Ca^{2+} and Ba^{2+} should be added to the alginate solution to crosslink into hydrogel. Other metal ions such as Cu^{2+}, Pb^{2+} and Co^{2+} are not appropriate for cells due to their cytotoxicity[94]. The rigidity of the gel increases when the affinity of ions with alginate becomes higher[95].

One limitation of alginate hydrogel is the widely existing pores, thus immune signaling cannot be effectively blocked[96]. For example, pore size of Ba^{2+}-alginate hydrogel can only protect allogeneic graft from immune recognition, but not the xenogeneic graft[97]. To ameliorate the immune response, synthetic polycations like PLL and poly-L-ornithine should be used to coat with alginate[98, 99]. Besides, glutaraldehyde, PEG, cellulose, etc. can also be applied as crosslinkers[100-102].

It is noted that even if the coupling materials are suggested to diminish the pore size of encapsulation with alginate, normal metabolism of the encapsulated cells should not be influenced by the material barrier, which otherwise may hinder substance transportation. In the study of islet cells encapsulation with PLL and

alginate, reactivity of islet cells to glucose is directly interfered. The degree of influence by PLL thickness even exceeds that of the islet size and capsule diameter. To minimize the impact, thickness of PLL layers should be less than 4.0μm, concentration should be lower than 0.1% and incubation time should be shorter than 10 minutes[103]. Otherwise the permeability may be decreased, leaving hazardous substances inside cells to cause damage.

Applications using other coating materials with alginate can also augment the rigidity of alginate encapsulation and reduce the permeability. PEG can be coated on capsules to increase the stability and prevent cells from overgrowth[104]. Even the low concentration of glutaraldehyde is capable of stabilizing the microcapsules[101].

Covalent crosslinking is another way to establish stable alginate gels. Photoactive crosslinking is the most preferred technique[105]. However, photoactive crosslinker solution will release a surge of free radicals in the process of bond formation, leading to cytotoxicity[106]. An alternative approach is to introduce aldehyde or hydroxyl groups to alginate. In this case, permeability is partly reserved and structure stabilized[107, 108]. Phenol may be applied together with horseradish peroxidase as a biological crosslinker, but the esterification would consume a plethora of carboxyl groups so that the capsules become unstable[107].

The purity of alginate is regarded as a potential factor affecting the immune response. Most natural polymers such as alginate contain immunogenic molecules including proteins and endotoxins. These substances can induce intensive adverse responses after diffusing out of the capsules[109]. Researchers assume that impure

alginate probably contains pathogen-associated molecular pattern molecules (PAMPs) which exist either in pathogens or in nature extensively with a highly conserved motif. These PAMPs are potent activator of immune system and can result in strong inflammation[110].

Complement system triggering is another procedure that strengthens the immune activation. The activated complement will lead to the generation of cytokines which penetrate into the capsules to cause damage[111]. However, the complement complex is usually too huge to cross the alginate coating. This effect is more prominent in encapsulation using alginate with high ratio of guluronic residue[112].

1.1.3.3.2 HA

HA is polysaccharide of high molecular weight, derived from connective tissues and fibroblasts. HA exists extensively in the organism, such as in cartilage and vitreum, to reserve water and keep lubrication. Therefore it is critical for synovium of joints. On the other hand, HA exhibits importance in cell-cell interaction as a structure supporter. For degradation, HA will enter the plasma and then get degraded by hepatic endothelial cells or directly by hyaluronidase[113].

HA has a highly conserved structure composed of 1,3-b-D-glucuronicacid and 1,4-b-N-acetyl-D-glucosamine. In the animal body, HA can be circulated and immobilized on glycosaminoglycans, receptors and proteins by electrostatic adsorption. Membrane receptors of HA have been identified into several categories that include intercellular adhesion molecule-1 (ICAM-1), hyaluronan mediated motility receptor (HMMR) and CD44. It is noted that expression of CD44 is

widespread in tumor cells, so that it becomes an ideal material for drug delivery targeting tumors. In general, HA is a component of ECM endowed with biocompatibility and biodegradability, thus suitable for most applications in tissue engineering and pharmacy[114].

HA can be modified to be functional with different techniques. Among them, chemical modification is the most used one. Carboxyl group, hydroxyl group and N-acetyl are the active sites for reaction. Therefore carbodiimide can mediate the esterification and amidation of carboxyl group. Etherification, esterification and crosslinking with divinyl sulfone are common methods for modifying hydroxyl groups[113]. The HA derivatives are divided into two types which include terminal-modified and partial-modified[115]. The terminal-modified HA will undergo different biological procedure and not be able to form bond. Conversely, partial-modified HA is still modifiable to form covalent bond after being applied in biological researches. In this context, partial-modified derivatives of HA are preferred in most occasions, but it should be aware that the biocompatibility is required when performing the chemical modification and the by-products have minimal toxicity.

In cell encapsulation, HA is especially favorable for cells of which the ECM contains a vast of glycosaminoglycans or HA. In the research of cartilage engineering, HA encapsulation was demonstrated to boost the chondrogenesis of mesenchymal stem cells (MSCs) and the establishment of supportive matrices[116]. It is also ideal in tissue engineering of nervous system. The improvement of neural regeneration and astrocyte activation has been verified in the application of artificial ECM fabrication

following nervous system disorders[117].

Modification of HA will be advantageous in many respects. Since HA is inheritably not adhesive to cells, adhesive motifs such as RGD can be coupled to increase the ability of adhesion[118]. Photoreactive HA polymer was synthesized by treatment of methacrylic anhydride. It is found that the mechanical properties of the polymer resemble that of neural tissues[117].

1.1.3.3.3 PSS

PSS is a polymer with thermoplasticity and featured by outstanding hydrophilicity. It has been extensively applied in encapsulation of tissues and cells, such as erythrocyte and pancreatic tissues[119]. Although PSS is able to interact with polycations such as poly PAH via the electrostatic adsorption to endow cells with a shield against immune recognition, the mechanical stability is a major concern for application of PSS[120]. Encapsulation with PAH and PSS is shown to be damaged by the shear force after transplantation[121]. Furthermore, PSS will provoke the activation of complement system so that the survival of encapsulated cells is impaired, especially for the mammalian cells[122].

1.1.3.4 Other Materials

Aside from natural and synthetic polymers, nanoparticles are applied in single-cell encapsulation. In 2009, Fakhrullin *et al.* encapsulated spores of *S. cerevisiae* and Trichoderma asperellum (*T. asperellum*) using Au and Ag nanoparticles together with PAH, bovine serum albumin (BSA) and PSS. However, they found that these different cells exert converse morphological changes and biological behaviors[123]. Some

applied multiwalled carbon nanotubes (MWNTs) in encapsulatin *S. cerevisiae* for investigating the electrochemical characteristics[124]. Graphite oxide is also proved to be suitable for encapsulation, with great biocompatibility[125].

Additionally, magnetic nanoparticles (MNPs) as a special type of nanoparticle, have attracted great attention in many fields such as biocatalysts, bioreactors and biosensors. MNPs provide the possibility of manipulating cells that are coated with MNPs in the 3D space via the external magnetic field. Either dead cells or living fungi were reported to be encapsulated[126]. The magnetizing encapsulation does not influence the enzyme activity within cells since the encapsulated cells still function as the biocatalyst[127]. Nevertheless, it is inevitable for MNPs to affect the viability of cells, especially when they are directly attached to the cell surface. Fakhrullin and colleagues probed into strategies of encapsulation with MNPs, indicating that adsorption of PAH with MNPs is a feasible and effective way to preserve the viability and functions of cells. Encapsulated fungi were easily performed with toxicity test and isolating[128]. Follicle epithelial cells and fibroblasts can be manipulated to form bilayered cellular structure in the magnetic field[129]. Additionally, it is acknowledged that encapsulation of HeLa cell line with PAH/MNPs is of enlightenment for cell research. Mammalian cells lack the cell wall, so that the fragile cell membrane is exposed to the toxic nanoparticles[130]. By applying PAH with MNPs, these nanoparticles will be immobilized outside the cell membrane to decrease the cytotoxicity.

1.1.4 The Interaction within LbL Self-assembly

LbL self-assembled multilayers are able to adsorb to interfaces firmly and alter their surface characteristics simultaneously. On the other hand, changes in the interacting force also mold the features of multilayers. As such, the premise of application of LbL is a comprehensive understanding of the interactions between polyelectrolytes and the encapsulated objects.

There have been studies about the feature variations led by coupling of polyelectrolytes with interfaces nowadays. These interfaces are divided into planar surface and colloidal particle. The interacting force on the surface was investigated via atomic force microscope (AFM), surface forces apparatus and totalinternal reflection microscope[131-133]. The assembly of the colloidal particles can be observed by means of turbidity measurement, time-resolved light scattering, and rheological technique[134-136].

Structures of LbL polyelectrolytes are either linear or branched. Strong polyelectrolytes such as PSS and branched PEI will possess charges almost permanently. On the contrary, charges of weak polyelectrolytes which include gelatin, chitosan, PLL and linear PEI are determined by variation of solution pH and ion strength. The degree of ionization can be measured with titration or patterned with electronic field[137].

1.1.4.1 Characteristics of Material Adsorption

The affinity of the polyelectrolytes with the oppositely-charged interfaces is resulted from force of electrostatic adsorption. Since the backbone of polyelectrolytes

is usually hydrophobic, van der Waals force and hydration force are playing important roles[13].

1.1.4.1.1 Interaction of Polyelectrolytes with Planar Interfaces

Visual techniques enable people to detect the interaction between materials and surfaces. For example, in the research of PDDA/SiO_2 combination, pH of polyelectrolyte solution was adjusted to be acidic and then it was incubated with SiO_2 substrate[138]. Initially, the mass of attached polyelectrolyte increased in a time-dependent manner, indicating the ongoing adsorbing procedure. Afterwards, the binding would not continue due to the saturation, although there were still materials in the solution. The surface was then rinsed but no detachment was found, suggesting that the material binding was hard to reverse[139]. Under some occasions using polyelectrolytes with low molecular weight, partial detachment will probably occur especially when solution composition changes or there are other materials in presence[140].

It was confirmed in these studies that the adsorption rate was proportional to the material concentration. This was also verified by mathematic model in a PDDA adsorption study[131]. The discrepancy was only a mere and might be resulted from the influence of hydrodynamics[141]. The adsorption rate on the plateau will be increased with the higher concentration of polyelectrolytes. This phenomena was explained by the finite relaxation of the material structure that when the concentration is increased, the lateral relaxation of the bound material will be inhibited by the rapid adsorption of adjacent polymers. The mechanism extensively exists in research of

protein adsorption[142].

1.1.4.1.2 Interaction of Polyelectrolytes with Colloidal Particles

Polyelectrolytes can attach to the surface of colloidal particles when they are mixed. When there are excessive polyelectrolytes, they will adsorb to the particles until the plateau reached; if the polyelectrolytes are insufficient, they will get attached without free polymers in the mixture. In this context, materials applied should be excessive to keep them homogenously distributed on particles[143].The adsorption was also verified to be irreversible and quantifiable in the experiment with PAA and sulfate particles, monitored by AFM[144]. Adsorbed materials on each unit of particle surface could be identified as mg/m^2, which was further confirmed via electrophoresis. However, heterogeneity of the mechanism above may occur due to the kinetics during the binding process[145].

1.1.4.2 Characteristics of the Polyelectrolyte Layers

1.1.4.2.1 Amount of Material Adsorption

As calculated under the condition of 50 mM salt solution, the saturated adsorption mass of PDDA on SiO_2 was about 0.3 mg/m^2 which was at small scale. The reason is that the innate ability of adsorption for a single layer of atoms is 1.0-2.0 mg/m^2. The mathematic model demonstrates the adsorption amount to be 0.01-1.00 mg/m^2 when the polymer coupling is saturated[146].

Adsorption amount of polyelectrolytes is directly associated with factors such as polymers' inherit features and solution composition. Among them, molecular weight, ion concentration and charge density of substrate are critical. For example, the amount

is weakly related to the molecular weight of linear polyelectrolytes, however, it is proportional to molecular weight of branched polyelectrolytes[147]. In addition, it is also dependent on the concentration of monovalent electrolytes. This has been verified in variant polymer-substrate mixtures and can be reversed only under extremely weak polymers or high concentration of salt solution[148].

Charge density of polymers is of significant discrepancy and their hydrophility changes accordingly. The charge density can be tuned by utilizing weak ion groups or adjusting pH. However, it may be different between bound complex and unbound complex since ionization happens during the binding. Generally speaking, when charge density of substrate increases and that of polymer decreases, the attached amount will increase, reaching maximum when charge density of polymer is at a minimal level[149].

1.1.4.2.2 Morphology of the Polyelectrolyte Layers

It has been verified that polymers are bound on the interfaces in a layer-by-layer way. Since the space in between is generated by the repulsion force from existing chains, the polymer films are heterogeneous laterally. Additionally, chains of polymers are flatten due to the robust electrostatic force with the interfaces. For weak polyelectrolytes under the condition of high salt density, they form films with homogeneity[137].

Thickness of the polyelectrolyte layers can be measured with different methods, for example, dynamic light scattering and quartz crystal microbalance measurements[150]. These indicate that the polymer films have the thickness of a few

nanometers. Since the diameter of polyelectrolytes is around 20-100 nm, it is acknowledged that these polymer chains are pressed to great extent when adsorbed. According to the thickness, water content of the pressed films is supposed to be only 20%-60%. However, under the condition of high salt concentration, films would be swollen and highly porous. Some researchers found that with the increase of salt content, mole mass, and the decrease of charge density, polymer films became thicker[151].

Even though dynamic light scattering exhibits a similar result, the figure could be higher than measured by surface technique, which could reflect the process of the film swelling. Application of substrates might underlie the deviation, but it was presumably caused by sub-layers within a single polymer structure. Thickness of these sub-layers varies with the concentration of salt solution alteration, leading to discrepancy of these methods. It is also noted that since the films are extremely thin and influenced by environmental factors, systematic errors are inevitable[152].

Lateral heterogeneity of coupled polymers have been confirmed with AFM technique. This feature is predominant for polyelectrolytes with high charges and condition with low salt. Popa *et al.* observed the dried branched PAA after adsorption. They observed that although there was still space among the polymer molecules, the adsorption had already reached saturation[153]. This was led by the potent repelling force from the branched macromolecules.

Various techniques have been applied to verify the lateral heterogeneity of attached polymers, however quantification is rare. As an exception, branched PAA-formed

films can be quantified at the single-molecule scale by AFM[154]. The attached single linear polymer and nucleic acid could be characterized statistically, but detailed description for structure of saturated layer of adsorbed linear polymers is still unavailable[155, 156]. Direct force measurement was used to prove that attached PAA and linear PSS were heterogeneous[157]. These findings indicated that linear polymers tended to generate films with high homogeneity. Hydrophobic polyelectrolytes with weak charges would construct films with higher homogeneity, in similarity to the cluttered lamellar phase[158].

1.1.4.3 Charge Balance of Polyelectrolyte Layers

1.1.4.3.1 Charge Reversal

A pronounced feature in the process of polymer-substrate adsorption is the charge reversal caused by excessive coating. It is acknowledged that combined polyelectrolytes and substrate are oppositely charged (except for some weak polyelectrolytes). A common sense is that when they have the same charge, polymers will be detached from the substrate. However, since the attached polymers are lateral heterogeneous, characteristics of the interface are critical only when it is adjacent to the polymers. Therefore, the polymer molecule would adsorb to the vacant binding site which is decided by local environment instead of the charge of substrate[159]. Moreover, other types of adsorption force which are not affected by charges of interfaces also exist, such as hydrophobic force and van der Waals force[160, 161].

Electrokinetic methods can be applied for detecting the charge of polyelectrolyte films. A good approach measuring capsules is electrophoresis. Electrophoretic kinetic

during the process can be converted into surface potential via mathematic model. Streaming potential or current techniques are commonly applied in measuring planner interfaces. Surface potential of both capsules and substrates can be monitored with direct force detection, by which the relative value is obtained[162].

Surface potential of amidine latex particles is an indicator to show a discrepancy in charge density between untreated and encapsulated particles[163]. In spite of it, the other characteristics may not be altered significantly since the polymer films are super thin. As a matter of fact, positive charges of non-encapsulated particles would be reversed by attached polyelectrolytes, exhibiting negative charges. These facts are confirmed by both surface potential and direct force techniques, with the exception of substrates with charge heterogeneity. In the process of coating, particles would remain positive when polyelectrolytes are at low concentration. When reaching a certain concentration threshold, the surface charges could be neutralized without additional adsorption[143]. Therefore, if polyelectrolytes are added continuously, negative charges on particles would aggregate till saturation with excessive polymers in the mixture.

1.1.4.3.2 Charge Distribution within the Multilayer Structure

Studies showed the pattern of charge density and surface potential. For substrate with positive charges, local layer characterization showed that aggregation of negative charges and depletion of positive charges could compensate the positive charges in the local charged group. However, the surface charges of saturated layer of polyanion can be over-compensated so that they can be neutralized by following addition of

polycations[164].

This procedure of compensation is slow, indicating that the net charge on the surface was decreased. The actual variation of charge distribution in the multi-layer films can be detected. It is because at the critical point of charge reversal, it is neutral on the interface so that chemical titration could be used to detect the charges by ion compensation. The counterions are important for charge balance in highly-branched polymers and substrates with low charges. For example, in the LbL assembly using branched PEI and PAA, the counterions are capable to compensate over 90% of the charges from bound polymers[165]. Even in layer of saturation, surface charges compensated by free polymers only accounts for a small proportion. Moreover, lateral heterogeneity-induced lateral deviation in the dissociated layer may underlie the discrepancy between adsorption amount and net charges.

Deviation of charge reversal point is explained by stoichiometry that depicts the necessity of high demand for weak polyelectrolytes in charge compensation[166]. Similarly, compensation of a few surface charges relies on the low amount of polyelectrolytes[167]. Also, it is acknowledged that weak polyelectrolytes are depended on solution pH[167]. For example, polycations will possess more charges with the decrease of environment pH. For the substrate with fixed charge distribution on the interface, the critical point for reversal tends to shift to high pH with promoted coupling of polymers simultaneously[168]. This phenomenon occurrs in the interaction of surface containing weak acidic or amphiprotic groups with strong polycations. It also applies under the opposite condition that weak polyanion attached

to positively-charged surface or strong polyanion attached to surface comprising weak alkaline and amphiprotic groups[169]. However, it is not applicable for polyelectrolytes and substrates which are pH-sensitive.

Deviation of the critical point of charge reversal is associated with molecular weight changes, explained by similar way either. For example, in the coupling with PAA which is densely structured, more charges will be compensated by the counterions when its molecular weight increased. In this context, the increase of net charges is slower than that of molecular weight, leading to the deviation of critical point towards high doses of polymers. Yet this has not been found in linear polyelectrolytes since they will interact in a flattened conformation, so that stoichiometrical changes are not in accordance with molecular weight variation[170].

1.1.5 Single-cell Encapsulation with Other Techniques

Aside from LbL self-assembly, other techniques such as metal reduction and mineralization have been used in the single-cell encapsulation. Gold ions can be reduced as nanoparticles to form a shell on *E. coli* cells, which could preserve the viability[171]. Afterwards, the toxicity to mammalian cells is alleviated and the gold particles can be utilized for photothermal therapy. Some thermophiles and archimycetes can aggregate gold ions to form protecting films, although the mechanism has not been fully unveiled[172].

Mineralization is another approach to induce shells at the micrometer-scale. Calcium carbonate was applied by Fakhrullin to encapsulate cells and these cells

stayed viable for months[173]. Mineralization of calcium phosphate, lanthanum phosphate and calcium carbonate could be used in combination with LbL technique on cells like *S. cerevisiae* and *E. coli*, with a survival rate of up to 40%[174, 175].

Bio-inspired silicification was recently introduced into cell encapsulation by Choi. They firstly encapsulated spores of *S. cerevisiae* with PDDA and PSS, and then put them into silicic acid so that nanoshell of SiO_2 was fabricated[25]. Although scattered single-cell encapsulation model was not achieved, this was a breakthrough for establishing the SiO_2 shell via genetic engineering. The engineered cells are able to produce lysozyme and silicatein that can be transported to cell wall. These components will react with precursor of SiO_2 to form deposition on the cell wall for protection[176].

Since these inorganic nanoshells can be manipulated for functional regulation, they hold significant potential. For example, the nanofilms can be functionalized to permit the permeability of certain substances[177]. There is a study that people conjugated SiO_2 precursor containing thiol groups on the SiO_2 shell to encapsulate *S. cerevisiae*. These cells are capable of capturing maleimide groups[178]. Thus, various types of functionalized shells can be designed on the basis of cellular biological features and material characteristics.

1.1.6 Functional Regulation of Encapsulated Cells

Manipulation of cellular functions by cell encapsulation has drawn attention increasingly, in the fields such as cell survival, dividing, differentiation and disguise.

There are studies demonstrating the cell protection against physical, chemical and biological factors by the encapsulation[174, 179]. Chemical modifications of materials also enable the functional regulation in multiple ways[180]. Naturally, the priority of the regulation relies on the stable encapsulation structure for required duration.

Under some circumstances, cell growth will be hindered by inappropriate encapsulation. SiO_2 layers with a thickness of 50 nm inhibit yeast cells from proliferation and it can be intervened by thickness reduction[43]. Although it is obscure how the encapsulation impairs the proliferation, it is generally believed that the proliferation is inhibited by the block of nutrients transportation due to the coating layers. Previous studies have found that the proliferation is prohibited mostly by mechanical features of the material layers such as rigidity and ductility[181]. When the outer layers are compromised, proliferation can be revived, as shown by Ishihara *et al.* who established cell encapsulation via droplet on HeLa cells and verified that cell proliferation will be hindered to a higher degree with the increasing rigidity of capsules[182].

Initial studies of cell protection suggest that cells can be protected from physical factors such as osmotic pressure and centrifugal force. Choi *et al*. encapsulated *S. cerevisiae* with silica films and these cells can still stay viable in pure water for one month[179]. As Maheshwari proved, Ca^{2+}-Au nanoparticles-modified graphene is able to keep encapsulated *S. cerevisiae* alive for 7 days in water[183]. It is even achievable for mammalian cells. HepG2 cells were coated with fibronectin and gelatin

and then performed in high-speed centrifuge. Surprisingly, more than 80% of encapsulated cells survived and less than 10% of untreated cells did[184].

Some studies investigated the heat-resistance endowed by the encapsulation. Chlorella was encapsulated with TiO_2/SiO_2 and exposed to 45 degrees Celsius for 2 hours, with no obvious viability impairment[185]. SiO_2 nanoparticles were also assembled on surface of yeast cells, and cells exerted higher survival rate than untreated cells did after the exposure to high temperature. These may be explained by the moisture-reserving feature of SiO_2 nanoparticles[186].

Biological insults can be diminished either. Resistance to lytic enzyme was obtained when *S. cerevisiae* were encapsulated[187]. Yeast cells are protected from lysosomal enzyme with the encapsulation using PAH and PSS, by the means of decreasing permeability of LbL films to the enzyme[7].

Besides the protection, drug-modification is achieved for functional regulation via the cell surface engineering. Li *et al*. applied gelatin and IGF-1 loaded alginate in encapsulating NSCs. Viability of NSCs is retained and IGF-1 can be released in a pH-sensitive manner to promote proliferation[26]. DPCs were encapsulated with basic fibroblast growth factor-2 (bFGF) loaded materials. The neurotrophic regulator is found being released to enhance the regeneration of hair[27]. These reports indicated versatile ways modifying LbL encapsulation on mammalian cells, so that this technique has the potential of adjusting grafted cells in cell therapy in the future.

1.1.7 Other Applications of Cell Encapsulation

Cell encapsulation has been becoming a powerful tool in research fields of biomaterial and cell biology since it was introduced by Decher *et al*. Thanks to the increasingly unveiled property of cell encapsulation and the utilization of versatile techniques and materials in the past decade, different applications of cell encapsulation begin to be achieved apart from functional regulation described above.

1.1.7.1 Drug Delivery

A controllable drug delivery is desired in the treatments for many diseases, especially those progressive disorders such as Parkinson's Disease (PD). The diseases are long-lasting, such that traditional therapies cannot provide sustained beneficial. Cell encapsulation provides a hope to develop novel treatment by endowing with controlled, lasting and widely distributed release of drugs. It takes advantages of the cell-secreting regulators with the capsule, which resembles to a movable apparatus. Encapsulation structure allows the diffusion of oxygen and trophic substances for cells' metabolism, and facilitates the transportation of the waste to outside of cells[188]. Further, the encapsulation layers provide cell protection by isolating immune and other detrimental factors from the cell surface[189].

Recent years have witnessed the application of cell encapsulation in drug delivery. Islet tissue has been the first to be encapsulated and applied in clinical trials. The purpose is to provide protective shell to islet cells which are from xenogeneic donors, genetically engineered or differentiated from stem cells. In 1994, islets were encapsulated and grafted intraperitoneally in human, showing effective glucose

control for 9 months[190]. There is a report on islets transplanted subcutaneously by means of the encapsulation with poly(acrylonitrile-co-vinyl chloride). Nearly no immune attack was detected by this approach[191]. Poly-L-ornithine was reported to encapsulate islet tissues together with alginate, and these grafts in patients' peritoneum exhibit promoted C-peptide level, declined insulin requirement and lack of side effects[192]. However in a study in which islet tissues were encapsulated in metal ion-crosslinked beads in 2013, the grafts were finally found aggregated in peritoneal cavity 3 months later. Even though the cells still function, the biocompatibility of the method remains questionable[193].As summarized, both potentials and obstacles exist in islet encapsulation. One problem is the responses of the organisms against encapsulating structures. Some materials will inevitably bring foreign factors to the recipients, resulting in inflammations which may cause necrosis of the encapsulated cells[194]. The second concern is whether the capsules are mechanically robust or not. Since the materials used in encapsulation are versatile, they possess different strength and elasticity which determine different extent of stability when transplanted[195]. Besides, interaction of the interfaces and condition of charges that are difficult to manipulate also influence the therapeutic efficiency after the transplantation[196].

Cell encapsulation is also practiced for drug delivery into nervous system. Because of the blood-brain barrier, drug transportation from vessels to the parenchyma is always a challenge. Additionally, the delivery requires both quality and quantity of the drugs during the transportation. To overcome these obstacles, cell encapsulation is

introduced and shows remarkable prospective. There are animal studies carried out implanting encapsulated cells in amyotrophic lateral sclerosis (ALS) and Huntington's Disease (HD) models, addressing satisfied cell survival and functional enhancement[197, 198]. Unfortunately, results are diverse in Phase I clinical studies. Some studies applied engineered fibroblasts encapsulated with polyethersulfone for providing nerve growth factor (NGF). Since these cells are extremely proliferative, the overgrowth will cause aggregated necrotic components. Therefore the permeability of the microcapsules decreases, inhibiting the cellular functions such as trophic factor-secretion in the end and the distribution of bioactive regulators with higher molecular weight[199]. In the studies involving ARPE-19 cells which are arising retinal pigment epithelial cells from human, clinical benefits are observed. These cells survive rigorous environments where there is a lack of nutrients. It was illustrated that encapsulated ARPE-19 cells can remain viable in brain and eyes for over 1 and 2 years[188, 200]. During the process, well-designed encapsulating materials play a pivotal role in maintaining the functions of cells and isolating the coated cells against inflammatory cytokines. Apart from NGF, secretion of glial cell-derived neurotrophic factor (GDNF) is also achieved by genomic engineering on ARPE-19 cells. The cells were encapsulated and transplanted to supply a considerable amount of GDNF for PD patients[201].

1.1.7.2 High-throughput Screen

This technique takes advantage of the microfluidic systems for performing single-cell assay and cell sorting. Uniformly dispersed mono-droplets are generated

from the channels and each of them works as an individual capsule[202]. Therefore it becomes a powerful tool for different applications such as cell encapsulation, since it enable cells to be encapsulated in the microfluidics droplets at single-cell scale[203].

One distinct feature of cell encapsulation by this method is the linkage of genotype with phenotype[204]. Cells and the secreted molecules will be compartmentalized within the droplets during the procedures of sorting[205, 206]. Due to the confined volume, the produced molecules in the droplets will be able to reach the measurable concentration easily[207]. As such, it remarkably facilitates the detection of the targeting molecules. Moreover, lysis and assays of biomolecules inside cells can be performed on the encapsulated cells. Different types of biological processes have been analyzed, since there are DNA and RNA amplifications ongoing in droplets[208, 209]. Therefore the high-throughput analysis is broadly extended, not just for the cell surface markers measured by fluorescence-activated cell sorting (FACS)[210]. Even though this encapsulation-based sorting system has a lower efficiency than FACS does, it still holds great potentials due to the versatility[211].

Microfluidic system which includes nano-scale microwells has already been applied for investigation into proliferation of cells and screening of antibody-generated cells[212, 213]. In most occasions of using conventional microwell analysis for cell sorting, the targeting cells ought to be harvested from the device manually, making it inconvenient for conducting high-throughput cell sorting. On the contrary, the microfluidic system applying cell encapsulation is capable of processing vast amount of encapsulated cells in a single trial with hyper speed and

readily harvest of capsules containing cells[214, 215].

However, high-throughput cell-encapsulation analysis system is not compatible for some purposes. For instance, washing is needed in some biological experiments so that the reagents have to be discarded and refilled, making it tough to endow on the cells compartmentalized. By means of capsule fusion and aqua injection, contents inside the droplets are able to be manipulated without the exchanges of buffers[216, 217]. Besides, the readout scope in encapsulation-based microfluidic techniques is much more rigid than that in traditional analysis[3].

People have developed the methodology for high-throughput screening of molecule-secreting cells from non-secreting cells on the basis of microfluidic cell encapsulation. The rapid procedure of assay and the satisfied viability of encapsulated cells manage to screen the targeting cells without the cell immortalization[3]. Furthermore, since the technique is compatible for fluorescence-based measurement, it can be utilized in detection of fluorescence-bound ligands. Additionally, the fluorescence-based assay can also be applied in sorting antibodies and anti-enzyme factors[215]. In short, the microfluidic screening system based on cell encapsulation enables multiple high-throughput analysis on diverse cell types such as bacteria, fungi and mammalian cells with the help of the proteins that are secreted, surface-bound or inside cells[214, 218, 219].

1.1.7.3 Decoding the Composition of Stem Cell Niches

In adult organism, stem cells locate in niches in different parts of the body. Niche is a critical milieu complex constituted of neighboring cells, supporting matrix and

trophic factors. Stem cells are nourished and maintained inside these delicate microenvironments. The complicated natural niche makes it tough to reestablish the structure in the *in vitro* environment. As such, clarification of specific factors which are the most influencing for stem cell functions is largely demanded[220-222]. It will be of great significance for any research aspects of stem cells which are either basic or translational. In this context, the controllable cell encapsulation synthesis can be used for bottom up establishment of niches.

Researchers took advantage of cell encapsulation with hydrogel on MSCs to identify the influences of chemical groups on the differentiation[223]. Following the cell encapsulation, MSCs were compartmentalized in mono-dispersed 3D microcapsules with the highly homogenous morphology. They would be cultured in basic culture medium without the addition of differentiating factors, and then the molecules of interest were supplemented individually to demonstrate their direct effect on the cell differentiation. In the conventional cellular assays in 2D culture, the effects of ECM on cells are hard to be deciphered[220]. However in the cell encapsulation by which cells are trapped in 3D structure, spreading of cells is confined due to the limited capsule size[224]. The cell-ECM interaction will be better unveiled under this circumstances, for example, adipogenesis is promoted in spherical capsules[225]. Furthermore, phosphate-modified encapsulation is verified to lead to osteogenesis and t-butyl to adipogenesis[226]. Besides the influences from ECM and chemical groups, other soluble factors can also be investigated with the help of encapsulation[227].

1.1.8 Expectations

Single-cell encapsulation has drawn tremendous attention in the past decade. It can be categorized as biotemplate, nano-encapsulation and artificial spores. These techniques not only combine biomaterials with cell biology technically, but also investigate the interaction of them functionally.

As the biotemplate, cells are not required to stay ideally viable since they are treated as tools. However, the biocompatibility of techniques and materials is becoming critical for the future applications like cell transplantation, cell sensors and cell catalysts which demand cell viability[4, 9, 10].

The established ultrathin, stubborn and functionalized films on the surface of mammalian cells resemble the cell wall of the plant cells. Due to the protective effects against physical, chemical and biological factors, the encapsulation is potentially applicable as the protective shield in cell transplantation therapy. Further, modification of the coating materials will endow cells with versatile functions including permeability adjustment, rigidity regulation and stimulation-responsibility. These expand the applications for basic and translational studies in the future.

The study of single-cell encapsulation is still at a preliminary stage. Obstacles such as how to design biocompatible, adjustable responsive materials and how to regulate cellular functions delicately should be overcome. In the near future, this technique is supposed to convert cells into manipulable individuals, boosting creative advancement in different fields.

1.2 Stem Cell Therapy in Neurodegenerative Diseases

1.2.1 An Overview of Stem Cells

Stem cells which exist in almost all the organisms are able to divide continuously and differentiate into discrepant sub-lineages of cells. Based on the sources, stem cells could be classified into embryonic stem cells and adult stem cells. The former one comes from blastocysts, while the latter one is derived from different adult tissues. As for potency, stem cells contain totipotent, pluripotent, multipotent, oligopotent and unipotent stem cells. For example, the zygotes are able to differentiate into a complete organism. However, multipotent stem cells such as NSCs and MSCs will differentiate into closely related family of cells[228]. Due to their extraordinary characteristics, stem cells are regarded as ideal candidates for cell transplantation therapy in diseases and trauma. Adult NSCs and induced-pluripotent stem cells (iPSCs) will be illuminated in the following parts since they have shown great potential in treating neurodegenerative diseases.

1.2.1.1 Adult NSCs

Although NSCs were observed in the adult brain over one century ago, they were only identified with immunostaining and isolated for two decades by researchers such as Palmer, Reynolds and Weiss[229, 230]. They isolated dividing cells from subventricular zone (SVZ) and subgranular zone (SGZ), and proliferated them into neurospheres. It was later found that the dividing of multipotent cells and neurogenesis could be modulated under diverse conditions such as exercise,

environment enrichment, learning, stress, and aging[231-233]. Meanwhile, the development of immunohistology, microscopy and stereological devices allowed researchers to better verify the proliferation and differentiation of NSCs in central nervous system(CNS)[232, 234-236].

With the development of experimental techniques, properties of NSCs have been gradually unveiled in the 2000s. Noticeably, the concept of “niche” has been suggested to be critical for NSCs. Niche refers to a microenvironment constituted by astrocytes, microglia, endothelial cells and blood vessels[237]. Survival, proliferation, migration and differentiation of NSCs require specific conditions in different niches. For example, in most parts of adult brain, NSCs only differentiate into glia, but not into neurons. However, when these cells are isolated and cultured under specific situation, neurogenesis could happen[238]. Similarly, NSCs isolated from SVZ and SGZ fail to differentiate into neurons when they are transplanted ectopically, but tend to generate astrocytes and oligodendrocytes instead[239]. Additionally, NSCs from non-neurogenic regions will regain the ability of neurogenesis after being transplanted into SVZ and SGZ[240]. In general, niche is proved to provide appropriate microenvironment for NSCs to support various functions.

Currently, NSCs have been identified in CNS including SVZ, SGZ and spinal cord. SVZ of lateral ventricles is the first identified place where the adult mammalian NSCs reside. In the niches along the SVZ in rodents, stem cells can be categorized into type A, type B, type C and ependymal cells. These cells are functionally related with each other: dividing type B cells with the phenotype of astrocyte are viewed as NSCs; type

B cells divide asymmetrically to produce type C cells which are known to amplify transiently; these transit-amplifying cells would subsequently give rise to type A cells that are immature neuroblasts[241]. NSCs can be further verified with two phenotypical characteristics: astrocyte-only CD15+ expression and CD24- expression. A better understanding of features and behaviors of NSCs would require more exclusive cell markers[242, 243]. In dentate gyrus of adult hippocampus, NSCs reside in SGZ between hilus and granule layer. NSCs in SGZ extend their processes vertically and exhibit astrocyte-like features, which are similar to that in SVZ. Nevertheless, these cells would directly give rise to immature neuroblasts while in SVZ, neuroblasts are derived from type A cells. Neuroblasts expressing polysialylated-neural cell adhesion molecule and doublecortin are known as type D1 cells. They would migrate into granule layer and gradually undergo morphological changes simultaneously to become type D2 and D3 cells, and finally differentiate into mature granular cells[244]. The major differences between NSCs in SVZ and SGZ lie in the *in vivo* behavioral patterns. NSCs from SVZ usually migrate long distance to olfactory bulb (OB). On the contrary, NSCs from SGZ only need to migrate a short distance to produce neurons. Additionally, NSCs in SVZ and SGZ exhibit different responses to some physiological factors and pathological influences. Regulatory factors for neuronal differentiation differ in these two niches as well[245]. Spinal cord is also a region where NSCs reside. In 1996, Weiss and colleagues extracted NSCs from spinal cord. Although stem cells in thoracic spinal cord account for only 0.1% and in lumbar spinal cord for 0.6%, they could generate neurospheres capable of

proliferation and differentiation[246]. Moreover, NSCs are identified in the central canal, especially in the dorsal part, and in parenchyma with limited proliferative capacity[247, 248]. Additionally, NSCs in spinal cord express glial fibrillary acidic portein (GFAP), and co-express CD133 and CD15, which are known markers for immature cells[249]. Neurospheres isolated from spinal cord illustrate heterogeneous compositions including NSCs, neurons, astrocytes, oligodendrocytic cells and radial glial cells[250]. Besides the neurogenic areas above, there are other controversial regions harboring cells with differential potentials. Newly produced neurons are found in cortex of adult monkey. These cells may be derived from SVZ and migrate into cortex. These neurons only exist temporarily in the cortex and no obvious neurogenesis can be detected in this area[251]. NSCs extracted from substantia nigra (SN) show differential potentials in cell culture. These cells are able to generate granule neurons after being grafted in hippocampus, however, there is a lack of neurogenesis when they are transplanted back to SN[252]. Besides, neurogenesis has been discovered in other noncanonical regions such as corpus callosum, piriform cortex and amygdala, broadly extending the knowledge of neuronal fate determination[253-255].

In stem cell niches, there are various types of regulators influencing the behaviors of NSCs. They can be generally divided into intrinsic factors, extrinsic factors, neurotransmitters and cell-related interactions. Intrinsic factors include transcriptional factors, epigenetic modification and energy metabolism-induced genome changes that alter the NSCs' behaviors[256-261]. Growth factors, morphogens and cytokines are

extrinsic factors which mediate versatile functions via their receptors[230, 262-264]. Further, the functions of NSCs can be influenced by neurotransmitters from dopaminergic projections, serotonergic axons and cholineacetyl transferase-positive axons[265-267]. In addition, cell-cell and cell-ECM interactions help shape NSCs properties. Cell-cell interactions via adherence junctions and gap junctions can affect proliferation of NSCs through the control of substance exchanges[268, 269]. The ECM components, such as laminin, integrins and vascular cell adhesion molecule 1 (VCAM-1) are known to influence proliferation and differentiation of NSCs[270].

1.2.1.2 iPSCs

iPSCs are genetically modified stem cells for achieving pluripotency. They are obtained by infusion off our genes that encode transcription factors with genome in adult cells. The four genes consist of Oct4,Sox2, cMyc and Klf4[271]. iPSCs are promising since they are able to proliferate infinitely and differentiate into all the cell types. As the manipulating process does not involve embryos, it will be more feasible to apply iPSCs. Also, less immune response will be provoked when the host’s own iPSCs are utilized[272].

There are challenges in iPSCs studies. To begin with, the efficiency of iPSCs conversion is low, due to technical limitations. The conversion rates are around 0.01%-0.1%, although there are improvement recently with more precise genetic modifications[273, 274]. In addition, iPSCs exhibit a high risk of genetic and epigenetic aberrances, such as chromosomal abnormality, mutation and aberrant DNA methylation, leading to tumor formation that is a major safety concern in the

practice[275-277]. The reasons might be frequent derivation, viral integration, oncogenes activation and culture adaptation[278-281].

Due to translational potentials, iPSCs drew significant attention of researchers. Onorati *et al*. cultured iPSCs in conditioned medium to obtain NSCs which were proved to generate neurons, astrocytes and oligodendrocytes[282]. Chambers reported a method to induce the differentiation of iPSCs into neurons with high efficiency[283]. It is well recognized that BMPs inhibitors are important neural inducers by blocking small mothers against decapentaplegic (SMAD) signaling pathway. Based on this fact, they found the combination of noggin and SB431542 for dual-inhibiting SMAD pathway can effectively convert iPSCs to neural precursor cells and neurons. Similarly, SMAD dual-inhibition together with retinoic acid is reported for induction towards oligodendrocytes[284].

1.2.2 Stem Cell Transplantation Therapy

1.2.2.1 Cell Transplantation

Since stem cells such as NSCs and iPSCs have shown their biological versatility in survival, proliferation, differentiation and integration, transplantation of these cells can be an ideal strategy in treating neurodegenerative diseases. This method still faces many obstacles, for instance the low expansion rate, graft tolerance and inefficient integration. Preclinical and clinical studies have yielded complex effects. They exert not only cell replacement effect, but also bystander effects regulating the microenvironment and promoting function recovery[285].

1.2.2.1.1 Cell Replacement Effect

Neurologic disorders are usually progressing with the deterioration of cells in nervous system, leading to the damage of microenvironment structure and inability of functional integrity[286, 287]. As such, transplantation of NSCs is promising since it aids to compensate the cell loss in lesion sites and promote the integration of the newborn cells[288]. So far, the general outcome of this method in CNS disorders implies the possibility in therapeutic aim, but the efficiency is closely related with the cells to be regenerated and the microenvironment in lesion areas.

In fact, for purpose of cell replacement by cell transplantation, there ought to be limited or localized inability of intrinsic or extrinsic factors as the reasons for the damage, for example the conditions in PD, SCI and stroke[289-291]. Conversely, if the microenvironment of the nervous system disorders is extensively and persistently impaired as in multiple sclerosis (MS), the cell replacement effect would become rather restricted[292]. Structural complexity of the tissue to be restored is also an important factor affecting the cell replacement. Functional integration of the differentiated cells from transplantation appears to be better formed when there are neural circuits retained[293].

1.2.2.1.2 Bystander Effects

Transplantation of NSCs was originally considered to serve for the lost cell replacement. However, recent findings suggest that the transplanted NSCs exhibit bystander effects such as prohibiting pathogenic processes, restoring damaged tissue and modulating immune responses[294]. Therefore, transplantation of NSCs may play

a pivot role in treating disorders which are caused by diffuse inflammation or neurodegeneration following inflammation, for example, MS, PD and HD[295-297].

1.2.2.1.2.1 Immunomodulation

Upon the NSCs are transplanted in injured areas, the complicated interaction of intrinsic and extrinsic regulations will start to determine whether immunomodulation or cell replacement is more prominent. Even though there are many on-going human trials applying NSCs, it seems that replacement of lost cells and functional recovery in host has not yet been achieved. In fact, sufficient survival of NSCs and circuitry integration are rarely observed in human trials of CNS disorders[298]. In a successful transplantation therapy for a PD patient, mesencephalic tissue was applied and resulted in abundant survived implant and integrated circuitry. The transplanted tissue was found to activate immune cells for reconstruction and also negative effects[299]. Moreover, NSCs transplanted in intact mice brain lead to immune response either, bringing about suppressed neurogenesis and promoted gliogenesis[300].

However in other disorders where inflammation prevails, undifferentiated NSCs respond to the environment after being grafted by secreting chemokines, cytokines, neurotrophins, etc. for immunomodulation and trophic effects[301]. For example, in an EAE model, NSCs transplantation via intravenous (i.v.) or intracerebroventricular (i.c.v.) routes increases apoptosis of T cells due to the production of death receptor ligands, LIF, etc[302]. Similarly in postacute phase of stroke, activation of microglia and infiltration of inflammatory cells are robustly inhibited by i.v. injection of NSCs[303]. Ameliorated immune response is also detected in postacute phase of SCI

by transplantation of NSCs through i.t. and i.p. administrations[304]. Strikingly, the immune suppression outside CNS can be achieved by NSCs transplantation as well. In animal models of EAE and stroke, inflammation alleviation in organs outside nervous system such as spleen and lymph nodes, is detected following i.v. transplantation of NSCs. It is believed to be the inhibition of phosphorylation of signal transducer and activator of transcription 3 by LIF. Therefore Th17 cell differentiation may be inhibited[305].

1.2.2.1.2.2 Endogenous Repair

Apart from the immunomodulatory factors, transplanted NSCs also provide trophic support. Prevention of cell damage and restoration of functional integration in the involved CNS can be achieved via the secretion of regulating factors by undifferentiated NSCs. In CNS disorders, endogenous NGF, BDNF, CNTF and GDNF from NSCs protect cells from apoptosis and scar formation, and enhance the neuron-glia interaction and remyelination[301, 306-308].

Meanwhile, transplanted NSCs secrete not only trophic regulators, but also guidance molecules which are initially from developmental stage such as thrombospondins. The combination of these factors contributes to the enhanced dendritic arborization and axonal projections during the recovery of disorders[309]. Under specific situations such as in SCI model, transplanted NSCs are able to form gap junctions with the survived neurons and thus help rescue the impaired tissues[310].

1.2.2.2 Transplantation Therapy in Neurodegenerative Diseases

Neurodegenerative diseases are featured by degeneration of neurons in CNS and periphery nervous system (PNS). The structural and functional compromises of neurons are pronounced. Abrupt insults such as stroke can lead to acute neurodegeneration in the lesion site. Progressive deterioration of neurons occurs in chronic neurodegenerative diseases such as PD, HD, Alzheimer's disease (AD) and ALS[311]. Even though many studies try to illustrate mechanisms and treatments, fully understanding of the diseases and effective therapeutic strategies are still elusive, especially for chronic neurodegeneration.

In cell therapy, tissues or cells are transplanted to the recipients. The main effects include providing cells for substitution and improving the local microenvironment. For cell replacement, different types of neurons should be used for different neurodegenerative diseases so that they can synapse and reestablish the neuronal network[287]. On the other hand, microenvironment in the focal area is always involved. Diverse pathological factors such as free radicals, toxic protein components, glutamate and inflammatory factors will accumulate in the injury site and may thus hinder the reconstruction[312]. In this context, the neurotrophic factors depicted above may be able to enhance the microenvironment to favor the proliferation, differentiation and integration of the grafts. These effects are emphasized discrepantly in different neurodegenerative disorders. In general, cell replacement is more demanded for diseases in which specific types of neurons are impaired, such as PD; bystander effects are more favored for diseases which cause pronounced environment

deterioration such as MS[295].

1.2.2.2.1 PD

PD is featured by the malfunction and death of dopaminergic neurons in substantia nigra of midbrain in a progressive way. Patients suffering from PD develop the signs like rigidity, tremor and difficulty in walking and posturing[313]. Current therapy aims at the dopamine supplementing which is proved to be effective at the early phase for relieving symptoms. These supplements include precursor of dopamine, agonist and L-dopamine[314-316].

However, this therapy is only temporary due to the failure of targeting the cause of disease, and most of the drugs have side effects. Therefore, researchers have been focusing on the substitution of lost dopaminergic neurons. Tissues from midbrain were grafted for providing dopaminergic neurons. Although results varied from trial to trial, it appeared that tissue therapy will benefit PD patients to certain extent. The obstacles involved in tissue transplantation are the shortage of available tissues and ethical concerns[317]. Cell transplantation is obviously another strategy to avoid such shortcomings. Neurons derived from stem cells like embryonic stem cells, NSCs and iPSCs are abundant and verified to improve the functions in PD animal models[318-320].

Aside from the cell replacement, bystander effects are also shown to improve the functions of dopaminergic neurons. By means of injection or genome engineering, neurotrophic factors have been utilized to protect the neurons and improve their functions in animals[321, 322]. Therefore, both effects should be combined to achieve

the therapeutic goals in PD treatment.

1.2.2.2.2 AD

As a chronic neurodegenerative disease, AD accounts for the major portion of dementia. At the early phase, patients have the loss of short-term memory. With time going on, they will progressively develop deficits in speech, executive function, motivation and other behaviors. The main pathological features of AD are the extensive neuronal destruction and impaired interaction in different brain parts, with the exclusive hallmarks of Aβ plagues and neurofibrillary tangles[323, 324].

Clinical treatments for AD are limited. Improvement of cholinergic activity at early stage is effective on improving behavioral and cognitive functions. Stem cell therapy shows encouraging outcomes from animal studies. BDNF-expressing NSCs when grafted show improved incorporation, synaptic building and functional recovery[325]. NGF is effective for AD when it was generated by genetically engineered somatic cells. As such, transplantation of NSCs along with the expression of NGF are supposed to be advantageous in treating AD[326].

1.2.2.2.3 ALS

ALS usually occurs in adults with a gradual deterioration of motor neurons. Therefore, patients often progressively lose motion coordination because of weakness of muscle strength[327]. ALS involves diverse types of cells which are primarily motor neurons, but the mechanism is largely elusive. Traditional therapy is not able to deal with the multiple targets[328]. In this context, stem cell therapy showed extraordinary potentials since they not only provide cell source, but also improve the

microenvironment. In animal studies, NSCs and MSCs expressing multiple neurotrophic factors such as GDNF and IGF-1 protect motor neurons and alleviate their degeneration[329, 330]. Especially, GDNF supplement in distal axon proves to effectively support neuromuscular junctions structurally and functionally.

There are ongoing clinical trials applying NSCs in ALS patients. The transplanted NSCs in spinal cord are verified to integrate and interact with the local motor neurons. The injection route has always been in optimization but delivery through lumbar/cervical intraspinal approach appears to be safe[331, 332]. Notably, the aim of these studies is to support the residual neurons, making the therapy appropriate for patients at early stage.

1.2.2.2.4 HD

HD is a disease of dominant inheritance caused by a plethora of cytosine-adenine-guanine (CAG) repetitions[333]. Pathologically, there is a loss of medium spiny neurons within neostriatum. Initially, patients exhibit subtle abnormalities in mood and mental activity. As it advances, inability of coordination and steady gait occur. Eventually, patients develop involuntary body moments and difficulty in speaking[334]. However, a thorough understanding of disease mechanism remains unavailable.

Cell or tissue transplantation therapy is probably with the most potential for HD. Transplantation of ganglionic eminence to provide medium spiny neurons shows the transplanted cells are able to incorporate with local circuitry. The graft results in a temporary enhancement and stabilization of motor functions. Ethical problems and

tumorigenesis still restrain the application[335]. Stem cells have been demonstrated to be potent in restoring loss of medium spiny neurons. After being transplanted, NSCs have been shown to integrate and migrate as expected[336]. In some studies, NSCs were engineered to over-express GDNF and thus showed robust neuroprotective effects to enhance the recovery[337].

1.2.2.3 Expectations of Stem Cell Therapy and Cell Encapsulation

Neurodegenerative disorders have brought about huge burden on both the patients and the society[311]. Stem cell transplantation is becoming a promising therapeutic strategy for treating the diseases, as verified by abundant studies. On one hand, the grafted stem cells can replace the lost cells to reestablish the neural circuits. On the other hand, the microenvironment in injury sites can be improved by stem cell secretion to alleviate the damage from toxic factors on local cells[338].

Although there are a plethora of successful studies on stem cell therapies for neurodegenerative diseases across the world, effective treatments that meet clinical criteria are still rare. The reasons are complicated. Biologically, risk of tumorigenicity is a major hurdle that limits the application of stem cell transplantation in clinical trials since there is a long-term expansion associated with the implants[339]. Tumor growth has been detected in an ataxia telangiectasia patient receiving fetal NSCs therapy[340]. Besides, neuronal differentiation and functional incorporation are also critical issues. Cues for neurogenesis and directional guidance of axons are present only in a narrow time window in normal animal, not to mention in the regions affected in neurodegenerative disorders[285]. Also, studies show that NSCs isolated

from different regions exhibit biased differentiation preference. For example when grafted or cultured, NSCs from dorsal and ventral SVZ generate cell patterns which resemble to that in their original sites. The region-specific information may be coded in the transcription factors. In transplantation therapy, appropriate stem cells and lineage induction methods should be considered[341]. In clinical trials, ethical issue is still a concern in the utilization of fetal-derived cells and the vehicle injection in control group[342]. Additionally, there are always insufficient patients enrolled in trials due to the variant conditions in each individual, such as age, gender, heath conditions and disease phase[343]. Further, for these neurodegenerative diseases, it takes a long time to ascertain the efficacy of cell therapy in patients[291]. Because of these complicated problems, significant benefits from stem cell therapy are rarely acknowledged.

From the above, we have described the basic knowledge and applications of both single-cell encapsulation and stem cell therapy. The involvement of single-cell encapsulation into the cell transplantation is a promising approach to deal with the obstacles in the cell therapy studies. Firstly, biological benefits will be obtained. LbL single-cell encapsulation is supposed to provide a protective shell on cells. The multilayers can also be tailored to adjust the permeability to various adverse factors including apoptosis inducers, complements or inflammation cytokines, thus enhancing the survival of the cells. For example, GDNF-expressing cells encapsulated in alginate were transplanted into the PD model and sustained for 6 months[344]. Immune isolation was also exhibited to maintain the long-term survival of

transplanted cells into ventricles in an *in vivo* study[345]. In this context, there will be sufficient amount of stem cells that can differentiate to supply the lost cells and secrete to nourish the local environment. Secondly, ethic concerns will be hopefully avoided. Due to the heterogeneity of different diseases, the demand for appropriate stem cells varies and thus rises the concerns about tissue collection from some sources. With the application of cell encapsulation, functions of stem cells such as survival, proliferation and differentiation can all be tailored. Potentially, it brings about the reduced number in stem cells collection and narrows the scope of sources where the eligible stem cells are extracted. Last but not the least, other applications including stimulation reactivity, cell catalysts and live cell imaging are also able to be realized in the cell therapy with the aid of cell encapsulation[346-348]. Eventually, cell transplantation strategy will be improved from diverse aspects and boosted from bench to bedside.

Chapter 2. General Hypothesis and Objectives

2.1 General Hypothesis

LbL single-cell encapsulation enables regulator delivery and survival enhancement.

2.2 Specific Objectives and Rationales

2.2.1 Specific Objective #1:

The first part of the project is to

1) Establish an LbL single-cell encapsulation model on NSCs with gelatin and alginate.

2) Verify the biosafety of encapsulation on NSCs.

3) Construct a pH-sensitive delivery system of loaded IGF-1 to regulate NSCs functions.

Rationale of Specific Objective #1:

LbL technique has been proven to be a potent tool in every field including single-cell encapsulation[12]. Most of the studies were performed on non-mammalian cells, exhibiting diverse functions endowed from the encapsulation[349, 350]. However, the research about mammalian cells such as NSCs is rare.

The advantage of the LbL encapsulation is the establishment of a delicate microenvironment for NSCs, leading to the functional regulation such as proliferation and differentiation via the delivery of bioactive regulators[351]. The basis is the abundant reactive groups on the biomaterials for coupling with different neurotrophic

factors[352]. Construction of the microenvironment for cell regulation is of great importance to therapeutic approach in nervous system diseases. As it is acknowledged, following the onset of neurologic disorders and trauma, homeostasis of microenvironment around neuronal cells is impaired by different pathological processes such as apoptosis, oxidative stress and excitotoxicity[353]. As a result, normal functions of neuronal cells will be seriously affected, especially the grafted NSCs[354]. For example, Hu *et al*. found that spinal cord injury would result in the acidification of the microenvironment, thus causing death of neurons by the activation of the acid-sensing ion channels[355]. G-protein coupled estrogen receptor 1(GPER1) and N-methyl-D-aspartate receptor (NMDAR) are crucial for promoting the cellular functions through the microenvironment maintenance[356]. As such, LbL single-cell encapsulation as an approach to tune cells' microenvironment, is potentially capable of enhancing the functions of transplanted cells for better therapeutic efficacy.

The pH sensitivity of the biomaterials should be taken into considerations in treating nervous system diseases. In the focal areas of spinal cord injury and traumatic brain injury, pH of the microenvironment is lowered to 6.5 due to the acidification, which restricts the selection of materials[355]. According to literatures and in our experience, type A gelatin and alginate are an ideal pair of polycation and polyanion. Both are biodegradable with biocompatibility. Since the isoelectric point (IEP) of gelatin is around 7 to 9 and alginate around 5.4, they exhibit opposite charges in neutral solutions and interact firmly under pH 6.5[357, 358]. Based on this feature, steady encapsulation and controlled release are achievable.

2.2.2 Specific Objective #2:

The second part of the project is to:

1) Establish the LbL single-cell encapsulation on PC12 cells with gelatin and HA under different parameters.

2) Detect the permeability of encapsulation layers under different circumstances.

3) Verify the improvement of cell survival via the cell encapsulation.

Rationale of Specific Objective #2:

Fabricating multi-layers on single cell via LbL technique has been proven to be successful in cell surface engineering. Significant progress have been made in its applications including cell therapy, cell regeneration and cell sensors, owing to versatile features of biomaterials[359].

Nevertheless, permeability of the encapsulation layers is barely investigated. In the early study using PAH and PSS, it was observed that substances with high molecular weight might be blocked by the encapsulation[360]. In following investigations, shell thickness, pH, temperature and modification were all suggested to influence the permeability of molecules[361]. Recently, researchers applied advanced techniques to control the permeability of encapsulation, for example high-gravity field and bio-inspired mineralization[362, 363]. Unfortunately, these techniques and materials are inappropriate for mammalian cells due to their incompatibility with the cell membrane.

Understanding the permeability of encapsulation on mammalian cells is challenging but necessary. Apparently, the artificial “cell wall” generated from the encapsulation is unnatural to cells although the technique is verified to be safe. The main concern is the influence on substance exchange through the cell membrane. Whether molecules can transport inward or outward is controversial based on the existing studies[364].

Illustration of the permeability in LbL encapsulation structure is crucial. Homeostasis of the microenvironment containing various regulators is a prerequisite for NSCs’ normal functions such as proliferation and differentiation. For example, Wnt activates a complex that involves T cell factor (TCF), lymphoid enhancer factor and β-catenin for improving neurogenesis[365]. Maintenance of proliferation and inhibition of differentiation are regulated by bFGF and epidermal growth factor (EGF)[366]. Estrogen secreted by glia cells protects neuronal cells via recognition of G protein-coupled estrogen receptor[356]. These signaling pathways are initiated on the cell membrane through ligand-receptor interaction. Therefore, the permeability of encapsulation layers will likely affect biological functions of the regulators. Meanwhile, functional regulation is mediated by multiple regulators through complicated pathways. Evaluation of the influence by an individual factor is thus often difficult, especially in the *in vivo* studies. As expected, selective permeability could be achieved via the adjustment of encapsulation parameters and modification of materials, for exploration of specific substances[367]. For nervous system diseases and trauma, diverse pathological processes such as apoptosis, complement system and

excitotoxicity are involved[368]. Most of these are initiated via the contact of adverse factors with the cells, leading to downstream incidents. In this context, LbL single-cell encapsulation could act as a protective mechanism for cells, which is especially applicable in cell transplantation therapy.

Among the detrimental factors, TNF-α is an appropriate model. It belongs to the extrinsic apoptotic factors and is expressed by immune cells in almost all the nervous system disorders. TNF-α binds to tumor necrosis factor-receptor 1 (TNF-R1) to recruit inhibitor of apoptosis proteins (IAPs), TNF receptor-associated factors (TRAFs), receptor-interacting protein 1 (RIP1), and TNFR-associated death domain protein (TRADD) for producing the complex called TRADD-dependent complex I. Next, complex II a/death-domain-containing proteins (DISC) is formed and then leads to thecaspase-3/8 cleavage which causes the apoptosis[369]. Single-cell encapsulation layers are supposed to provide a barrier to prohibit the diffusion of TNF-α, thus the activation of apoptotic pathway is decreased and cell survival is preserved.

Chapter 3. Materials and Methods

3.1 Materials

bFGF (catalog no. 100−18B), EGF (catalog no. AF-100−15), Neurocult proliferation medium(catalog no. 05771), neurobasal medium (catalog no. 21103049), andB27 supplement (catalog no. 17504-044) were obtained from Cedarlane, Ontario, Canada.Gelatin (catalog no. G2625), alginate (catalog no. A2158), poly-D-lysine (PDL; catalog no. P6407), PEI (catalog no. P3143), chitosan (catalog no. 50494), fluorescein 5(6)-isothiocyanate(FITC; catalog no. F3651), rhodamine B (catalog no. 283924), ethanediamine(catalog no. 00589), EDC (catalog no. E6383), BSA (catalog no. A2153), FITC-dextran (FD) (catalog no. 46944; FD20S, FD40 and FD250S), proximity ligation assay (PLA) kit (catalog no. DUO92101), Hoechst 33258 (catalog no. 94403), propidiumiodide (PI; catalog no. P4170), bromodeoxyuridine (BrdU; catalog no. B5002), and anti-BrdU (catalog no. B2531) were obtained from Sigma-Aldrich, Ontario, Canada. HA was purchased from Freda Biopharm, China. TNF-α (catalog no. 400-14) was obtained from Peprotech, New Jersey, U.S. 3-(4,5-Dimethylthiazol-2-yl)-2,5-diphenyltetrazoliumbromide (MTT; catalog no. 30006) and Phallodin CF488A (catalog no. 00042) were obtained from Biotium, California, U.S. Bicinchoninic acid (BCA) kit (catalog no. 23225), cDNA synthesis kit (catalog no. K1641) and SYBR Green quantitative real-time polymerase chain reaction (qPCR) kit (catalog no. F-415) were obtained from Thermo Scientific,

Massachusetts, U.S. Protein G magnetic beads (catalog no. 1614023) was obtained from Bio-rad, Ontario, Canada. Anti-microtubule-associated protein-2 (anti-MAP-2; catalog no. sc-20172), anti-β-tubulin III (catalog no. sc-51670), anti-glial fibrillary acidic protein (anti-GFAP; catalog no. sc-6170), anti-nestin (catalog no. sc-33677), anti-β-actin (catalog no. sc-69879), anti-TNFR1 (catalog no. sc-8436) and TNF-α antagonist (catalog no. sc-358755) were obtained from Santa Cruz, Texas, U.S. Anti-TNF-α (catalog no. ab6671) was from Abcam, Ontario, Canada. Secondary antibodies for immunofluorescence staining and TRIzol reagent (catalog no. 15596−026) were obtained from Invitrogen, Massachusetts, U.S. Secondary antibodies for Western blot and IGF-1enzyme-linked immunosorbent assay (ELISA) kit (catalog no. MG100) were obtained from R&D Systems, Minnesota, U.S. IGF-1 protein (catalog no. 01-208) and IGF-1 antibody (catalog no. 05−172) were obtained from Millipore, Ontario, Canada. Oligonucleotides for real-time PCR were synthesized by Invitrogen, Massachusetts, U.S.

3.2 NSCs Isolation and Culture

NSCs were extracted from E15.5 embryos of pregnant mouse (provided by Animal Center of University of Manitoba). Mouse was anesthetized with 5% isoflurane and then euthanized. The mouse was placed on a pad and sprayed with 70% alcohol on the abdominal skin. The skin was held with tweezers and the V-shaped incision was made with scissors. The skin was then isolated apart and muscles were cut by sterilized scissors. A chain of embryo sacs was exposed and extracted to be transported in a dish with cold Hank’s balanced salt solution (HBSS). The brains of embryos were

dissected out with another pair of sterile scissors and placed in a dish containing HBSS. After careful removal of the midbrain, hindbrain and meninges, the cortices and hippocampus were washed three times with cold HBSS, and then cut into small pieces with a scalpel. They were collected in a 15 ml tube and added with 5 ml of accutase. The tube was placed in the water bath at 37 ℃ for 5 min. The mixture was then pipetted for 20 to 30 times to shatter the undigested blocks and filtered through a 70 μl filter. The filtered mixture containing NSCs was centrifuged at 1200 rpm for 7 min. The supernatant was discarded and the cells were seeded in plates with low attachment, which were maintained in a 5% CO2/95% air incubator with 100% humidity. The medium was replaced every 3 days.

3.3 LbL Single-cell Encapsulation

Cell suspension of 2×10^6 cells was put into a 15 ml centrifuge tube. The tube was centrifuged and supernatant was discarded. Then 1 ml of 0.1% gelatin solution was added to resuspend the cells. The tube was gently shaken for 10 min. The suspension was next centrifuged at 2000 rpm for 5 min and the supernatant was aspirated. In the next washing step, the cell pellet was gently disassociated with 5 ml of Dulbecco's phosphate-buffered saline (DPBS), followed by another centrifuge and supernatant discard. After washing the cells for three times, 1 ml of 0.1% alginate (or HA) was added to the cell pellet for 10 min. The process was repeated for predetermined times in each experiment by alternatively adding polycation and polyanion to achieve the LbL single-cell encapsulation.

3.4 Cell Viability Test with Hoechst/PI Staining

Firstly, 0.1% solutions of alginate, gelatin, chitosan, PEI, and PDL were prepared. After the LbL assembly on NSCs was accomplished with alginate and different polycations, these different groups of NSCs were rinsed with cold DPBS solution thoroughly for three times. A fresh 1:1000 dilution of Hoechst 33258 stock in DPBS (Final concentration was 0.12 μg/ml) was added. The solution was incubated in the dark for 15 min at room temperature. After it was rinsed for three times with DPBS, a 1:1000 dilution of PI (final concentration was 2 ug/ml) was added. The solution was again incubated in the dark for 3 min at room temperature, followed by DPBS rinsing for about three times. Finally, the samples were observed on a fluorescence microscope (TE2000-E, Nikon). Images taken from ten random fields were used for analysis.

3.5 MTT Assay

NSCs and LbL-NSCs were seeded at the density of 1×10^4 per well in a 96-well plate which was coated with 0.01% PDL. The medium was replaced every 3 days. At time points 0, 1, 3, and 6 days, 10 μl of MTT was added to each well and the plate was incubated in an incubator for 4 h. Then the solution was removed, followed by the addition of 200 μl of dimethyl sulfoxide (DMSO) to each of the wells. Afterwards, the plate was placed on a shaker to dissolve the precipitate gently and consistently for 10 min. The absorbance was examined at the wavelength of 570 nm with a multilabel plate reader (Model No. 1420, Wallac).

3.6 Preparation of Fluorescent Reagents with Gelatin and Alginate

To prepare the gelatin-FITC, 20 mg of gelatin was fully dissolved in 2 ml of 0.1 M sodium bicarbonate buffer. 10 mg of FITC was dissolved in 1 ml of DMSO at the same time. While magnetically stirring the gelatin solution, FITC solution in DMSO was slowly added. The reaction was incubated overnight at room temperature with continuous stirring. Then, the mixed solution was dialyzed against dialyzing buffer which was changed every 4 h for 3 days and lyophilized. For the alginate-rhodamine B, ethanediamine was used as a bridge for binding alginate and rhodamine B since they lack reactive amino groups. 10 mg of alginate in 1 ml DPBS was activated by 10 mg of EDC for 30 min. Then 3 mg of ethanediamine was added and the mixture was stirred overnight at room temperature. After the solution underwent dialysis and lyophilization, alginate-ethanediamine powder was obtained. Then the powder was put into 2 ml of rhodamine B solution (2.5 mg/ml in DPBS). The resultant solution was stirred overnight at room temperature. Therefore the alginate-rhodamine B was obtained after dialysis and lyophilization.

3.7 Fluorescence Intensity of LbL Encapsulation

2×10^6 NSCs were taken and encapsulated with gelatin-FITC and unmodified alginate according to the protocol described above. After the encapsulation, LbL-NSCs with different number of layers and the uncoated NSCs were grafted in the 96-well plates with 1×10^4 in each well, and the cell suspension was then diluted to 100 μl with DPBS. Next, fluorescence intensity was examined using a multilabel counter (1420, Wallac) at the excitation wavelength of 490 nm.

3.8 Transmission Electron Microscopy (TEM)

Cells for TEM were processed as described previously[370]. Untreated cells and cells encapsulated with different parameters were directly fixed in the solution of 2.5% glutaraldehyde that was diluted with 0.1 M Sorensen's buffer for 1 h. Then the samples were washed with 5% sucrose solution which was prepared in 0.1 M Sorensen's buffer, for 5 min×3 times and put into a refrigerator at 4 ℃ overnight. Postfixation was processed by adding 1% OsO_4 to the cell samples for 2 h. After being dehydrated with 30%, 50%, 75%, 90% and 100% ethanol and methanol for 10 min × two times, samples were embedded in epoxy resin, followed by drying in an oven at 60 ℃ for 24 h. A microtome (Model No. 318423, Reichert Nr.) was used to obtain the thin sections, which were further mounted on copper grids. Finally, 2% uranyl acetate and 1% lead citrate were used to stain the samples for 2 h. These prepared grids were analyzed with a TEM (CM-10, Philips) at 25 ℃.

3.9 Zeta-Potential Assessment

NSCs at the density of 2×10^6 were nanocoated with gelatin and alginate, as described above. The same amount of untreated NSCs, NSCs encapsulated with gelatin, gelatin/alginate, and $(gelatin)_2$/alginate was taken respectively and then the zeta-potential was determined by the instrument (Brookhaven).

3.10 Scanning Electron Microscopy (SEM)

NSCs and LbL-NSCs at time points 1, 3, 5, and 7 days were fixed in 0.1 M Sorensen's buffer containing 2.5% glutaraldehyde for 2 h. Then the samples were rinsed with 0.1 M Sorensen's buffer which contained 5% sucrose for 5 min×3 times.

Next, 1% OsO_4 was added to the cell samples for 2 h at 4 ℃, followed by three cycles of washing. After being dehydrated with 30%, 50%, 75%, 90% and 100% ethanol and drying, the samples were sprayed with gold prior to the observation with a SEM (JEOL 5900).

3.11 Loading Efficiency of IGF-1 on Alginate

Different amount (10ng, 100ng and 1000ng) of IGF-1 was mixed with 1ml 0.1% alginate for 24h and put in to a dialysis bag (for molecular weight 13,000D). Sample from the dialysis bag was taken to test the IGF-1 with the IGF-1 ELISA kit every day (three days in total). 100ng IGF-1 in 1ml of DPBS solution acted as the control. The unbound IGF-1 would leak from the bag, so that the ELISA result would indicate the amount of loaded IGF-1 on the material.

3.12 Atomic Force Microscopy (AFM)

Untreated cells and cells encapsulated with different parameters were seeded on cover slides and were observed under the atomic force microscope (EasyScan 2, NanoSurf). All samples were scanned under the “Phase contrast” mode with 2.5 s/ line and 512 points/ line. After obtaining the images at lower magnification, an area of around 25 μm^2 on cell surface was focused to scan under a higher magnification. Furthermore, average roughness value (indicated as S_a which was calculated by the software) per 1 $\mu m^2$was obtained by selecting 10 spots randomly on each cell.

3.13 FITC-dextran (FD) Permeability Investigation

PC12 cells were encapsulated with gelatin and HA with different parameters. 0.5 ml of 1 mg/ml FD with different molecular weights were then incubated with cells in

medium with varying pH for 30 min. After the incubation, cell samples were washed with DPBS for three times. Samples were examined under the fluorescent microscope (Axio Imager Z.2, Zeiss). Intensity of the fluorescence was detected by a plate reader (Model No. 1420, Wallac) at the excitation wavelength of 490 nm by diluting 1×10^4 cells to 100 μl in a 96-well plate as addressed above.

3.14 Proximity ligation assay (PLA)

TNF-α (20 ng/ml) was incubated with cells in control group and encapsulation groups for 5 min. Fixation of cells was immediately performed by applying 4% PFA, followed by DPBS washing for three times. Duolink blocking solution was used to block samples for 30 min under 37 °C. Next, blocking buffer was discarded and primary antibodies were added to incubate for 1 h at 37 °C. After washing, PLA probes were added to samples for 1 h at 37 °C and subsequently, cells were incubated with ligation solution for 30 min at 37 °C. Finally, samples were treated with polymerase in amplification solution followed by Hoechst staining and mounted on slides. Images were taken by the fluorescent microscope (Axio Imager Z.2, Zeiss), in which the red dots represented for the direct interaction of TNF-α and TNF-R1.

3.15 Immunofluorescence

Cells grown on the coverglasses in the plate were taken and fixed in 4% PFA for 15 min at 4 ℃. Then they were rinsed with DPBS for 5 min×3 times, and 0.25% TritonX-100 in DPBS (TBST) was added to permeabilize the cells for 10 min. The samples were incubated with 1% BSA in TBST for 30 min to block the unspecific binding. Next, the cells were incubated with primary antibodies in DPBS containing

1% BSA overnight at 4 ℃. On the following day, after being rinsed three times with DPBS (5 min each), the cells were incubated with secondary antibodies for 1 h in the dark at room temperature. The mixture of the secondary antibody solution was decanted, and the cells were rinsed with DPBS for 5 min×3 times in the dark. The cells were stained with 0.12 μg/mL Hoechst 33258 in DPBS for 1 min in the dark and rinsed with DPBS. Finally, the cells were mounted on coverslips with a drop of mounting medium. The primary antibodies used were as follows: BrdU (mouse, 1:500), MAP-2 (rabbit, 1:1000), β-tubulin III (mouse, 1:500), GFAP (goat, 1:2000), and nestin (mouse, 1:1000). Secondary antibodies were as follows: Alexa-488 conjugated chicken anti-mouse (catalog no. A21200, 1:1000), Alexa-488 conjugated rabbit anti-goat (catalog no. A11028, 1:1000), Alexa-594 conjugated rabbit anti-mouse (catalog no. A11062, 1:1000), Alexa-594 conjugated chicken anti-mouse (catalog no. A21201, 1:1000), and Alexa-488 conjugated goat anti-rabbit (catalog no. A11034, 1:1000). Images of 10 random fields were taken with a fluorescent microscope (TE2000-E, Nikon), and positive cells were quantified systematically.

3.16 Real-Time PCR

The total RNA of NSCs and LbL-NSCs was extracted with the TRIzol kit. Then, the reverse transcription was operated to synthesize cDNA. Quantitative real-time PCR was processed for the amplification of cDNA target with the ABI 7500 qPCR system (Applied Biosystems, Foster City, CA) following the manufacturer's recommendations. Glyceraldehyde 3-phosphate dehydrogenase (GAPDH) mRNA was used for normalization. Sequences of primers are included in Table 1.

3.17 Western Blot Analysis

NSCs and LbL-NSCs were grafted on 0.01% PDL coated 6-well plate at the density of 3×10^5 per well. The cells were cultured in proliferation medium for 1 day, and the medium was replaced with neurobasal medium containing B27 supplement for 3 and 6 days. The cells were treated with radio immunoprecipitationassay (RIPA) lysis buffer containing protease inhibitor cocktail to extract the total protein. Protein concentration was determined with a BCA kit. Then, the samples (20 μg of each) were loaded per lane on sodium dodecyl sulfate-polyacrylamide gel electrophoresis (SDS-PAGE) gel (10% acrylamide) and subjected to immunoblotting. The primary antibodies were as follows: MAP-2 (rabbit, 1:1000), nestin (mouse, 1:2000), β-actin (mouse, 1:3000). Secondary antibodies used included: horseradish peroxidase (HRP)-conjugated goat anti-rabbit (catalog no. HAF008, 1:3000), and HRP-conjugated donkey anti-mouse (catalog no. HAF018, 1:3000). The results were quantified using QuantityOne software (Bio-Rad).

3.18 Co-immunoprecipitation (Co-IP)

TNF-α (20 ng/ml) was added in control group and encapsulation groups. After 5 min of incubation, cells were washed with cold DPBS for three times, followed by being lysed for 20 min in lysis buffer (150 mM of NaCl, 50 mM of pH 7.4 Tris-HCl, 5 mM of EDTA, 0.1% of NP-40, and protease inhibitor cocktail). After the magnetic beads were rinsed with PBST containing 0.1% Tween 20 for three times, 2 μg of antibodies of TNF-α and TNF-R1 were incubated with beads separately for 10 min. Cell lysate was incubated with the antibody-loaded beads, with 100 μl for each. The

mixture was rotated for 1 h at room temperature. The protein-loaded beads were then magnetized and washed, followed by elution with 6×Laemmli buffer for 10 min at 70 ℃. The eluent was moved to new tubes and ready for SDS-PAGE. Input samples were extracted immediately after the lysis of cell samples and denatured for 5 min at 95 ℃. Samples were loaded on SDS gel (12% acrylamide) and then performed Western blot. The primary antibodies were: TNF-α (rabbit, 1:500), TNF-R1 (mouse, 1:300). Secondary antibodies used included: HRP-conjugated goat anti-rabbit (1:5000) and HRP-conjugated donkey anti-mouse (1:5000). The results were quantified with Image Studio software (LI-COR Biosciences).

3.19 ELISA Assay

NSCs encapsulated with gelatin and IGF-1-loaded alginate were grafted in the medium with pH 7.4 and 6.5 separately. At the time points 24, 48, 72, 96, 120, 144, 168, 192, 216, and 240 hours, 50 μl of each sample was taken to add to the ELISA microplate, which was coated with anti-IGF-1. They were left for antigen-antibody reaction for 2 h. After being washed with washing buffer for five times, the conjugation solution was added to each well for 2 h. After the washing step, substrate solution was pipetted into the plate for 30 min in the dark. Finally, immediately after adding the stop solution, a multilabel counter (Model No. 1420, Wallac) was used to determine the optical density at the wavelength of 450 nm. Therefore, the cumulative release curve would then be obtained.

3.20 Statistical Analysis

Means plus or minus the standard error of the mean were used to express the values.

The expression of the error bars was the standard error of the mean. Analysis of variance (ANOVA) in the study was used to compare different groups with Tukey HSD in post-hoc. Difference was considered to be significant when the P value was less than 0.05.

Chapter 4. Results (Specific Objective #1)

4.1 Safety of LbL Single-cell Encapsulation on NSCs

NSCs were encapsulated, as shown in Scheme 1. The polycation and polyanion attached to each other in a layer-by-layer way due to the interaction of the opposite charges. In the end, the NSCs had multiple layers of materials on the cell surface. The polyelectrolytes we used in this research were gelatin and alginate. Gelatin, derived from collagen, was a cell-compatible protein similar to native ECM and presented polycation properties under appropriate conditions[371]. The polyanion alginate was also biocompatible and widely used in tissue engineering, especially in the central nervous system[372]. As such, gelatin and alginate are both biocompatible natural polymers and ideal polyelectrolytes for LbL encapsulation. NSCs were encapsulated in a polycation−polyanion−polycation way, marked as $(\text{polycation})_2$/polyanion. In the viability test (Figure 1), Hoechst/PI staining was applied to show the viability of cells in different groups because the Hoechst could permeate cell membrane to bind to minor groove of DNA; PI, as an impermeable fluorescent reagent, is known to only bound to DNA in dead cells. It showed a viability of 10.4, 7.5, 13.7, 92.3, and 96.5%, respectively, in PEI, PDL, chitosan, gelatin, and untreated group after counting the percentage of live cells in 10 random fields of each group, indicating that gelatin was anamicable polycation to NSCs, unlike other synthetic polycations which would compromise the cell membrane[81, 373]. In Figure 2, the cytotoxicity of LbL encapsulation with $(\text{gelatin})_2$/alginate was further confirmed by the MTT assay.

LbL-NSCs and NSCs showed similar MTT absorbance on day 0, 3, and 6, revealing that the LbL encapsulation would not influence the NSCs viability significantly in a dynamic period. In short, gelatin and alginate are suitable for LbL encapsulation of NSCs.

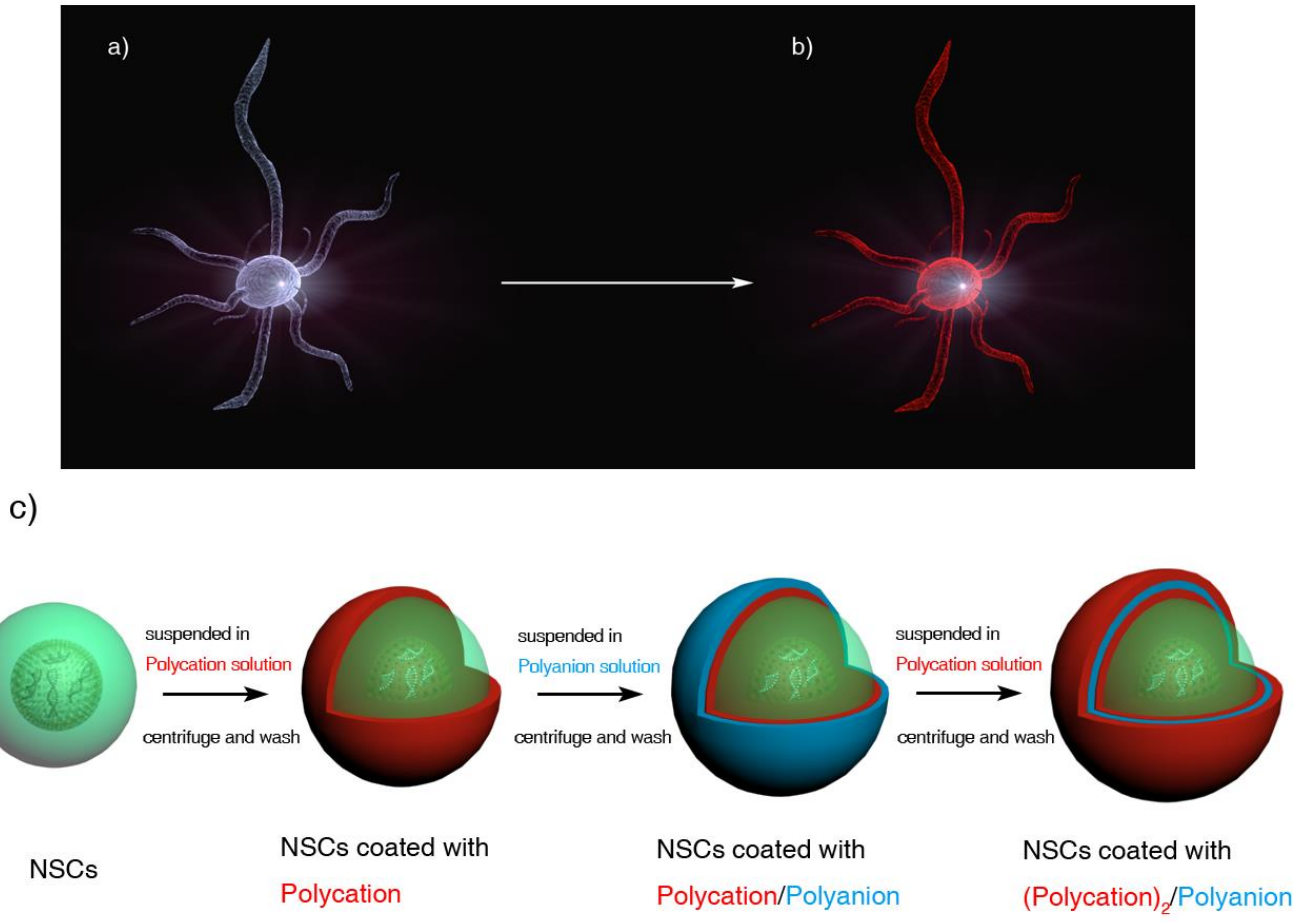

Scheme 1. The scheme of LbL encapsulation. The objective of the LbL encapsulation was to build a single-cell encapsulation model by coating nano materials on the cell surface. Specifically, a natural cell (a) was converted to a surface-modified cell (b) which was endowed with potential for further applications. The illustration of the major steps involved in the LbL encapsulation was shown in (c).

NSCs were firstly suspended in the polycation solution and then centrifuged and washed. The polycation layer would attach to the cell surface. Next, the polycation-coated NSCs were put in the polyanion solution to add a second layer. In the end, the LbL encapsulation would be completed after several repeats.

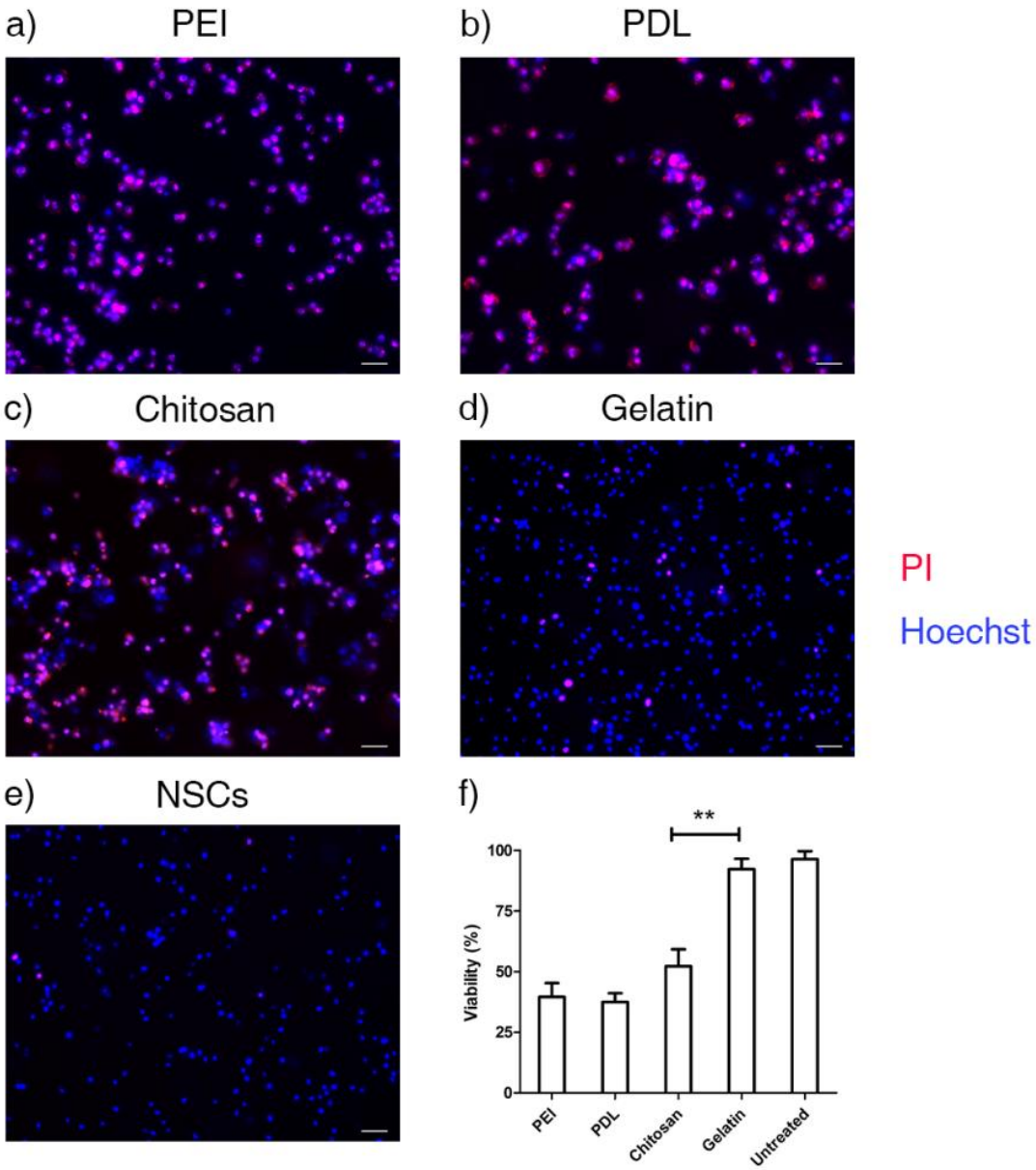

Figure 1. Cell viability of NSCs encapsulated with different polycations by

Hoechst/PI staining. a)-e) Hoechst/PI staining of NSCs encapsulated with $(PEI)_2$/alginate, $(PDL)_2$/alginate, $(chitosan)_2$/alginate, $(gelatin)_2$/alginate and untreated NSCs. Cells with dark blue were viable cells; cells with bright blue and red were apoptotic and necrotic cells. Scale bar in (a)-(e): 50μm. f) Quantification of viability of NSCs in different groups. **: $p<0.01$.

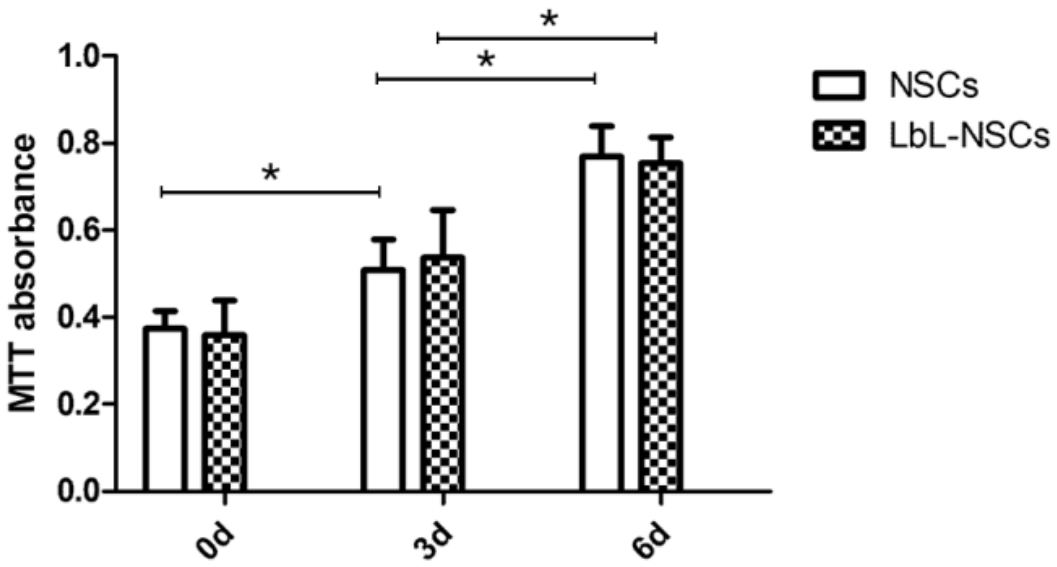

Figure 2. MTT test of NSCs and LbL-NSCs at different time points. NSCs encapsulated with $(gelatin)_2$/alginate and untreated NSCs were cultured in a 96-well plate with three repeats (n=3). On the 0d, 3d and 6d of the culture, MTT was added and the absorbance was measured. *: $p<0.05$.

4.2 Characterization of LbL Single-cell Encapsulation

Gelatin-FITC and alginate-rhodamine B were employed to enable us to visualize the LbL encapsulation on NSCs,(Figure 3a−c). A lower magnification of the general view of NSCs encapsulated with $(gelatin\text{-}FITC)_2$/alginate was also exhibited (Figure 3d). Fluorescence intensity of varied layers of gelatin-FITC was measured as an

alternative characterization (Figure 3e). The fluorescence intensity of one layer of gelatin-FITC was much higher than that of untreated NSCs. When the original alginate was coated on gelatin-FITC, the intensity showed some extent of decline. The reason was probably the fluorescence blocking by the added alginate layer. When another layer of gelatin-FITC was added, the intensity increased distinctly. The 3D scanning of a single NSC encapsulated with $(\text{gelatin-FITC})_2$/alginate also confirmed the feasibility of encapsulation (Figure 4). TEM further demonstrated LbL coating on NSCs (Figure 5a) and the untreated NSCs (Figure 5b). The material layers around cells were around 6 ± 2.3 nm as calculated by ImageJ, which agreed with other reports[40, 90].

Zeta-potential test, a common measurement of LbL self-assembly, was performed to obtain the change of the potential of cells with varied layers of materials (Figure 6). When the negatively charged NSCs were encapsulated with gelatin and alginate subsequently, the zeta-potential changed accordingly since the oppositely charged polyelectrolytes were able to bind together and overcompensate for each other[374].

The persistence of the materials on the surface of NSCs was observed by encapsulating NSCs with gelatin-FITC and alginate (Figure 7). The persistence time should be noted since any application of LbL nanocoating required the persistence of materials for a period of time. Figure 7 showed the decrease of the fluorescence, which marked gelatin on the cell surface with time going on from 1 to 10 days. As a result of this observation, it indicated that the encapsulation would be able to persist for about 10 days, providing sufficient time for most applications. The encapsulated

cells could still contact each other as observed. The reason might be that the materials were biocompatible and biodegradable, and only three layers of materials with low concentration were used.

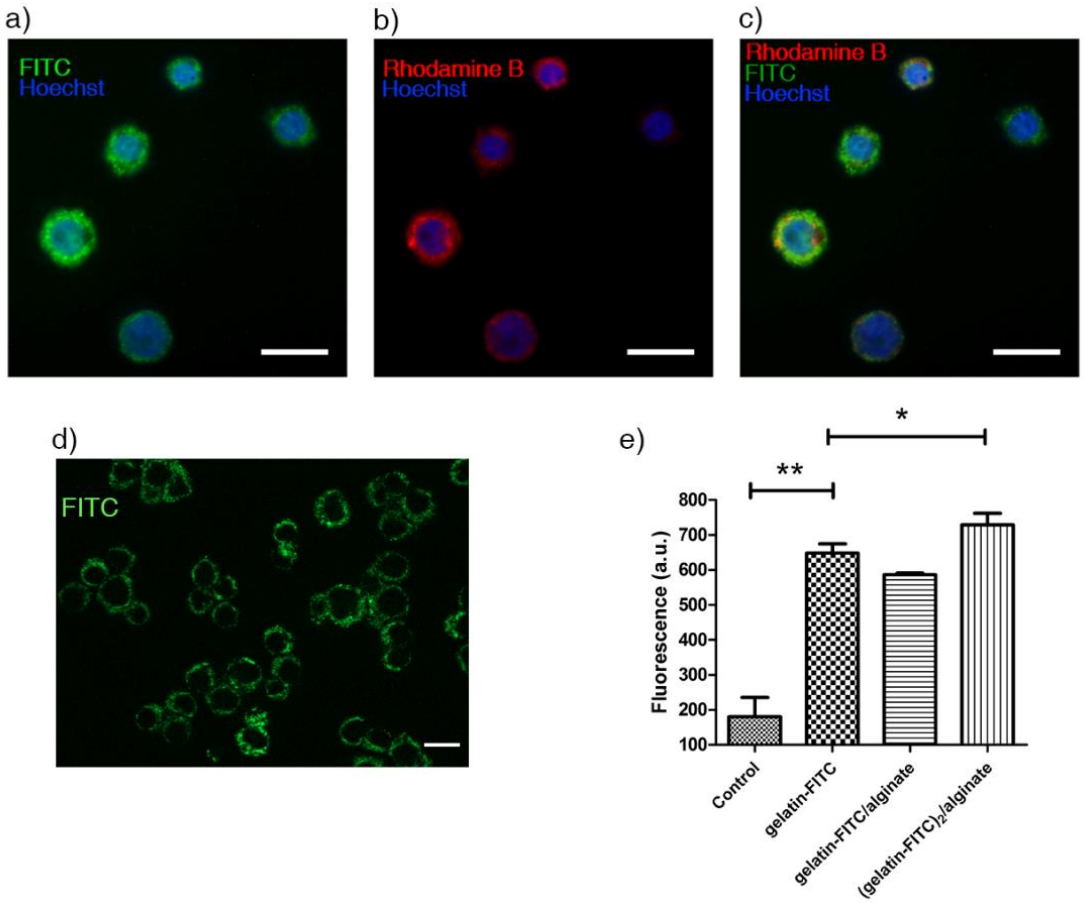

Figure 3. Characterization of LbL encapsulation with fluoresceins labeling. a)-c) Gelatin was conjugated with FITC, while the alginate was conjugated with rhodamine B. NSCs were LbL-coated with these materials, so gelatin-FITC (a) and alginate-rhodamine B (b) could be detected. c) Merged image of (a) and (b). d) A lower magnification of FITC-gelatin and alginate encapsulated NSCs. Scale bar in (a)-(d): 10μm. e) The fluorescence intensity of different layers of gelatin-FITC was measured. Untreated NSCs, NSCs encapsulated with gelatin-FITC,

gelatin-FITC/alginate and (gelatin-FITC)$_2$/alginate were taken to measure the fluorescence intensity which acted as an alternative way of characterization. *: $p<0.05$; **: $p<0.01$.

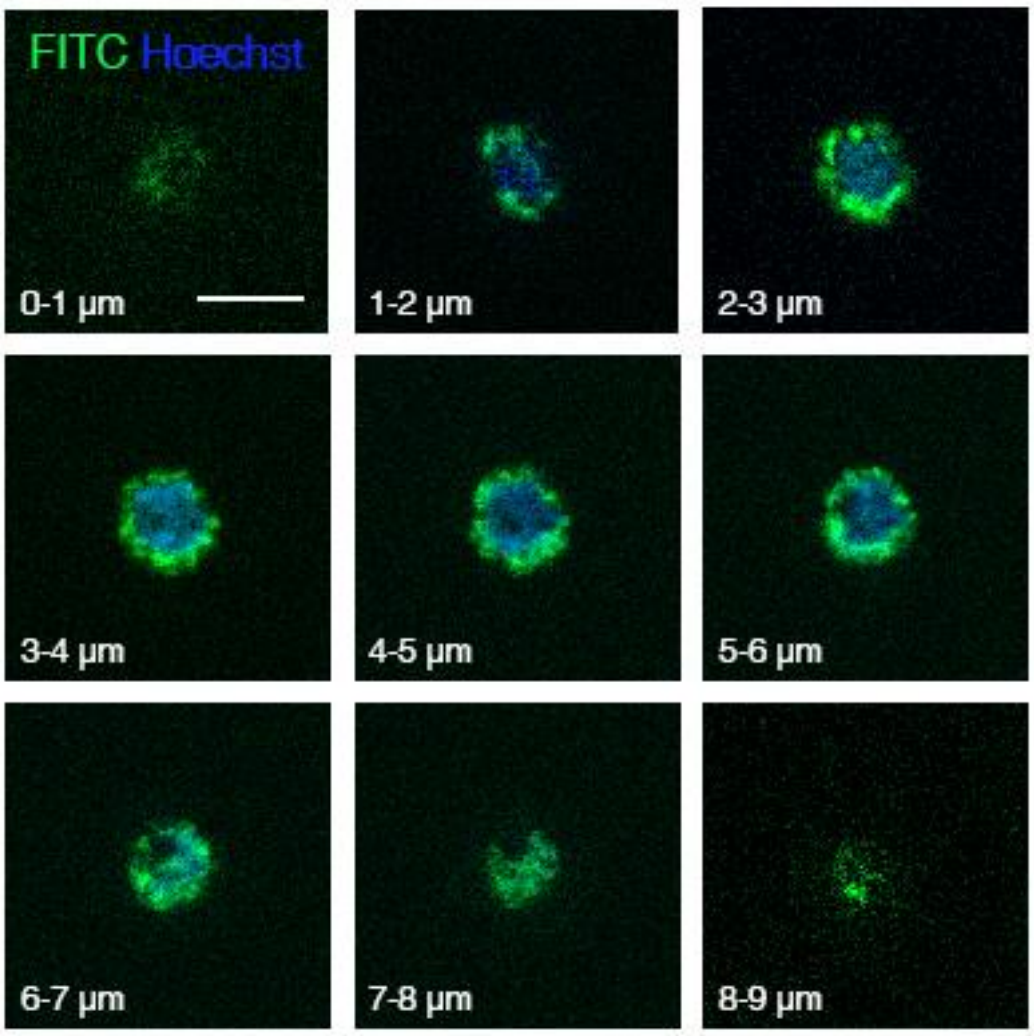

Figure 4. 3D scanning sections of LbL encapsulated cells. NSCs were encapsulated with FITC-gelatin and alginate. Under the Zeiss Apotome imaging system, homogenous encapsulation of NSCs was observed through the 3D scanning. (Green: gelatin; blue: Hoechst). Scale bar: 10μm.

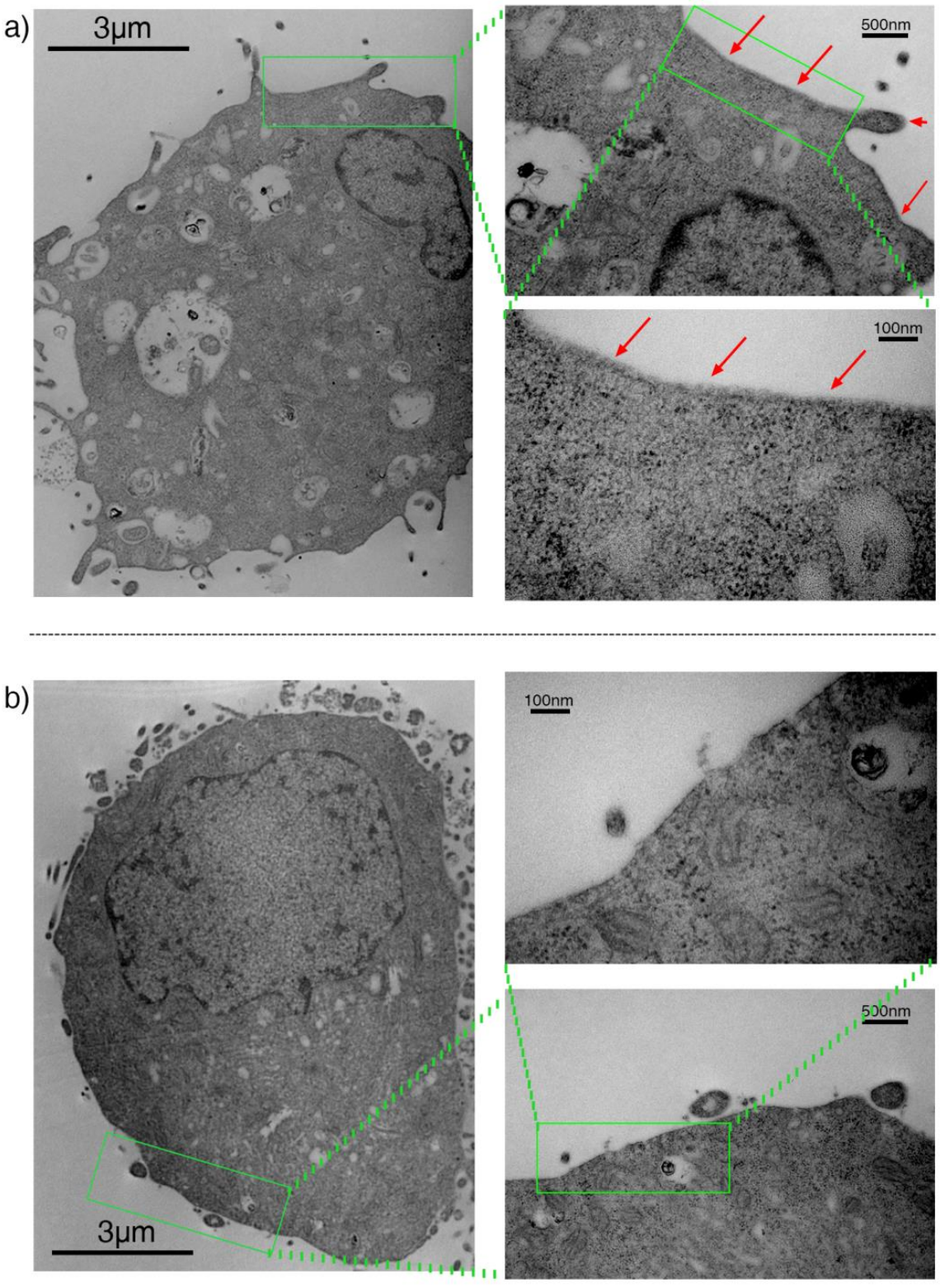

Figure 5. Characterization of LbL encapsulation with TEM. a) Different magnification of TEM images of (gelatin)$_2$/alginate encapsulated NSCs. b) Different

magnification of TEM images of untreated NSCs. Arrows indicated the materials on the cell surface.

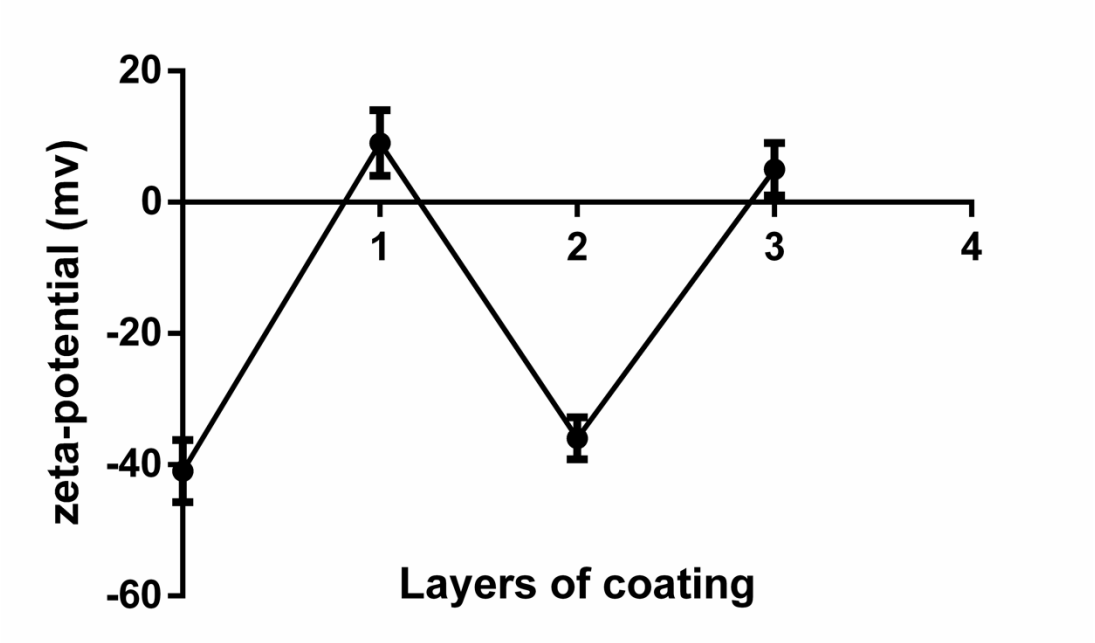

Figure 6. Zeta-potential assessment of NSCs nanocoated with different layers of materials. The zeta-potential of untreated NSCs, NSCs nanocoated with gelatin, gelatin/alginate and $(gelatin)_2$/alginate (marked from "0" to "3" on the x-axis) was shown.

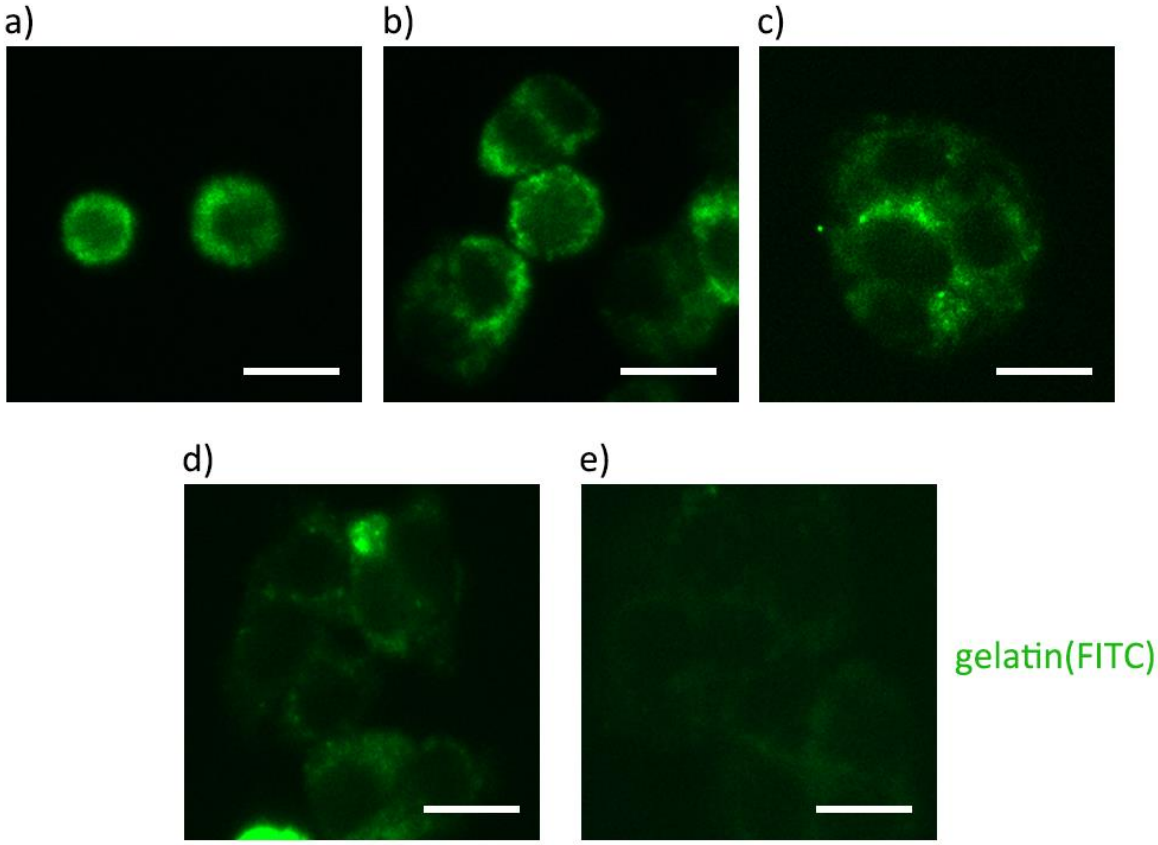

Figure 7. Persistence of coated materials. NSCs were encapsulated with gelatin-FITC (green) and alginate. At the time point 0d, 1d, 3d, 7d and 10d (a-e), the existence of biomaterials on the cell surface was characterized by means of a fluorescent microscope. Scale bar in (a)-(e): 10μm.

4.3 Morphologic Changes of Encapsulated NSCs

For morphology evaluation, SEM was performed to observe the NSCs and LbL coated NSCs on day 1, 3, 5, and 7 (Figure 8a). LbL coated NSCs showed spheroid-like morphology while the untreated NSCs stretched broadly. F-actin staining by phalloidin showed the effect of encapsulation on NSCs cytoskeleton compared with that of untreated NSCs (Figure 8b). On day 1, 3, and 7, the

cytoskeleton of encapsulated NSCs was much more restrained than that of untreated NSCs. Spreading area of each cell stained with phalloidin was calculated with the help of ImageJ. In Figure 8c, the area of NSCs at any time point was distinctly broader than that of LbL-NSCs. The versatile methods of characterization of LbL encapsulation above proved that LbL coating on NSCs was indeed existent and demonstrated the morphological changes of coated NSCs compared with untreated ones.

a)

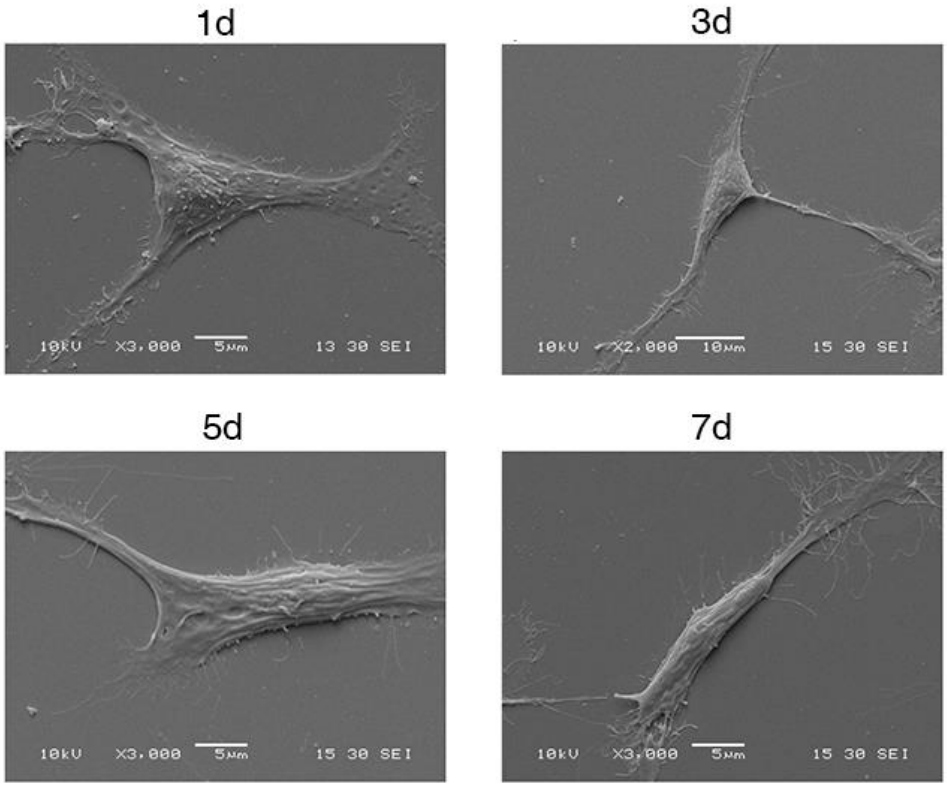
1d
3d
NSCs
5d
7d
10kV X3,000 5μm 13 30 SEI
10kV X2,000 10μm 15 30 SEI
10kV X3,000 5μm 15 30 SEI
10kV X3,000 5μm 15 30 SEI
1d
3d
LbL-NSCs
5d
7d
20kV X3,000 5μm 10 50 SEI
20kV X3,000 5μm 10 50 SEI
20kV X3,000 5μm 10 50 SEI
20kV X3,000 5μm 12 50 SEI

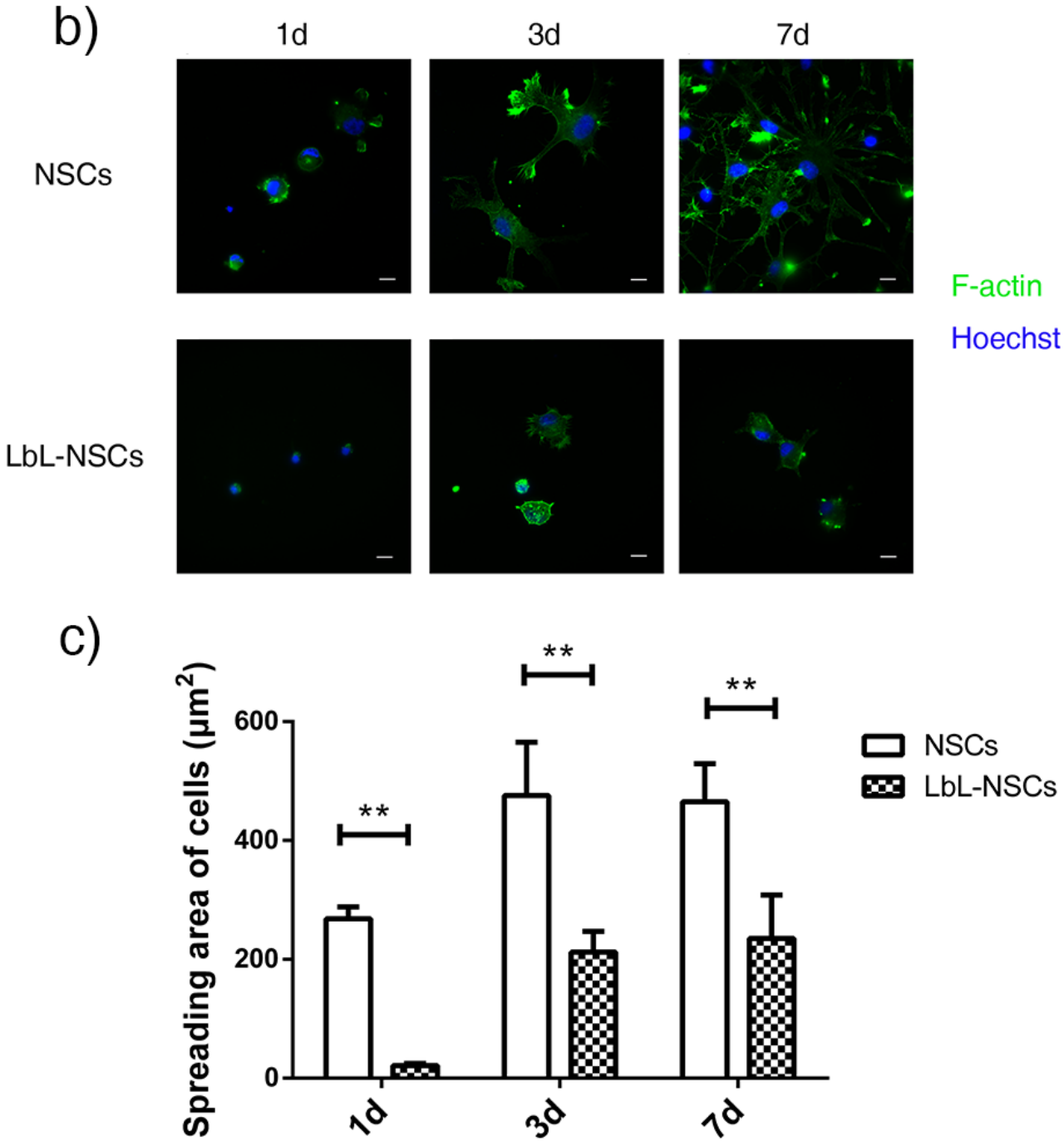

Figure 8. Morphologic changes of NSCs and LbL-NSCs. a) Characterization of LbL encapsulation with SEM. Untreated NSCs and $(gelatin)_2$/alginate coated NSCs

were grafted on a 24-well plate. They were processed for SEM microscopy on 1d, 3d, 5d and 7d. The processes of untreated NSCs stretched broadly. The spheroid-like LbL encapsulated NSCs at different time points were shown in the lower part. b) Cytoskeleton change of NSCs and LbL-NSCs. Encapsulated with $(gelatin)_2$/alginate, LbL-NSCs and untreated NSCs were cultured and stained with phalloidin (green) to show the F-actin of cells on 1d, 3d and 7d. The F-actin reflected the cytoskeleton. Like in SEM images, the coated NSCs were more spheroid-like than the untreated ones. (Blue: Hoechst). Scale bar in (b): 10μm. c) The spreading area of each cell was quantified by ImageJ based on the cytoskeleton staining results. **: $p<0.01$.

4.4 Influences of Encapsulation on NSCs' Functions

To test whether the changes in cellular morphology would lead to the difference in NSCs functions, we first observed the proliferation of encapsulated NSCs by BrdU assay (Figure 9a−d). Because BrdU could incorporate with the newly synthesized DNA as a substitute of thymidine during DNA replication, it was commonly used to detect the proliferation[375]. Images of 10 random fields of each group were taken to count the BrdU positive cells that were considered to be new cells, per se. As shown in Figure 9e, the proliferation of LbL encapsulated NSCs showed no significant changes ($p > 0.05$)[376, 377]. Therefore, it is suggested that LbL encapsulation with gelatin and alginate would not greatly impact the proliferation of NSCs.

In Figure 10a, the ratio of neurons and astrocytes in both groups of NSCs and LbL-NSCs was quite similar. Among them, 15% differentiated into neurons and 22%

into astrocytes (Figure 10b). Real-time PCR also showed that the transcription of related genes in LbL-NSCs was not influenced compared to that in NSCs groups at different time points (Figure 10c), though there were morphologic changes found on coated cells. As a promising cell therapy for nervous system disorders, NSCs have the ability to generate different types of neural cells. During the NSCs culture, EGF and bFGF were two most important cytokines to maintain NSCs stemness[378]; however, once these were withdrawn, NSCs would differentiate quickly[379]. To demonstrate whether LbL encapsulation would impact NSCs stemness, we performed withdrawal of two cytokines after they were seeded. The results suggested that the LbL encapsulation would not impact the differentiation of NSCs. On the other hand, NSCs could be induced to a specific type of cells when cultured in a specific inducing medium. Neurogenesis of NSCs in LbL group and control group was induced by B27 supplement for 3 and 6 days, and then all NSCs were detected with the antibody of β-tubulin III (Figure 11a). Similarly, Western blot also confirmed that the expression of nestin, a marker of NSCs, decreased day 3 to day 6, while the expression of MAP-2 increased (Figure 11b). From immunofluorescence staining and Western blots, even after encapsulation, NSCs were still able to differentiate into specific cell types such as neurons. It is suggested that LbL coating should not lead to the loss of the stemness by presenting the differentiation into multiple cell types after cytokines withdrawal and the neurogenesis induced by B27 supplement.

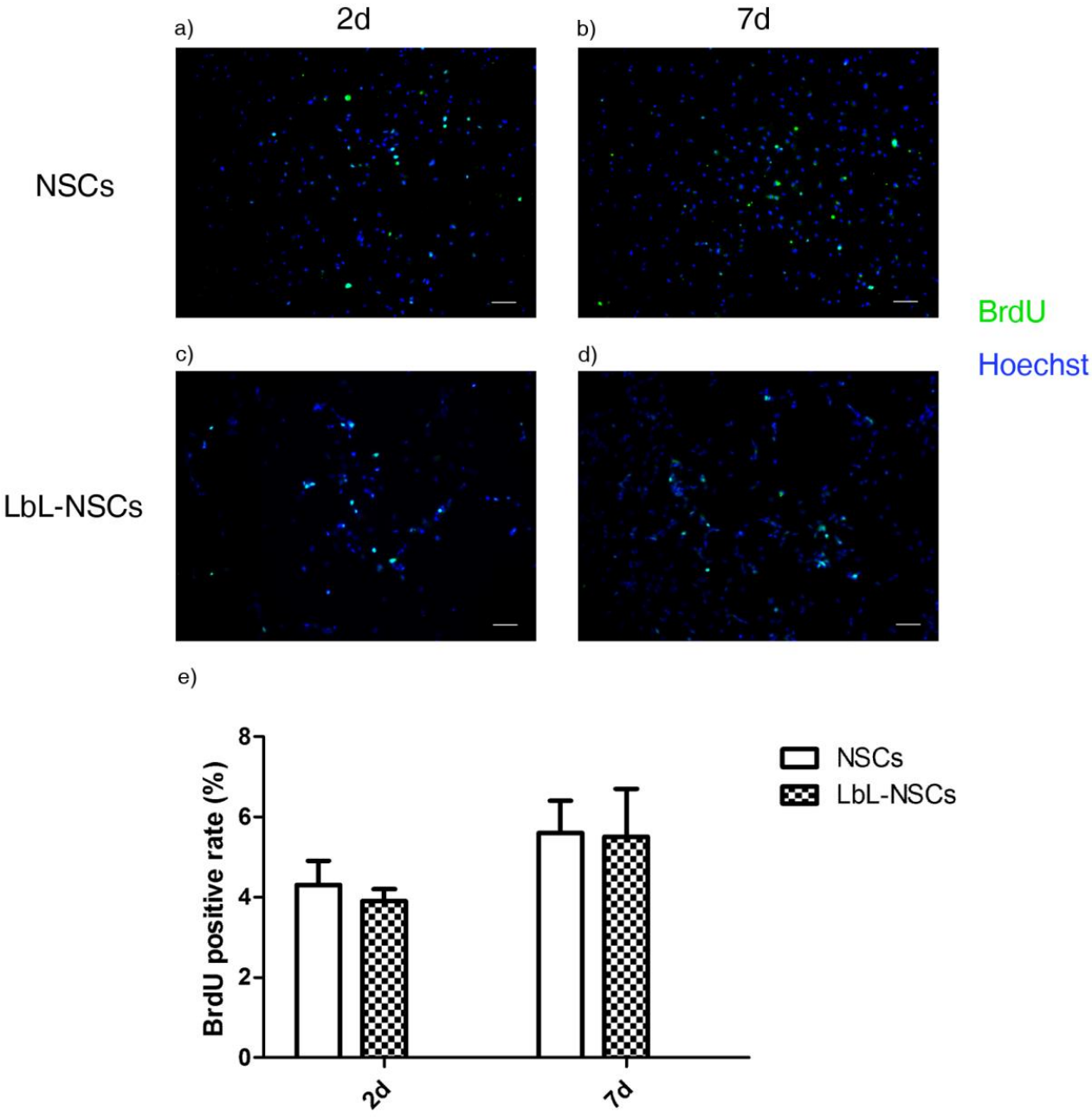

Figure 9. Proliferation assay of NSCs and LbL-NSCs. Untreated NSCs and NSCs coated with $(gelatin)_2$/alginate were cultured in a 24-well plate for a week. BrdU was added on 1d and 6d, and then the cells were taken for anti-BrdU staining on 2d and 7d to show the newly generated cells during the 24h. a)-b) Proliferation of NSCs detected by BrdU assay at different time points. c)-d) Proliferation of LbL-NSCs detected by

BrdU assay at different time points. (Green: BrdU; blue: Hoechst). Scale bar in (a)-(d): 100μm. e) Quantification of BrdU-positive cells in different groups on 2d and 7d. The percentage of new cells was counted in ten random fields of each group to quantify the proliferation rate; (n=3).

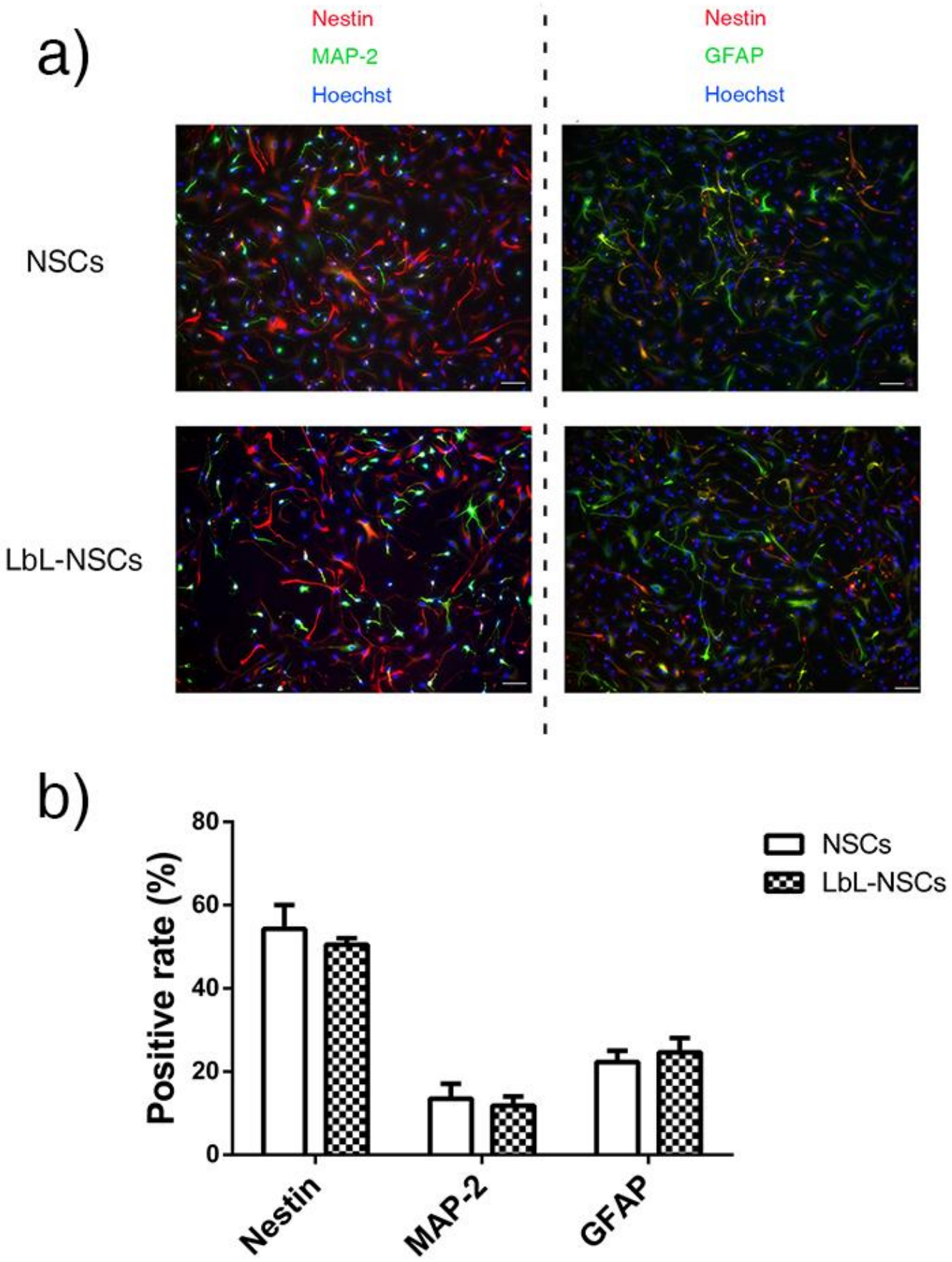
a)
Nestin
MAP-2
Hoechst
Nestin
GFAP
Hoechst
NSCs
LbL-NSCs
b)
Positive rate (%)
80
60
40
20
0
NSCs
LbL-NSCs
Nestin
MAP-2
GFAP

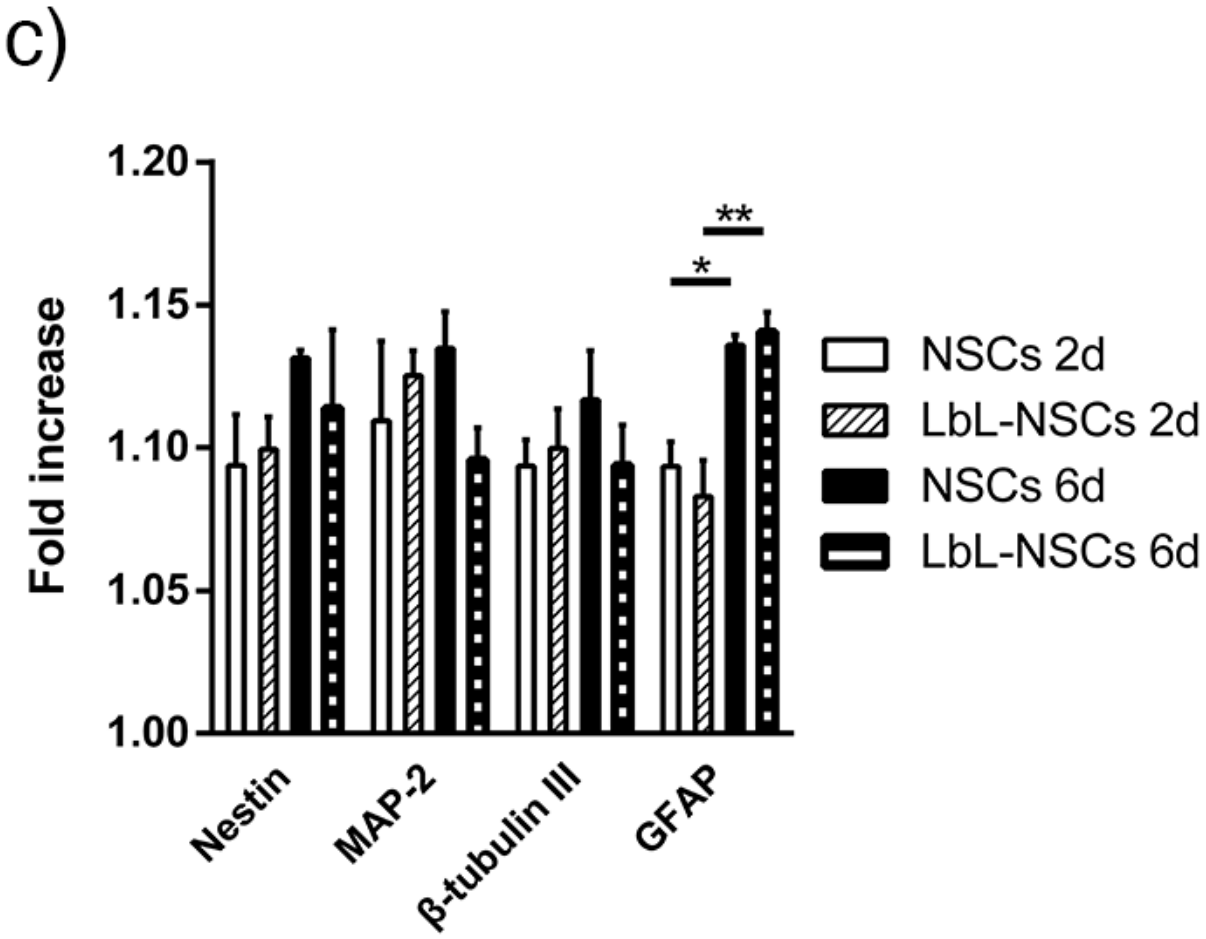

Figure 10. Differentiation of NSCs and LbL-NSCs after cytokines withdrawal. a) The stemness of cells was detected by immunofluorescence staining after 6d of cytokines withdrawal. Markers of MAP-2, GFAP, and nestin were used to detect neurons, astrocytes and NSCs. Scale bar in (a): 100μm. b) Quantification of the rate of cells with different markers in both groups after cytokines withdrawal. The percentage of cells was counted in ten random fields of each group to quantify the differentiation; (n=3). c) Real-time PCR of related genes at 2d and 6d after cytokine withdrawal was shown. Fold increase of each gene has been normalized against GAPDH; (n=3). *: $p<0.05$; **: $p<0.01$.

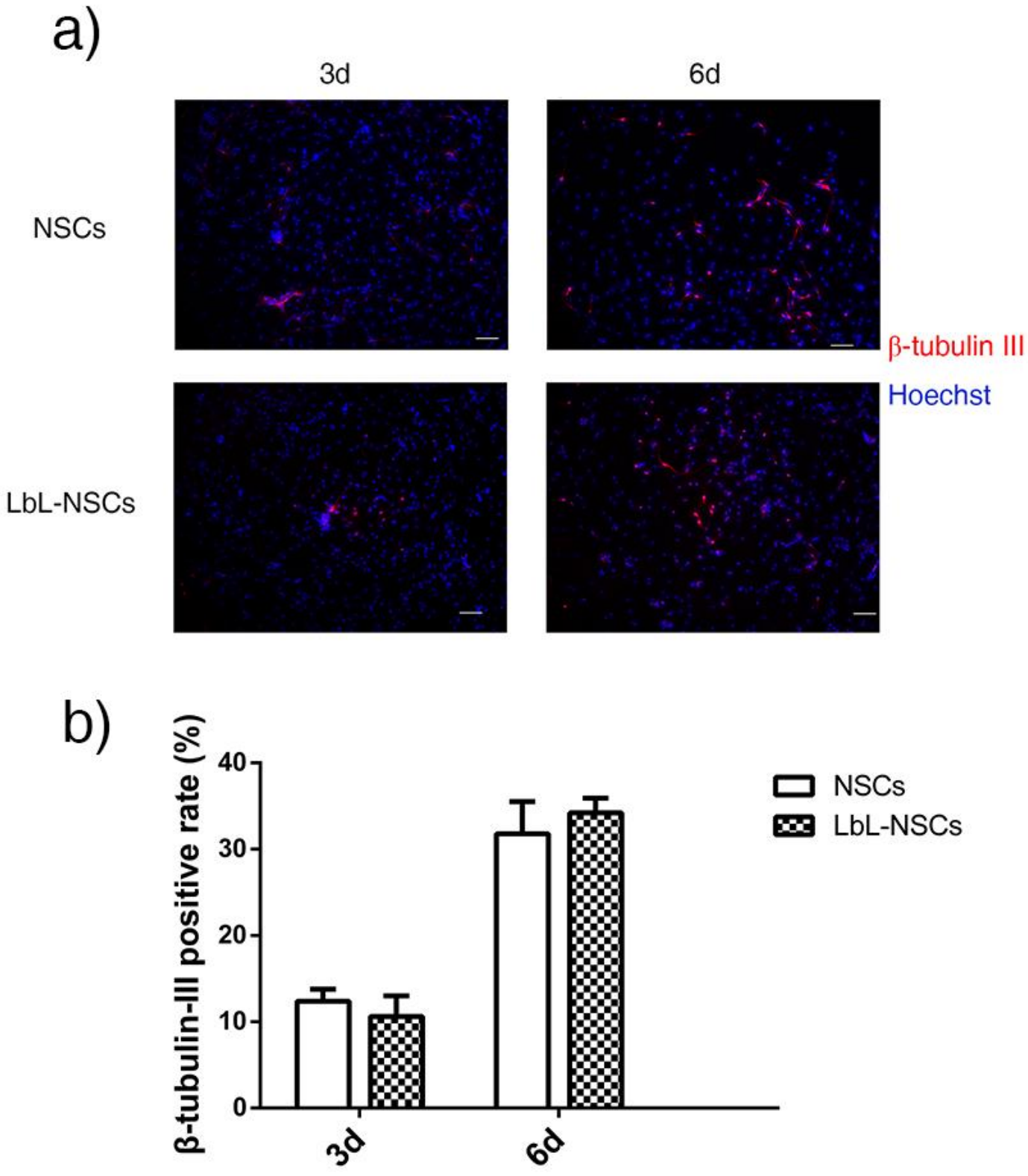
a)
3d
6d
NSCs
LbL-NSCs
β-tubulin III
Hoechst
b)
β-tubulin-III positive rate (%)
40
30
20
10
0
3d
6d
NSCs
LbL-NSCs

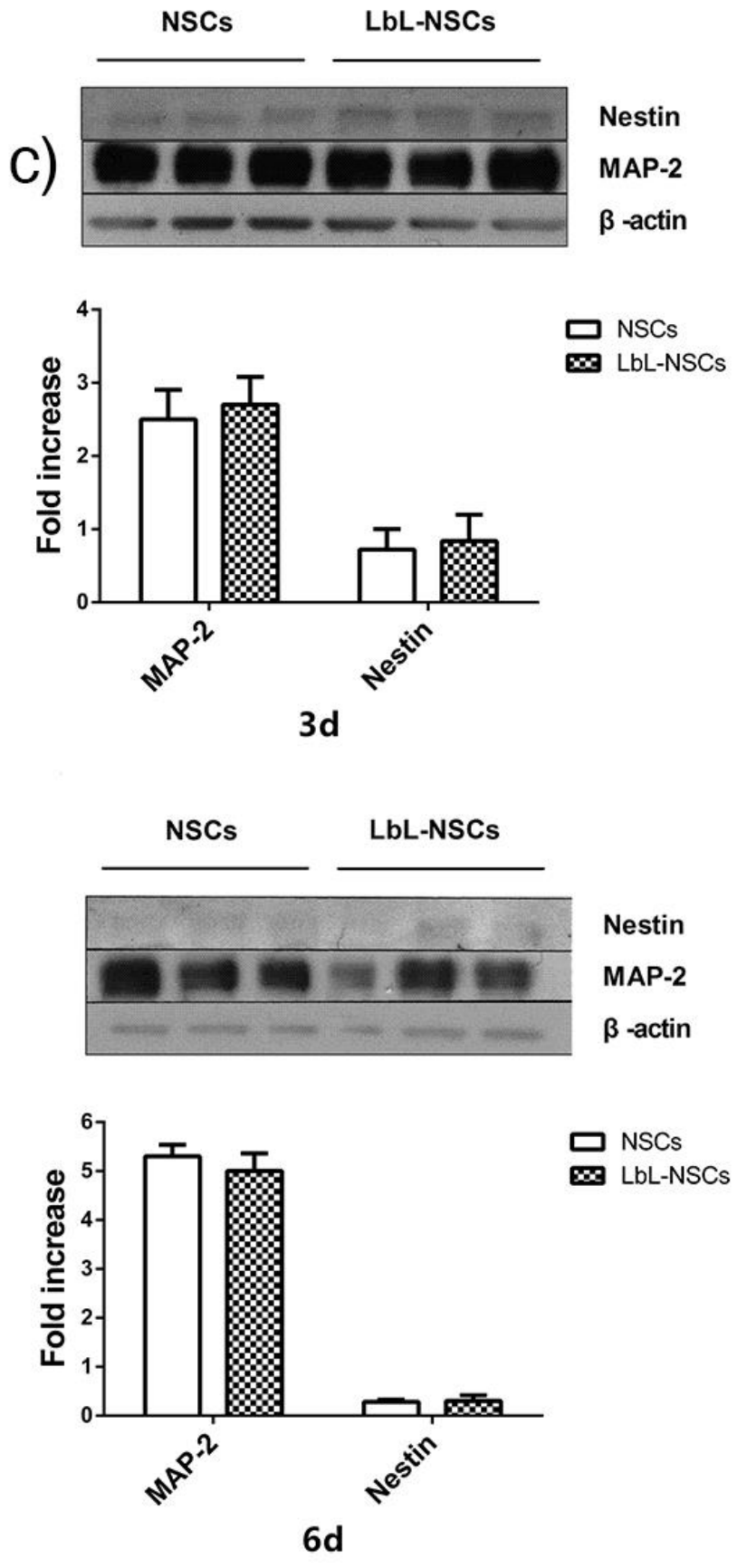
NSCs
LbL-NSCs
C)
Nestin
MAP-2
β -actin
Fold increase
0
1
2
3
4
NSCs
LbL-NSCs
MAP-2
Nestin
3d
NSCs
LbL-NSCs
Nestin
MAP-2
β -actin
Fold increase
0
1
2
3
4
5
6
NSCs
LbL-NSCs
MAP-2
Nestin
6d

Figure 11. Neurogenesis inducing of NSCs and LbL-NSCs. Untreated NSCs and $(gelatin)_2$/alginate coated NSCs were seeded for 1d and then induced with neurobasal medium containing B27 supplement for 3d and 6d for neurogenesis. a) β-tubulin III (red) was used as the neuronal marker to demonstrate the neurogenesis of untreated NSCs and LbL-NSCs at different time points. (Blue: Hoechst). Scale bar in (a): 100μm. b) Quantification of the rate of neurons in both groups after neurogenesis inducing. The percentage of β-tubulin III positive cells was counted in ten random fields of each group to quantify; (n=3). c) Quantification of induced neurogenesis by Western blot. Untreated NSCs and $(gelatin)_2$/alginate coated NSCs were induced for neurogenesis for 3d and 6d. Expressions of MAP-2 (a neuronal marker) and nestin (a marker for NSC) were shown by Western blot assay. Expression levels of each marker have been normalized against β-actin; (n=3).

Primers	Sequences	Annealing (°C)	Product (bp)
Nestin (Fw)	GAAGAGGGCAGAGAAGAAAG	60	108
Nestin (Rv)	CAGATCCCACTTTGGAGAAG		
GFAP (Fw)	CTCTAAGGTCCCTCCCTTT	60	121
GFAP (Rv)	GCCTCTGACACTGTCTTTATT		
MAP-2(Fw)	CTTCCACCGAGCATTCTTT	60	119
MAP-2 (Rv)	CATGGCTGCATCTGTAACT		
β-tubulin III (Fw)	GCTGGCCATTCAGAGTAAG	60	127
β-tubulin III (Rv)	GTGCTGTTGCCGATGAA		
GAPDH (Fw)	TGCTGAGTATGTCGTGGAG	52	288
GAPDH (Rv)	GTCTTCTGAGTGGCAGTGAT		

Table 1. Primers used for the real-time PCR.

4.5 Application of LbL Single-cell Encapsulation in Drug Delivery

Whether the LbL encapsulation structure could be employed as a drug carrier to regulate NSCs functions by loading bioactive molecules would be crucial for extensive applications of LbL nanocoating. LbL self-assembly technique has been applied on controlled drug delivery in previous studies[380, 381]. For examples, insulin, doxorubicin, bone morphogenetic protein-2 (BMP-2) were reported to be loaded on the LbL structure, demonstrating distinct effect of sustained release[382-384]. In Figure 12, anti-IGF-1 was incubated with NSCs in different groups to show the presence of IGF-1 on the surface of cells which were encapsulated with gelatin and IGF-1 loaded alginate (100 ng IGF-1 with 1 mL 0.1% alginate; loading efficiency is shown in Figure 13), which, at the same time, indicated the success of encapsulation. Its release profiles at pH 7.4 and 6.5 were shown in Figure 14, exhibiting a prolonged release at pH 6.5. IGF-1 was proven to be effective to enhance the proliferation of NSCs so that it was regarded as the target molecule of drug delivery of LbL nanocoating[385]. A pH value of 6.5 was used to mimic the ischemic environment in the study to investigate the influence of pH on the molecule release because the low pH is common in central nervous disorders such as stroke[386]. Taken together, the potential applications of this technique to deliver functional regulators together with NSCs in diseases such as stroke were implied. The reason why IGF-1 could be released for a longer period of time at lower pH might be that the pH 6.5 was closer to the middle between the IEP of gelatin and alginate than pH 7.4, making the LbL shells more stable, or the permeability of LbL materials

changed due to different pH [387]. It needed to be clarified in the future.

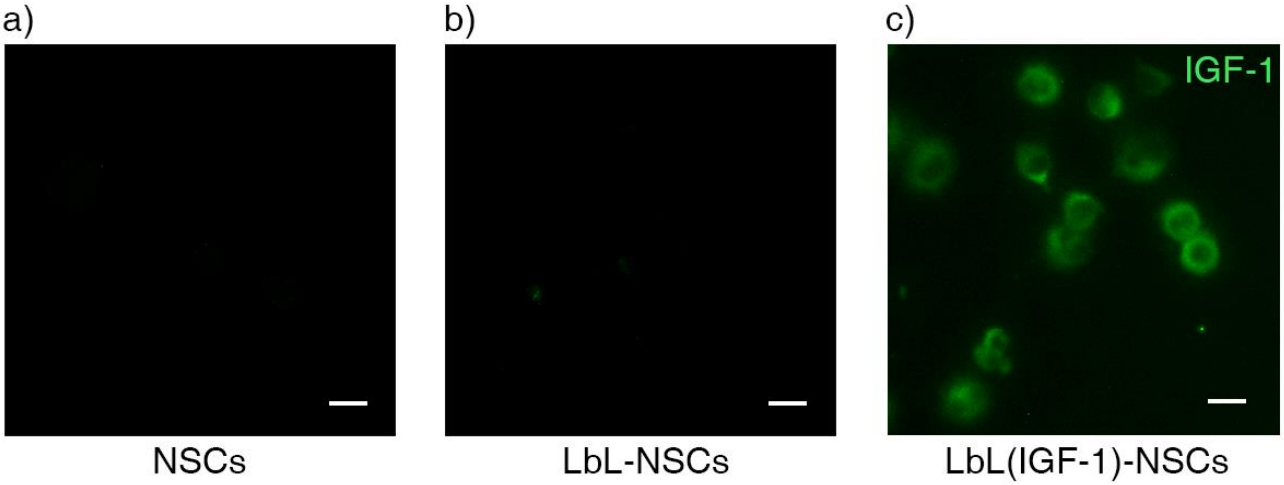

Figure 12. Characterization of LbL (IGF-1)-NSCs. IGF-1 was mixed with alginate to make them adsorbed. NSCs were encapsulated with $(gelatin)_2$/alginate and $(gelatin)_2$/alginate-IGF-1. a)-c) NSCs, LbL-NSCs and LbL (IGF-1)-NSCs were stained with anti-IGF-1 to illustrate the presence of IGF-1 (green) on the cell surface. Scale bar in (a)-(c): 10μm.

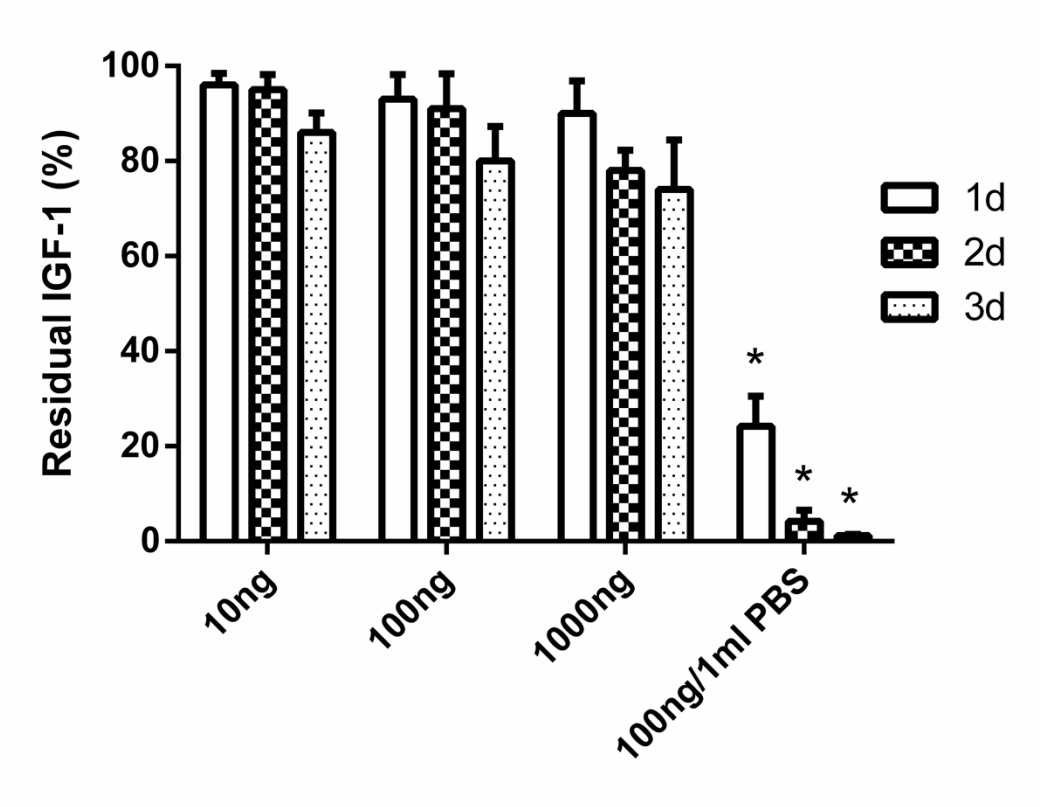

Figure 13. Loading efficiency of IGF-1 on alginate. The amount of IGF-1 remained in the dialysis bag from 1d to 3d was tested. *: $p<0.05$.

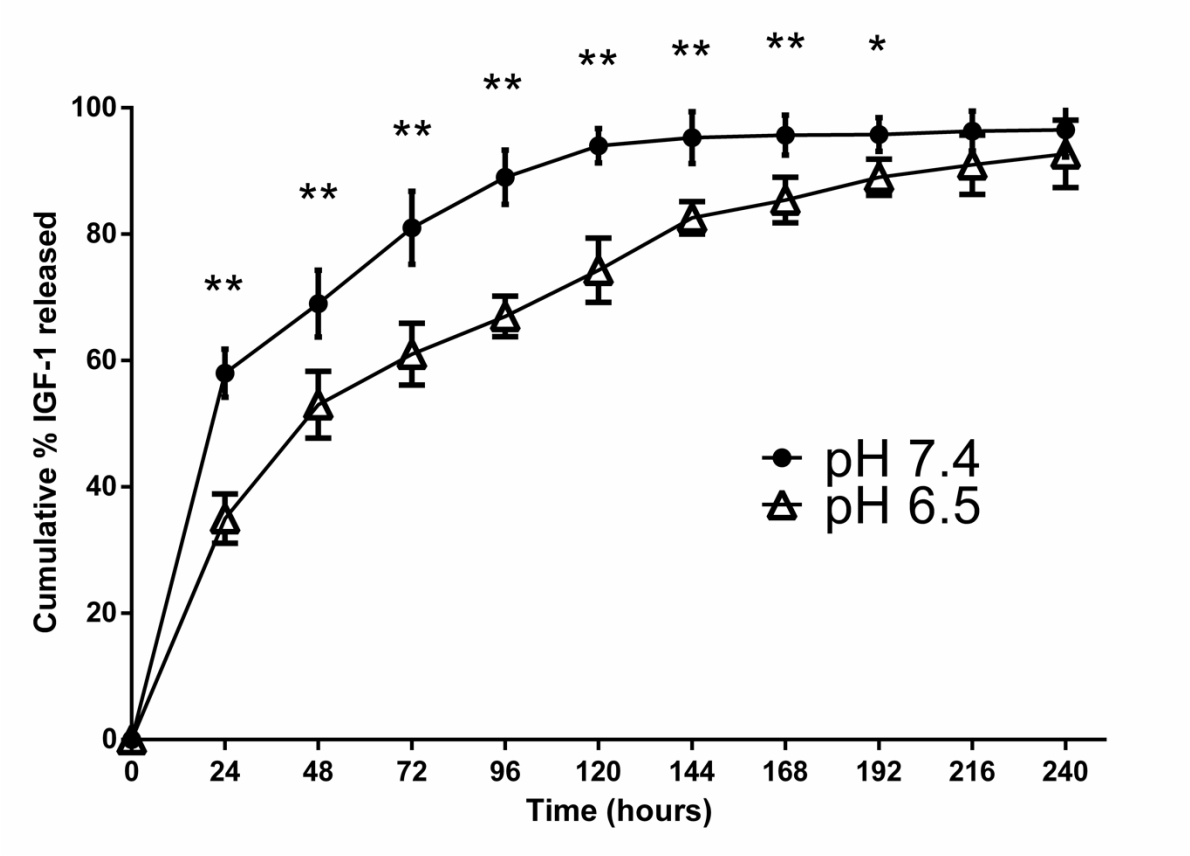

Figure 14. Cumulative IGF-1 release curve. IGF-1 was mixed with alginate to let it physically adsorb to alginate. NSCs were coated with $(gelatin)_2$/alginate-IGF-1 and cultured under different pH in 24-well plates. The medium was taken to test the IGF-1 concentration with the ELISA kit at time points from 0 h to 240 h; (n=3) and the cumulative release curve of IGF-1 was obtained. *: $p<0.05$; **: $p<0.01$.

4.6 IGF-1 Loaded on LbL Encapsulation Layers Was Released to Regulate NSCs

At 2, 5, and 7 days, the proliferation of NSCs in different groups were tested with BrdU assay (Figure 15). The groups were defined as the NSCs group (Figure 15a−c), in which there were only untreated NSCs; the NSCs+IGF-1 group (Figure 15d−f), in which 20 ng/mL IGF-1 was added to the normal NSCs; the LbL-NSCs group (Figure 15g−i), in which there were NSCs encapsulated with $(gelatin)_2$/alginate; and the LbL

(IGF-1)-NSCs group (Figure 15j−l), in which the NSCs were encapsulated with $(gelatin)_2$/alginate-IGF-1 (100 ng IGF-1 with 1 mL 0.1% alginate). The proliferation rate of cells in NSCs+IGF-1 group and LbL (IGF-1)-NSCs group was similar, yet much higher than the rate in the other two groups at 5 and 7 days (Figure 15m). In addition, since the effect of IGF-1 for proliferation is dose-dependent[388], when a higher amount of IGF-1 was loaded onto alginate, the proliferation rate of encapsulated NSCs on day 7 increased (Figure 16). Therefore, it provided evidence that the coating materials could function as a carrier for IGF-1 and was able to promote the proliferation of NSCs successfully.

Finally, because the IGF-1 could still effect after being loaded on the materials and had a more sustained release profile at pH6.5, survival rate of LbL (IGF-1)-NSCs (100 ng IGF-1 with 1 mL 0.1% alginate) was examined with other groups under this condition (Figure 17). The survival rate of NSCs+IGF-1 group (20 ng/mL) was higher than that of untreated NSCs. However, it began to decrease after about 3 days. On the contrary, the viability of LbL (IGF-1)-NSCs was maintained at 90%, indicating the effect of the sustained release of IGF-1 at pH 6.5. This NSCs-regulator model was able to reduce the burst release, which was disadvantageous for drug delivery[389], and prolong the effect of functional regulators at the same time, and thus, it could be applied as a novel treatment strategy for nervous system diseases in the future.

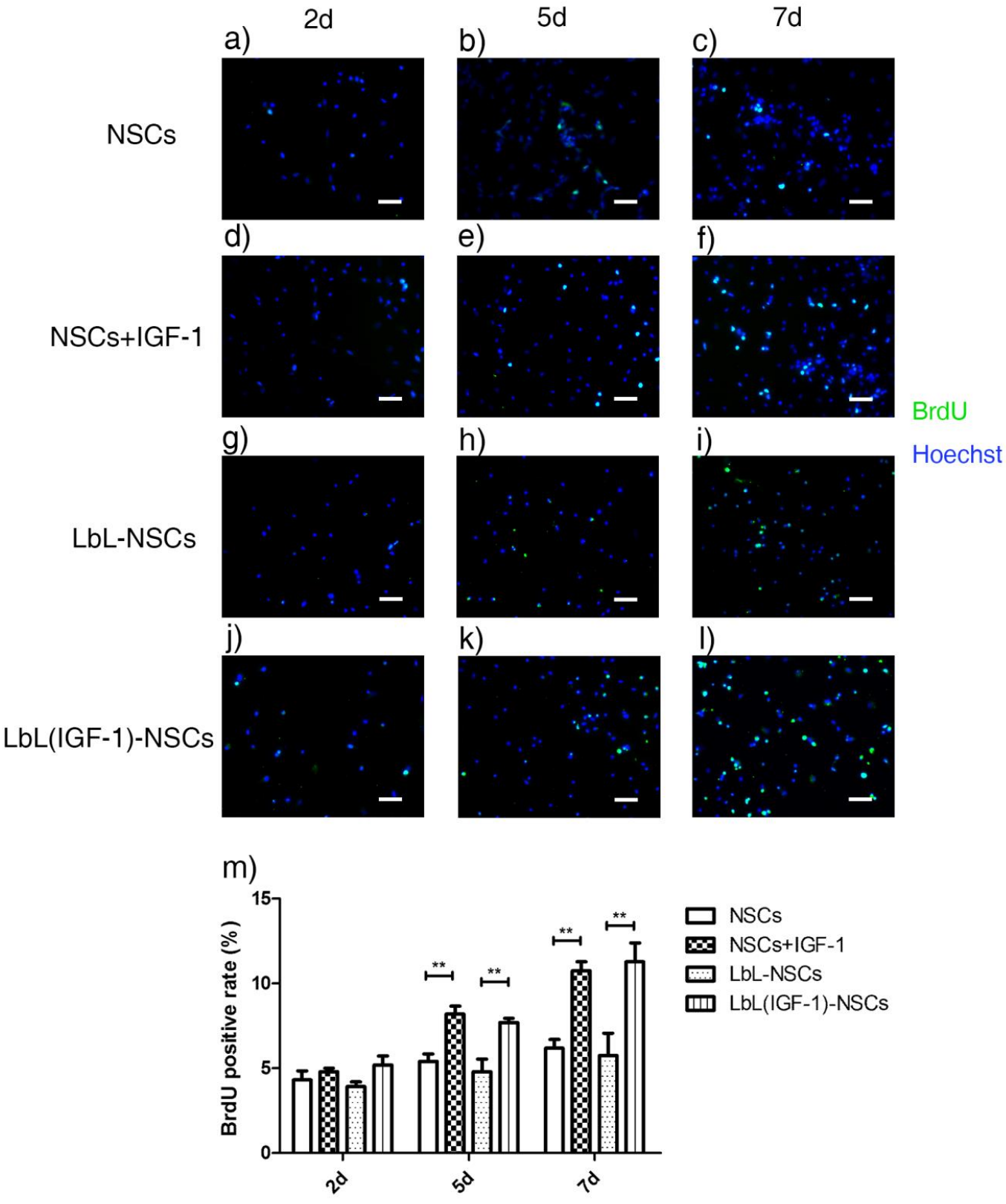

Figure 15. Proliferation assay of untreated NSCs, NSCs treated with IGF-1,

LbL-NSCs and LbL (IGF-1)-NSCs. NSCs were coated with $(gelatin)_2$/alginate and $(gelatin)_2$/alginate-IGF-1. Untreated NSCs, LbL-NSCs and LbL (IGF-1)-NSCs (100ng IGF-1 mixed with 1ml 0.1% alginate) were cultured without adding extrinsic IGF-1. NSCs in another group would be added IGF-1 protein (20ng/ml every three days). On 1d, 4d and 6d, BrdU was added to these four groups. At time points 2d, 5d and 7d, cells were taken for anti-BrdU staining to show the newly generated cells. a)-c) Proliferation of untreated NSCs detected by BrdU assay at different time points. d)-f) Proliferation of NSCs treated with IGF-1 protein. g)-i) Proliferation of LbL-NSCs. j)-l) Proliferation of LbL (IGF-1)-NSCs. (Green: BrdU; blue: Hoechst). Scale bar in (a)-(l): 50μm. m) Quantification of BrdU-positive cells in different groups on 2d, 5d and 7d. The percentage of new cells was counted in ten random fields of each group to quantify the proliferation rate; (n=3). **: $p<0.01$.

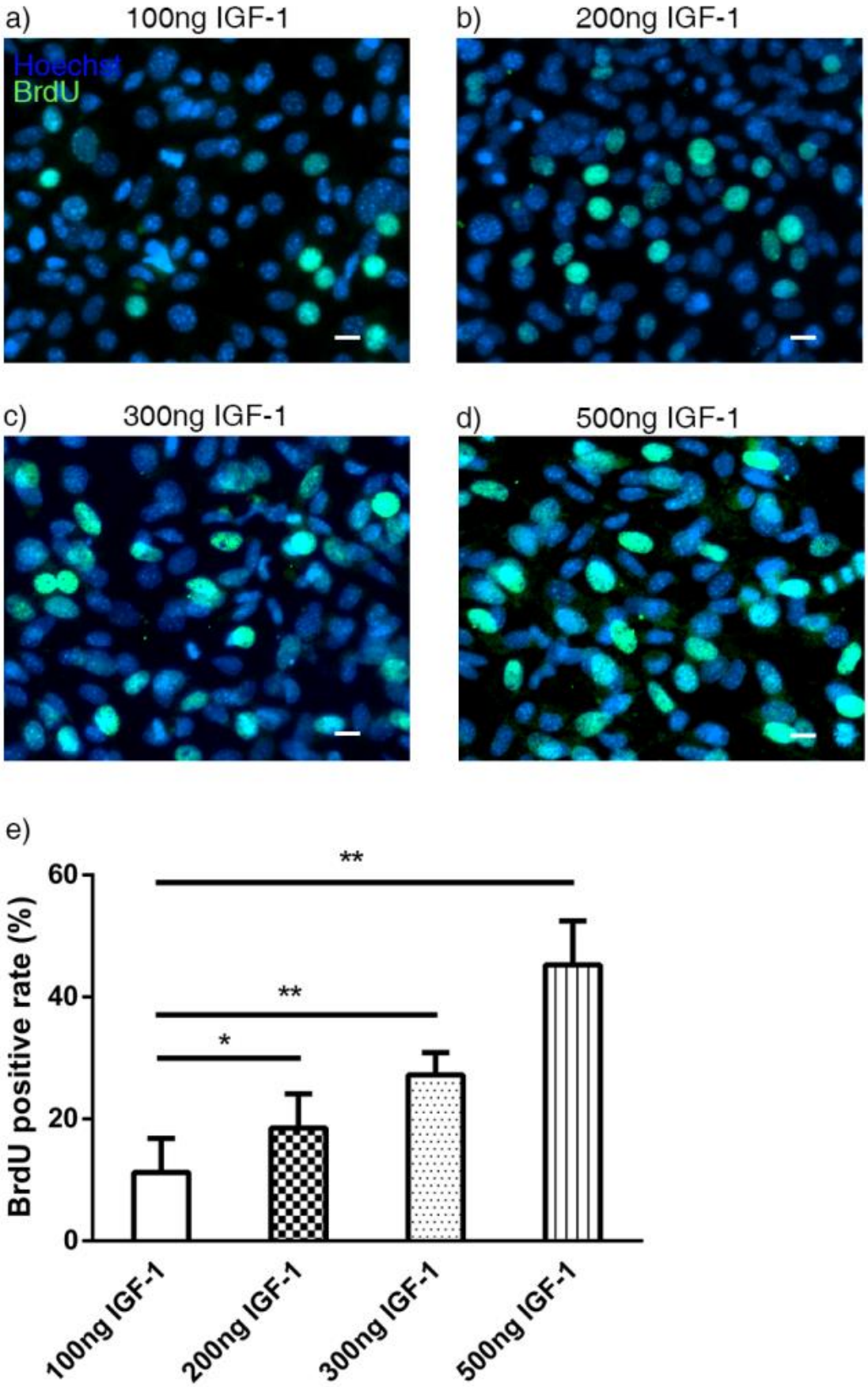
a)
100ng IGF-1
Hoechst
BrdU
b)
200ng IGF-1
c)
300ng IGF-1
d)
500ng IGF-1
e)
BrdU positive rate (%)
60
40
20
0
**
**
*
100ng IGF-1
200ng IGF-1
300ng IGF-1
500ng IGF-1

Figure 16. Proliferation rate of encapsulated NSCs with different amounts of IGF-1 loaded on 7d. 100ng, 200ng, 300ng and 500ng IGF-1 were mixed with 1ml 0.1% alginate respectively and then NSCs were encapsulated with gelatin and different groups of alginate-IGF-1.At the time point 7d,the proliferation rate of NSCs in these different groups were tested by BrdU assay (a-d). (Green: BrdU; blue: Hoechst). Scale bar in (a)-(d): 10μm. e) Quantification of BrdU-positive cells in different groups on 7d. The percentage of new cells was counted in ten random fields of each group to quantify the proliferation rate; (n=3). *: $p<0.05$; **: $p<0.01$.

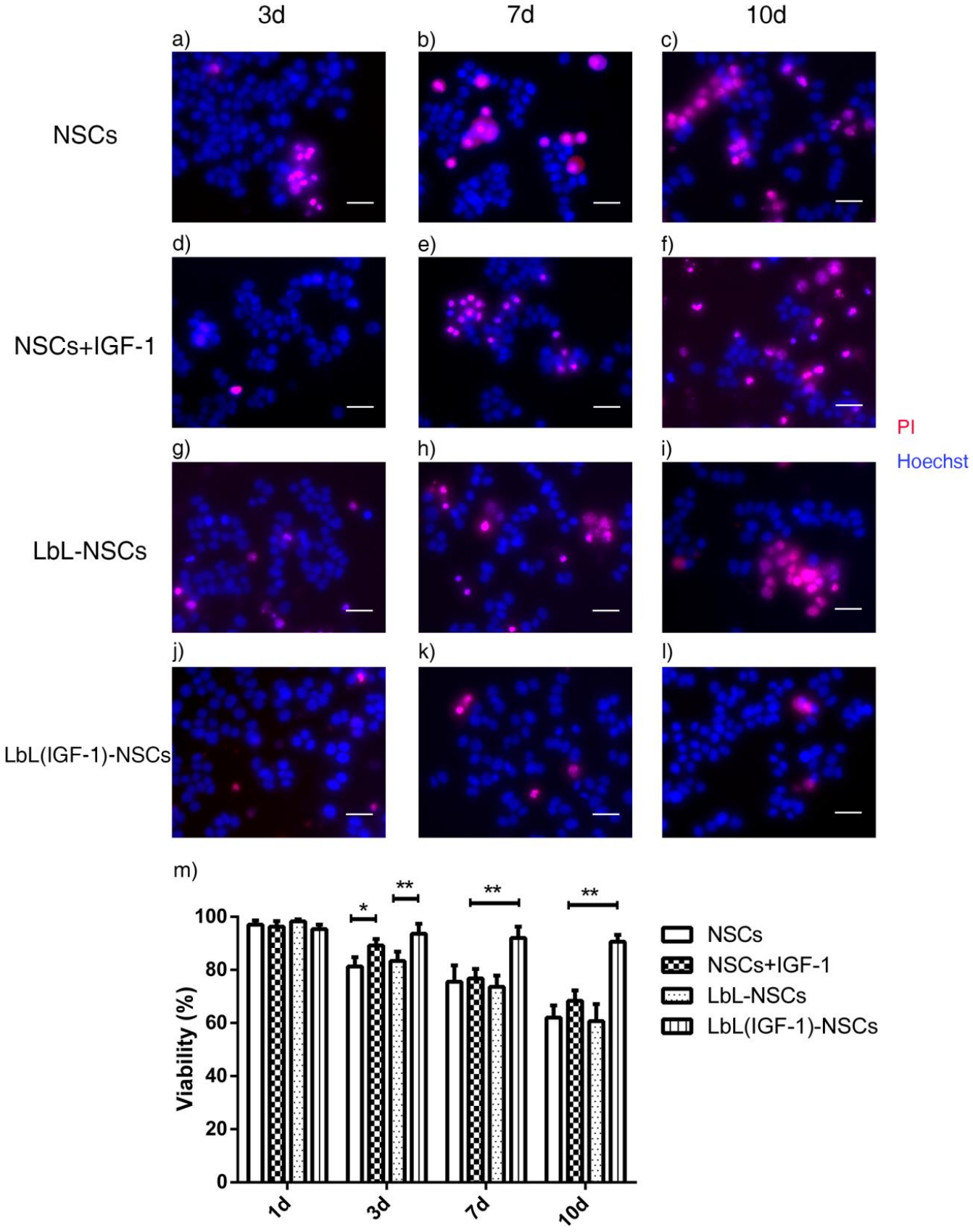
3d
7d
10d
a)
b)
c)
NSCs
d)
e)
f)
NSCs+IGF-1
PI
Hoechst
g)
h)
i)
LbL-NSCs
j)
k)
l)
LbL(IGF-1)-NSCs
m)
Viability (%)
100
80
60
40
20
0
1d
3d
7d
10d
*
**
**
**
NSCs
NSCs+IGF-1
LbL-NSCs
LbL(IGF-1)-NSCs

Figure 17. Survival rate of untreated NSCs, NSCs treated with IGF-1, LbL-NSCs and LbL (IGF-1)-NSCs at pH 6.5. NSCs were coated with $(gelatin)_2$/alginate and $(gelatin)_2$/alginate-IGF-1. Untreated NSCs, LbL-NSCs and LbL (IGF-1)-NSCs were cultured without adding extrinsic IGF-1. NSCs in another group would be added IGF-1 protein (20 ng/ml every three days). The pH of the medium was adjusted to 6.5. On 1d, 3d, 7d and 10d, Hoechst/PI staining was performed to examine the viability of the cells. Results of 3d, 7d and 10d were shown from a)-l). (Blue: Hoechst; red: PI). Scale bar in (a)-(l): 20μm. m) Survival rate of NSCs in different groups on 1d, 3d, 7d and 10d. The percentage was counted in ten random fields of each group to quantify; (n=3). *: $p<0.05$; **: $p<0.01$.

Chapter 5. Results (Specific Objective #2)

5.1 Cell-compatible Study of Single-cell Encapsulation with Gelatin and HA

PC12 cells, extracted from rat adrenal medulla, were used since they are acknowledged as the neuronal cell model[390]. Gelatin (type A) with an isoelectric point of 7.0-9.0 and HA with that of 2.5 were chosen as the polycation and polyanion, respectively. They are both FDA-proved natural polyelectrolytes with reputable biocompatibility and are able to form multilayers under neutral pH[81, 391].

According to our previous study of encapsulation on NSCs, cellular properties such as the viability, differentiation and proliferation were not impacted distinctly when NSCs were treated with 3-layer encapsulation with 0.1% gelatin and alginate. The present research were further moved forward to its extremity in the parameters of LbL single-cell encapsulation.

Cell viability of PC12 cells encapsulated with different parameters was detected by Hoechst/PI staining. After being coated with 0.1%, 0.5% and 1% of materials for 4, 8 and 12 layers, cells were stained with Hoechst/PI reagents. PI can permeate cell membrane of dead cells to bind to DNA and display red fluorescence. As illustrated in Figure 18, cell viability was not affected by encapsulation, indicating the biocompatibility of this technique on PC12 cells.

Proliferation represented by cell counting and Ki-67 staining at different time points was applied to indicate the feasibility of the materials and encapsulation methods. Cell number counted at different time points during the cell culture is direct

evidence demonstrating the survival and proliferation of cells. Ki-67 is closely related with proliferation since it is found to be expressed in mitotic cells in all the cell cycles except the G0 phase [392]. Therefore, the Ki-67 staining is generally accepted as a technique for detection of proliferation[393]. In Figure 19, the increase of cell number on day 0, 3, 5 and 7 was shown. Although cells proliferated consistently in all the groups, the increase of cell number was obviously hindered in groups of 0.5% of materials 12-layer and 1% of materials encapsulation groups after day 3. The results of Ki-67 staining also conformed to the cell counting that the proliferation of cells in these groups were 45.3 ± 6.5%, 42.4 ± 4.2%, 37.2 ± 9.4% and 35.4 ± 8.1% on day 3, on the contrary, the rates were 48.3 ± 65.3%, 51.0 ± 8.7%, 47.2 ± 9.7%, 52.7 ± 2.9%, 47.7 ± 11.0% in 0.1% of materials groups, 0.5% of materials for 4-layer and 8-layer groups. Besides, in consideration of the undifferentiated survival rates of cells in all the groups, it was assumed that gelatin and HA were biocompatible materials for single-cell encapsulation, however, the proliferation would be negatively impacted by encapsulation with high-concentration materials and excessive layers. As such, permeability investigation will be then performed on cells encapsulated with the appropriate parameters such as 0.1% of materials for 4, 8 and 12 layers; 0.5% of materials for 4 and 8 layers.

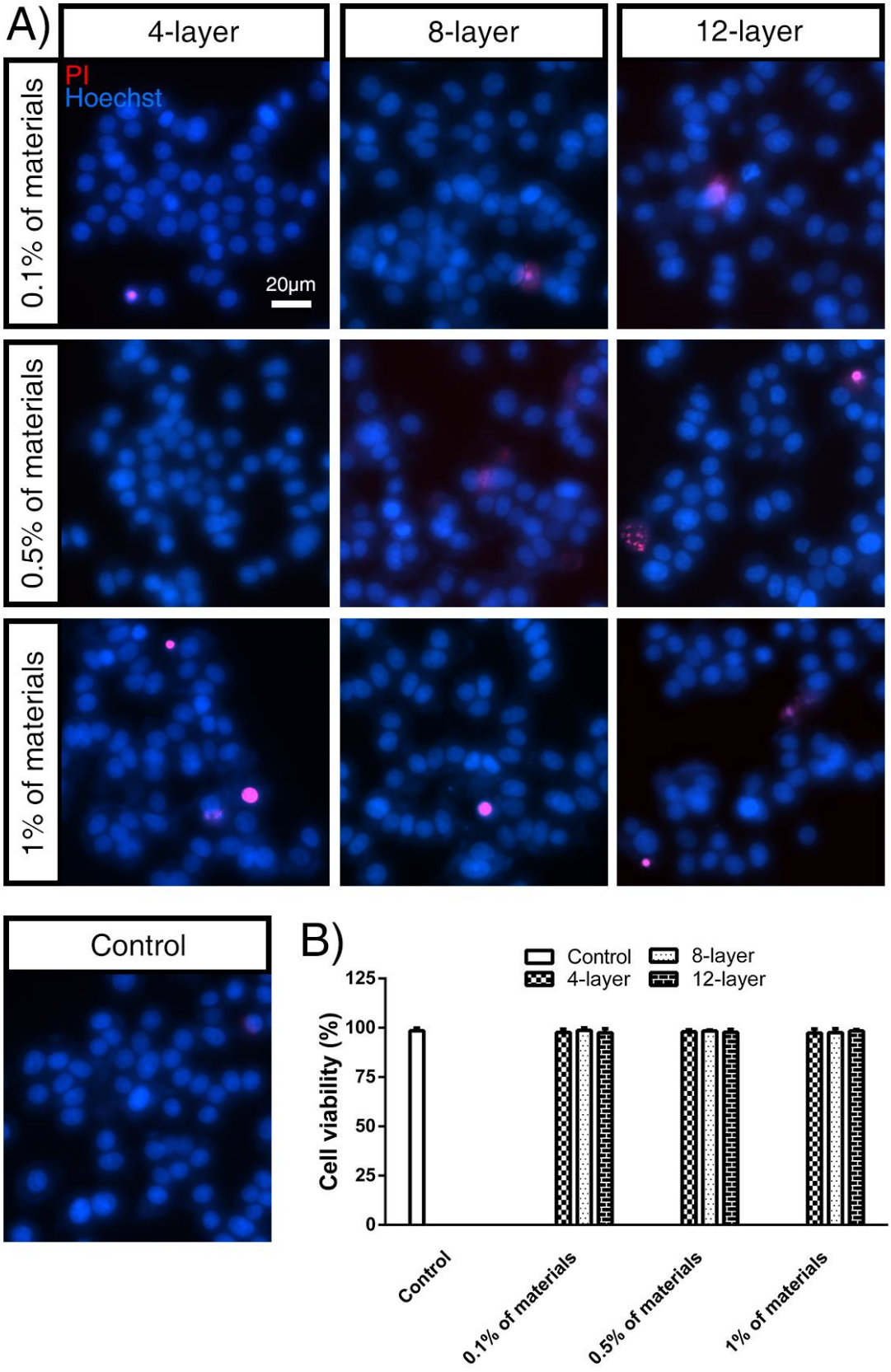

Figure 18. Cell viability of untreated PC12 cells and PC12 cells encapsulated with different parameters by Hoechst/PI staining. A) Hoechst/PI staining of

untreated PC12 cells and cells encapsulated with 0.1%, 0.5% and 1% of materials for 4, 8, and 12 layers. Cells with blue were viable ones. B) Quantification of viability of PC12 cells in different groups.

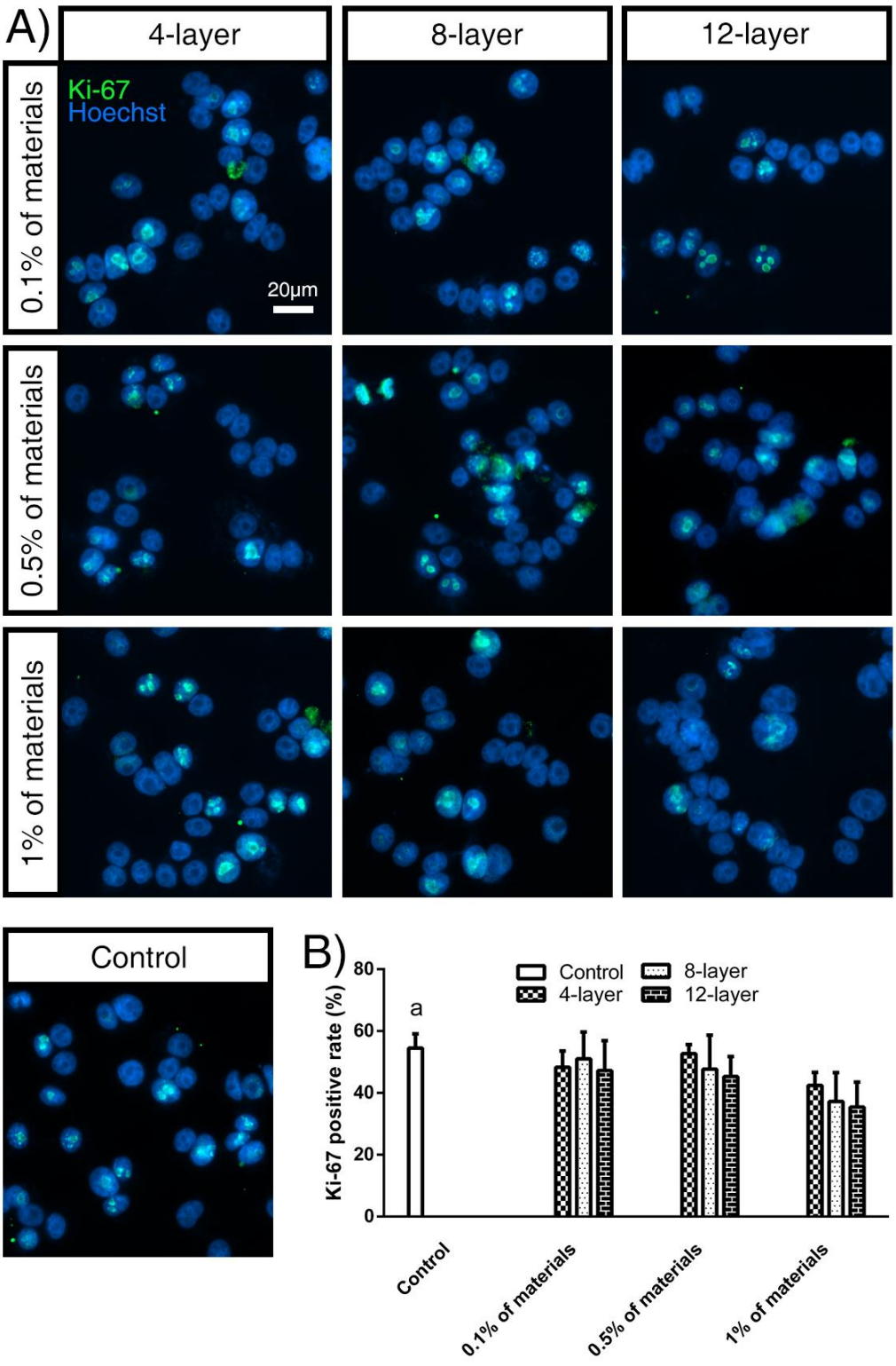

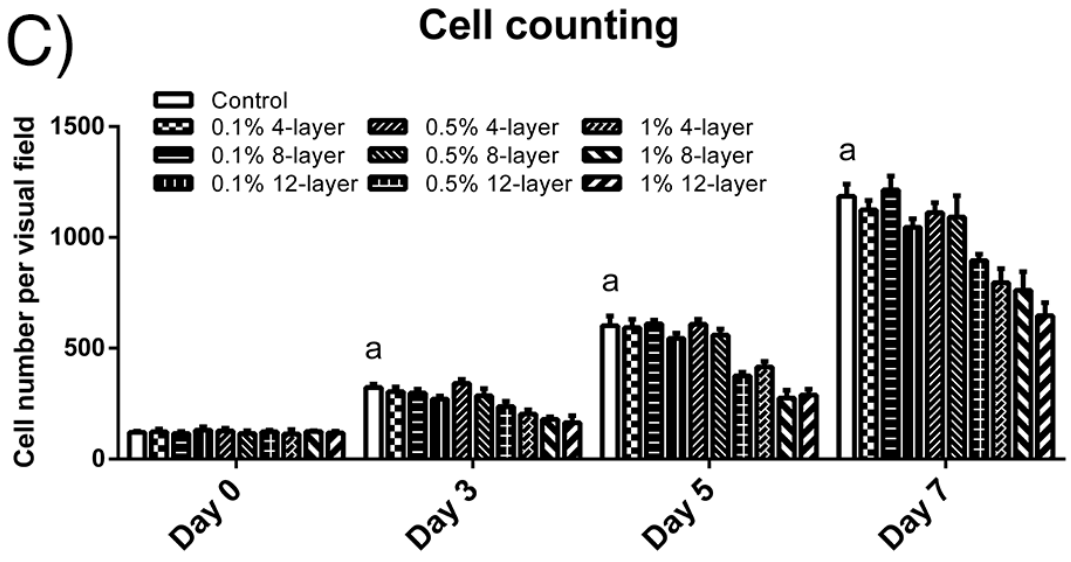

Figure 19. Proliferation assay of untreated PC12 cells and encapsulated cells. A) Ki-67 staining of untreated PC12 cells and cells encapsulated with 0.1%, 0.5% and 1% of materials for 4, 8, and 12 layers on day 3. B) Ki-67 positive rates quantified from each group on day 3. The ratio was calculated from five random fields of each group; (n=5). a: $p<0.05$ when control vs. 0.5% 12-layer and 1% groups. C) Cell counting of untreated PC12 cells and cells encapsulated with 0.1%, 0.5% and 1% of materials for 4, 8, and 12 layers on day 0, day 3, day 5 and day 7. Average cell amount in each visual field (0.15 mm^2) was counted from five random fields; (n=5). a: $p<0.05$ when control vs. 0.5% 12-layer and 1% groups.

5.2 Characterization of Single-cell Encapsulation on PC12 Cells

Characterization was performed by TEM and fluorescence labeling of gelatin. Cell samples from groups of control, 0.5% 4-layer and 0.5% 8-layer were observed under electron microscope for examining the surface of cells. Apparently seen from Figure

20, the cytoplasmic membrane was free from materials on cells in control group. As measured by ImageJ, materials formed the layers of 20.5 ± 6.6 nm in the 4-layer group and 34.4 ± 4.2 nm in the 8-layer group. Coating with FITC-labeled gelatin also confirmed the establishment of the encapsulation. 0.5% of gelatin-FITC and 0.5% of HA were applied in the LbL encapsulation on PC12 cells for 8 layers. Under the fluorescence microscope, the encapsulation was demonstrated clearly. In short, LbL self-assembly technique was successfully applied to encapsulate PC12 cells at single-cell scale with gelatin and HA.

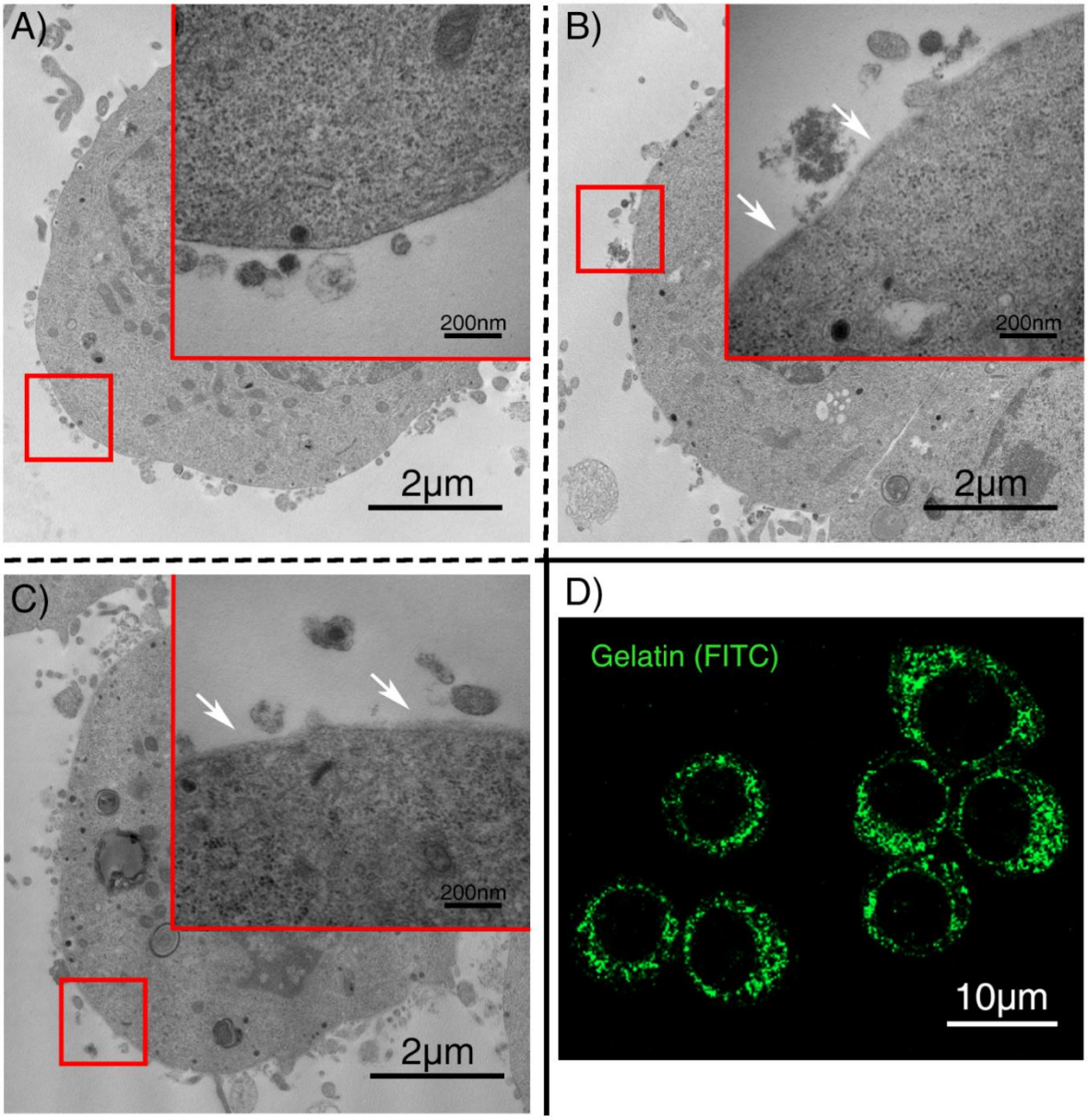

Figure 20. Characterization of encapsulated PC12 cells with TEM and fluorescence labeling. TEM of untreated PC12 cells and cells encapsulated with 0.5% of materials for 4 and 8 layers were shown in A)-C). Arrows indicated the materials on cell membrane. D) Fluorescence characterization of PC12 cells encapsulated with FITC-labeled gelatin and HA.

5.3 Cell Surface Topography on PC12 Cells

As foreign materials, gelatin and HA were supposed to alter the surface status of cells after being encapsulated on cell membrane. AFM is frequently utilized to reflect the surface conditions of various interfaces, including cell surface[394].

In Figure 21, the shaded map and 3D images were taken for untreated PC12 cells and encapsulated cells. Cell surface on untreated PC12 cells were smoother and had smaller bulges (with the area of approximately 0.016 μm^2) on it. On the contrary, there were more well-arranged rectangle-like structures (with the area of more than 0.043 μm^2) on the cell membrane in all the encapsulation groups, especially in 0.5% 8-layer group. With time going on, the rectangle-like structures on cell surface in 0.5% 8-layer group became less and eventually similar to that in control group. The quantitative average roughness (Sa) of the surface topography also conform to the map of the AFM result. Sa gradually increased as materials of higher concentration were used or more layers were coated. At the time points day 3, 5 and 7, Sa was reduced gradually, implying the degradation of materials.

These phenomena suggested that the LbL encapsulation would form additional structures on cell surface and thus change the roughness. This could provide direct evidence for the characterization of LbL encapsulation since the surface change was markedly straightforward. The dynamic presence of LbL structures in the first 5 days also explained the time-course change of the permeability which would be discussed later.

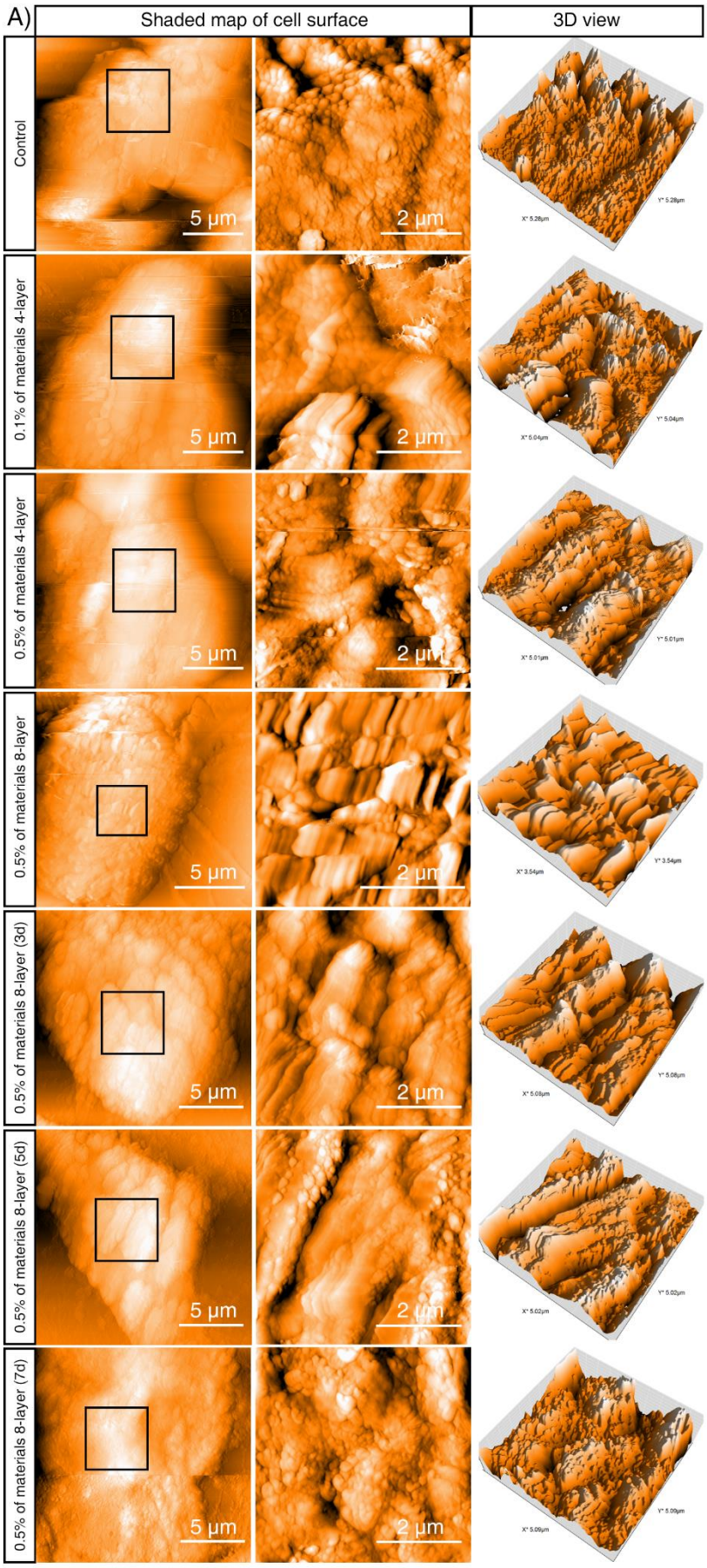
A)
Shaded map of cell surface
3D view
Control
0.1% of materials 4-layer
0.5% of materials 4-layer
0.5% of materials 8-layer
0.5% of materials 8-layer (3d)
0.5% of materials 8-layer (5d)
0.5% of materials 8-layer (7d)
5 μm
2 μm

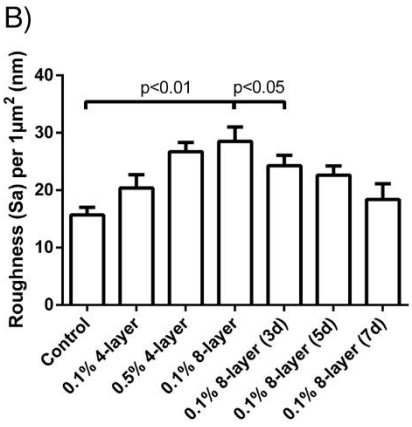
B)
Roughness (Sa) per 1μm² (nm)
40
30
20
10
0
p<0.01
p<0.05
Control
0.1% 4-layer
0.5% 4-layer
0.1% 8-layer
0.1% 8-layer (3d)
0.1% 8-layer (5d)
0.1% 8-layer (7d)

Figure 21. Representative AFM images of untreated PC12 cells and encapsulated PC12 cells. A) Shaded map of cell surface on untreated cells, cells encapsulated with 0.1% of materials for 4 layers, 0.5% of materials for 4 layers and 0.5% of materials for 8 layers at different time points. Images in middle column showed the magnified view of the fields in left column. 3D view of these magnified images was demonstrated in right column. B) Average roughness value per 1 μm^2 in each group; (n=4).

5.4 Permeability of LbL Encapsulation to FITC-dextran (FD)

Semi-permeability has been recognized as a remarkable feature of LbL structure. Since the substance transportation is of great importance to cells, it is necessary to describe the extent to which the permeability of materials changes under different situations. Dextran is a polysaccharide which can display a wide range of molecular weights since it can be customized with chains of varying length[395]. FITC-labelled dextran with different molecular weights is used as a tool for investigating the permeability, as previously described in many studies[396-399].

The general procedure of the experiments could be elucidated in Scheme 2. Untreated PC12 cells and cells encapsulated with 0.5% of materials for 8 layers were incubated with FD of 4 kDa and 250 kDa respectively on day 0, 3, 5 and 7. Under a fluorescence microscope, permeability of encapsulation to 4 kDa was found increased after day 3 and permeability to 250 kDa in encapsulation groups at all the time points decreased compared to that of control groups (Figure 22A). Simultaneously,

fluorescence intensity of each group obtained by the spectrometer exhibited similar results. To be specific, the encapsulation contributed to 22.9 ± 11.9% of reduction for the permeability to 4 kDa only on day 0, while, there was no difference on the following days. Likewise, permeability to 250 kDa was reduced by 35.4 ± 27.1%, 33.7 ± 40.6%, 18.2 ± 21.5% and 20.0 ± 20.8% on day 0, 3, 5 and 7 respectively (Figure 22B). Together with the results of permeability to FD of 40 kDa in Figure 23, a conclusion could be drawn that the permeability of LbL structures to FD would decrease as the molecular weight of FD became higher. From the above, since the permeation of small molecules and the blocking of large molecules were irrelevant to encapsulating parameters, FD of 4 kDa and 250 kDa were not suitable probes for examining the permeability of LbL structure.

FD of 40 kDa was proven to be a better probe since its moderate molecular weight helped to evaluate the permeability of LbL structure with different parameters. Untreated PC12 cells; cells encapsulated with 0.1% of materials for 4, 8 and 12 layers; 0.5% of materials for 4 and 8 layers were incubated with FD of 40 kDa on day 0, 3, 5 and 7. In Figure 23, images of fluorescence showed that encapsulation with 0.1% of materials failed to exert blocking effect against FD. On the contrary, permeability of FD in cells encapsulated with 0.5% of materials was significantly decreased. As further confirmed in fluorescence intensity test, FD was effectively blocked by 34.9 ± 8.8% and 16.9 ± 13.1% in 0.5% 4-layer group on day 0 and day 3; 33.2 ± 9.4%, 22.6 ± 16.8% and 12.3 ± 10.0% in 0.5% 8-layer group on day 0, day 3 and day 5. As such, permeability to molecule with a certain molecular weight was reduced when higher

concentration and more layers were applied. Encapsulation with 0.5% for 4 or 8 layers can maintain the balance between the satisfactory proliferation rate and distinct blockade against molecules with molecular weight of 40 kDa.

As suggested in Figure 24, pH of medium might affect the permeability of LbL multilayers. To determine the change of materials under different medium pH, PC12 cells were encapsulated with gelatin-FITC and HA for 8 layers and then cultured in medium with pH of 3.0, 5.0, 7.0, 9.0 and 11.0 for 12 h. Under a microscope, it could be observed that the coating materials largely vanished in the groups of medium with pH of 3.0, 9.0, and 11.0 (Figure 24A). When cells were encapsulated with 0.5% for 4 and 8 layers and incubated with FD 40 kDa for 30 min, the permeability decreased by 24.5 ± 12.4% and 10.7 ± 9.3% in groups of pH 5.0 and 7.0 respectively (Figure 24A and 24B). This outcome was attributed to the interfered integrity of LbL structures on cytoplasmic membrane since the two polyelectrolytes tended to gain the same electric property when pH was extremely high or low, which resulted in a weak adsorption of the polyelectrolytes. Another explanation might be the damaged internal bonds between each layer[137].

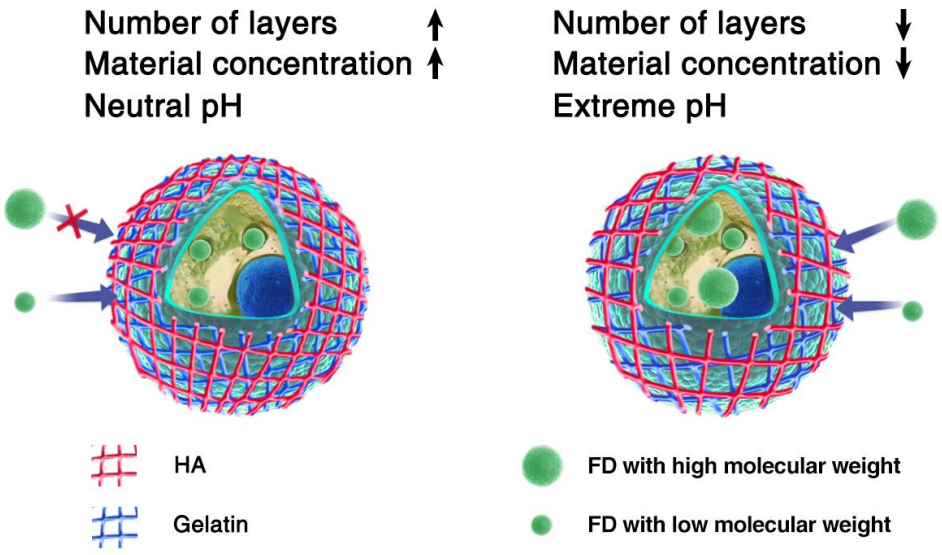

Scheme 2. The scheme of permeability of FD through LbL encapsulation. In neutral pH, when material concentration and number of layers increases, the pore size of the encapsulation structure is smaller, allowing passage of only molecules with lower molecular weight. Reversely, when pore size is enlarged, molecules with both high and low molecular weights are allowed to pass.

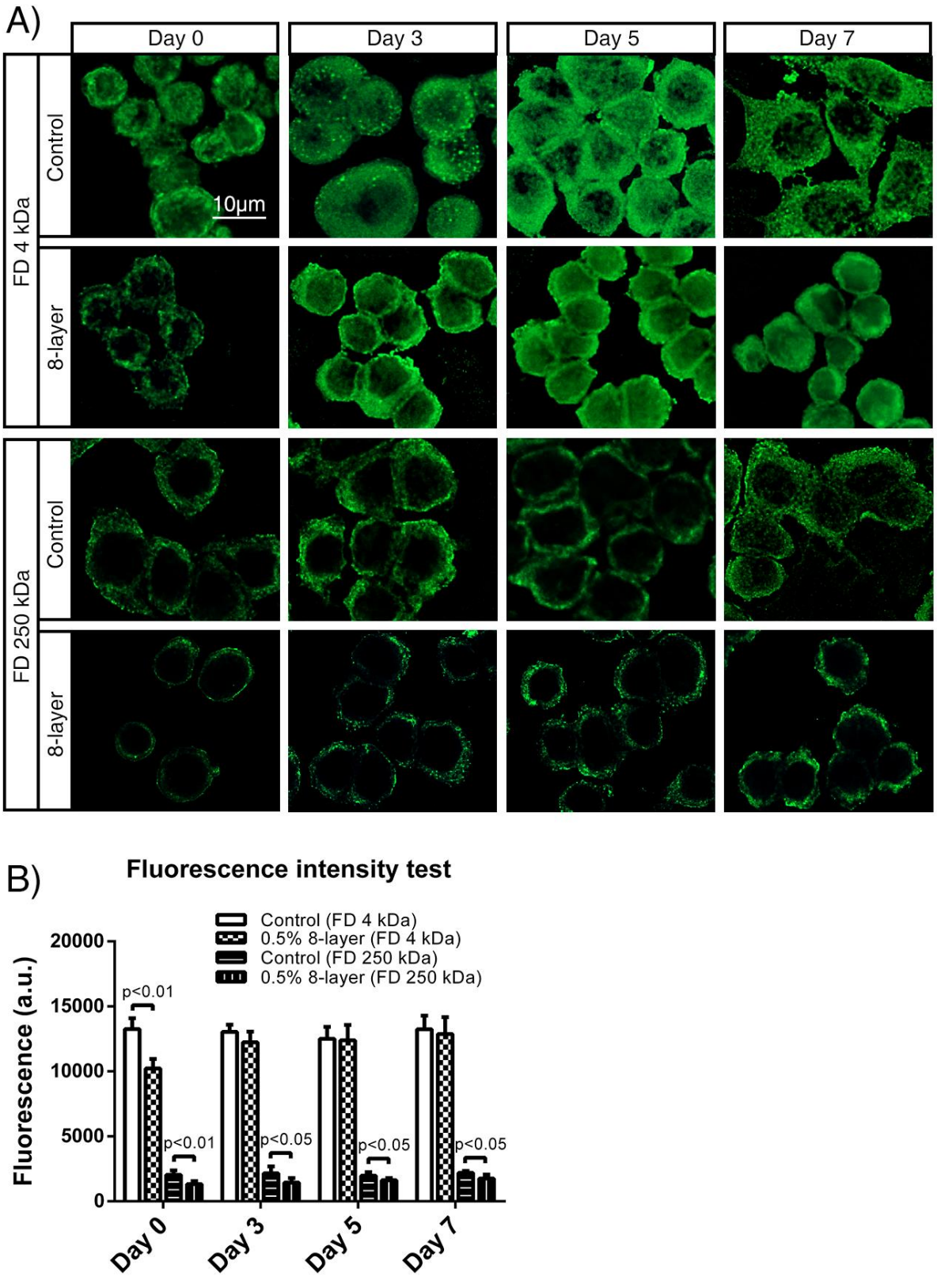

Figure 22. Permeability of encapsulation with 0.5% 8-layer to FD 4 kDa and 250 kDa.A) FD 4 kDa and 250 kDa in untreated PC12 cells and cells encapsulated with

0.5% of materials for 8 layers after 30-minute incubation at different time points. B) Fluorescence intensity test of FD 4 kDa and 250 kDa in different groups. a: $p < 0.01$ when FD 4 kDa in control group vs. that in encapsulation group; (n=5).

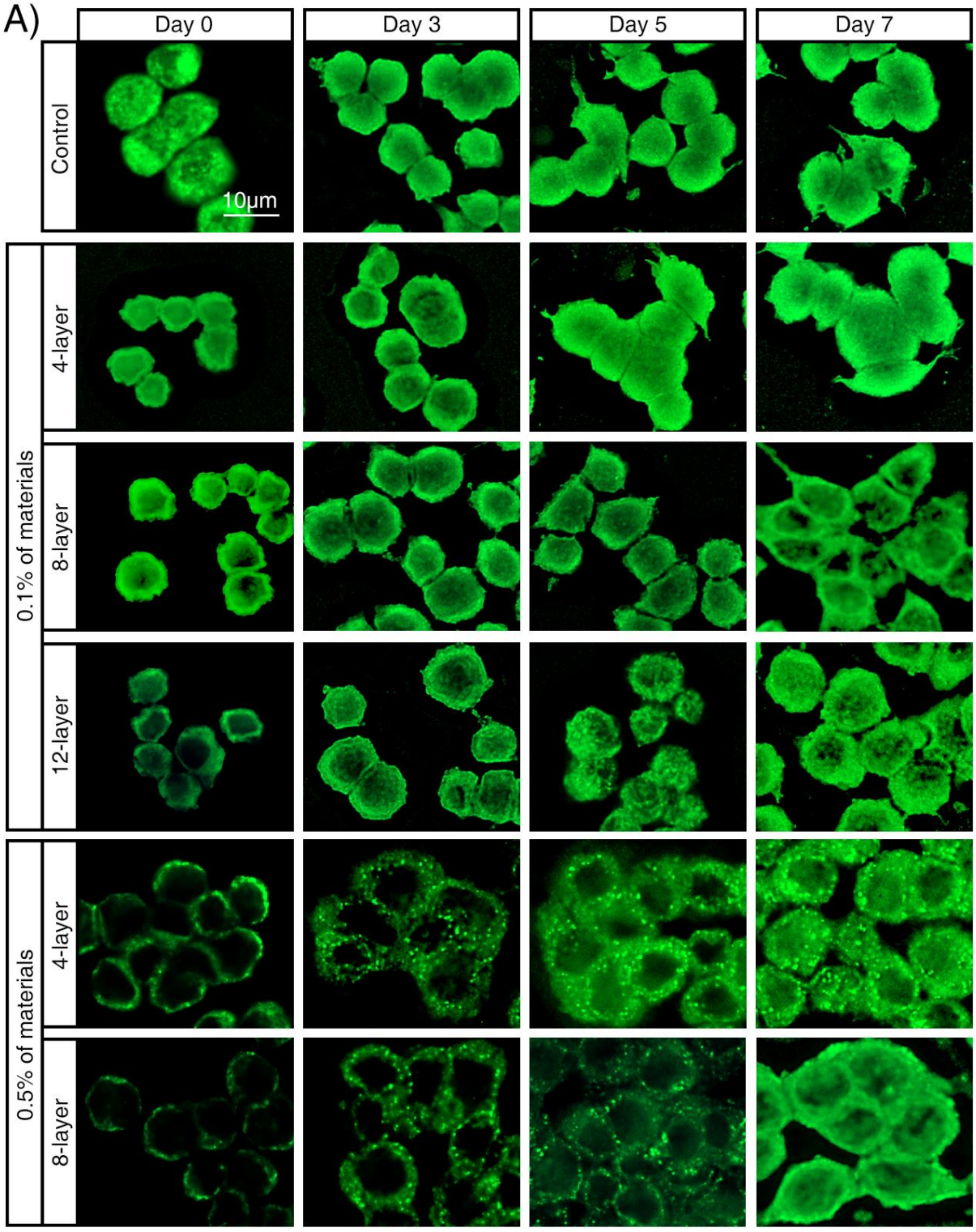

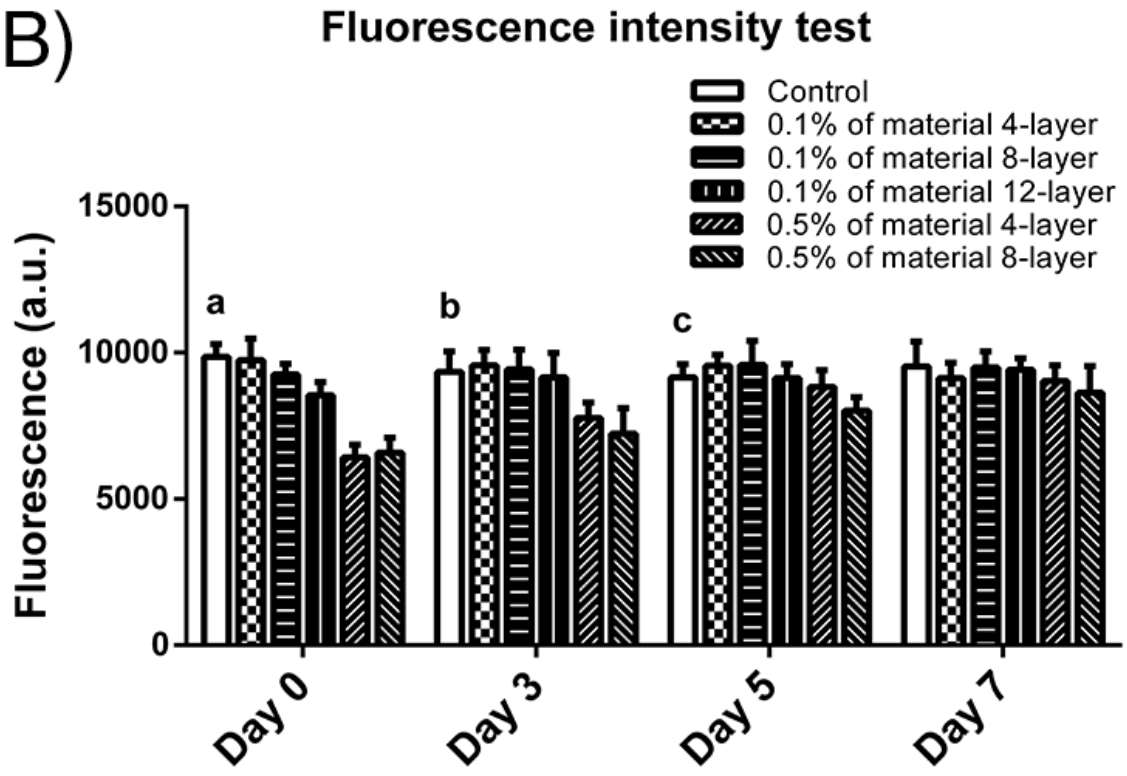

Figure 23. Permeability of encapsulation with 0.1% and 0.5% of materials to FD 40 kDa.A) FD 40 kDa in untreated PC12 cells and cells encapsulated with 0.1% of materials for 4, 8, and 12 layers and 0.5% of materials for 4 and 8 layers after 30-minute incubation at different time points. B) Fluorescence intensity test of FD 40 kDa in different groups. a: $p < 0.01$ when FD 40 kDa in control group vs. that in 0.1% of materials for 12-layer encapsulation group and 0.5% of materials groups; b: $p < 0.01$ when FD 40 kDa in control group vs. that in 0.5% of materials encapsulation group; c: $p < 0.01$ when FD 40 kDa in control group vs. that in 0.5% of material for 8-layer encapsulation group; (n=5).

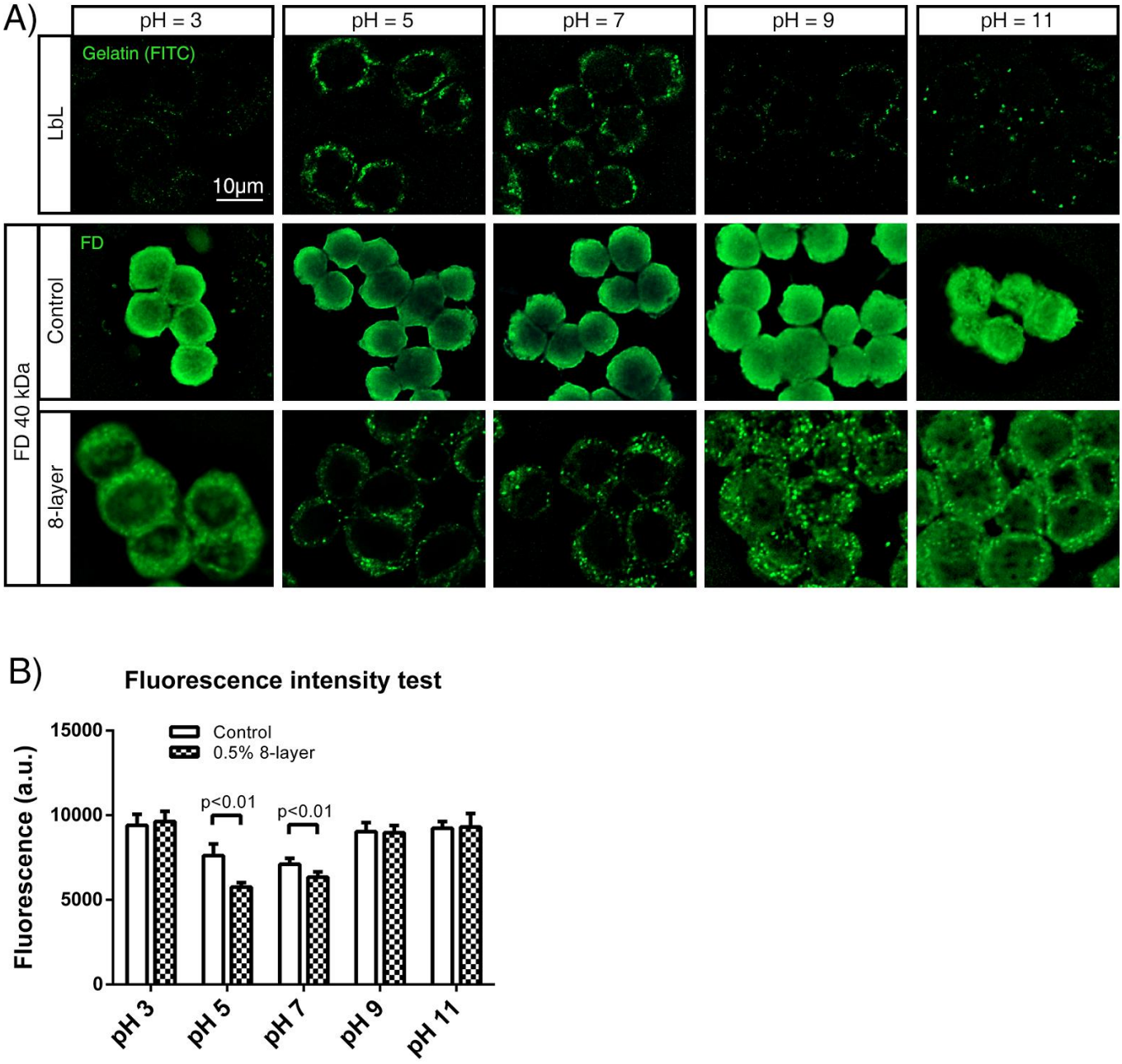

Figure 24. LbL encapsulation and permeability of encapsulation to FD 40 kDa under different medium pH. A) In the upper panel, PC12 cells were encapsulated with FITC-labeled gelatin and HA. They were cultured in medium with different pH value for 12h. In the lower two panels, untreated PC12 cells and cells encapsulated with 0.5% of materials for 8 layers. After being cultured in medium with different pH,

cells were incubated with FD 40 kDa for 30 minutes. B) Fluorescence intensity test of FD 40 kDa in different groups.

5.5 Using LbL Encapsulation to Block TNF-α-induced Apoptosis

The knowledge of permeability would assist to extend the application of single-cell encapsulation in many fields. For example, in the transplantation therapy for neurological diseases, TNF-α plays a major role in apoptosis of transplanted cells[400, 401]. This process requires the binding of TNF-α and its transmembrane receptor which is known as TNF-R1. After the TNF-R1 activation by binding with TNF-α, TRADD, RIP1, TRAFs and IAPs are recruited to form the complex which is acknowledged as TRADD-dependent complex I. Subsequently, complex II a/DISC is formed to trigger the caspase-3/8 activation leading to apoptosis[402]. As such, I hypothesize that LbL encapsulation is impermeable to TNF-α and blocks the activation of TNF-R1.

To test this hypothesis, proximity ligation assay (PLA) was applied to show the blocking effect of LbL encapsulation against TNF-α/TNF-R1 interaction. PLA is an assessment of protein-protein interaction. Primary antibodies to the two proteins are firstly applied to bind to proteins respectively. Next, specifically designed secondary antibodies recognizing the primary antibodies, which have short DNA strands attached, are incubated. Therefore, when the two proteins interact with each other (with a distance < 40 nm), the DNA strands from each secondary antibody will form a circle-like structure through the subsequent addition of ligase and oligonucleotides.

Finally, after the incubation with polymerase and fluorescent complementary oligonucleotides, the DNA circle is tremendously amplified to yield the fluorescence that indicates the interaction visible under a fluorescence microscope. PLA is of critical importance for investigation of TNF-α/TNF-R1 interaction since it is able to exhibit directly the functional blockade effect of LbL encapsulation in situ[403].

To begin with, untreated PC12 cells were stained with CFP-membrane staining reagent and gelatin-FITC was used in the encapsulation groups. Then the uncoated cells and cells encapsulated with 0.5% of materials for 4 and 8 layers were incubated with 20 ng/ml of TNF-α for 5 min on day 0, day 3 and day 7 (as shown in Scheme 3). Together with the negative control and cells treated with 10 μM of TNF-α antagonist, they were used for PLA. Red dots in Figure 25A represented for the interaction between TNF-α and its receptor TNF-R1. From Figure 25 and 3D reconstruction (Movie 1-3), the interaction was significantly reduced by 32.2 ± 27.0% in 4-layer group and 60.0 ± 23.5% in 8-layer group on day 0; it decreased in 8-layer group by 34.5 ± 21.1% on day 3; no difference was found among all the groups on day 7. The blockade effect of 8-layer encapsulation was proven to be satisfied since it showed no difference from that of antagonist group on day 0. FD 20 kDa was also applied for investigating the permeability since the molecular weight of TNF-α is close to it (Figure 25D). From the FITC fluorescence inside cells of different groups, it could be drawn that 8-layer nanogel was able to effectively inhibit the penetration of molecules around 20 kDa within 3 days. In general, encapsulation with 0.5% of materials for 8 layers exerted distinct effect on inhibiting the binding of TNF-α and TNF-R1 on day 0

and day 3.

TNF-α/TNF-R1 interaction was further verified by Co-IP. Uncoated PC12 cells, cells encapsulated with 0.5% of materials for 4 and 8 layers were incubated with 20 ng/ml TNF-α for 5 min. From the blotting (Figure 26), the TNF-α/TNF-R1 interaction was decreased in the encapsulation groups. This was consistent to the PLA results that encapsulation was effective in blocking the TNF-α/TNF-R1 interaction.

Effect of LbL encapsulation on TNF-α-induced apoptosis was examined on PC12 cells. Uncoated PC12 cells and cells encapsulated with 0.5% of materials for 8 layers were incubated with 20 ng/ml of TNF-α and 1 nM of Actinomycin D (ActD) on day 0, day 3 and day 7[404]. Cell counting was performed on cells incubated with TNF-α, ActD, both and none. The number of cells decreased dramatically in groups with both TNF-α and ActD. Significantly more cells in the encapsulation group survived than in the uncoated cells on day 3 and day 7 (Figure 27A). TUNEL apoptosis staining showed the apoptosis in 8-layer encapsulation was much lower than that in 0-layer group at different time points (Figure 27 B-C). These data indicate that encapsulation with 0.5% of materials for 8 layers protects the cells from apoptosis induced by TNF-α. Therefore by tuning the encapsulation parameters, TNF-α-induced apoptosis can be blocked. This enlightens the potential of LbL single-cell encapsulation in transplantation studies in the future.

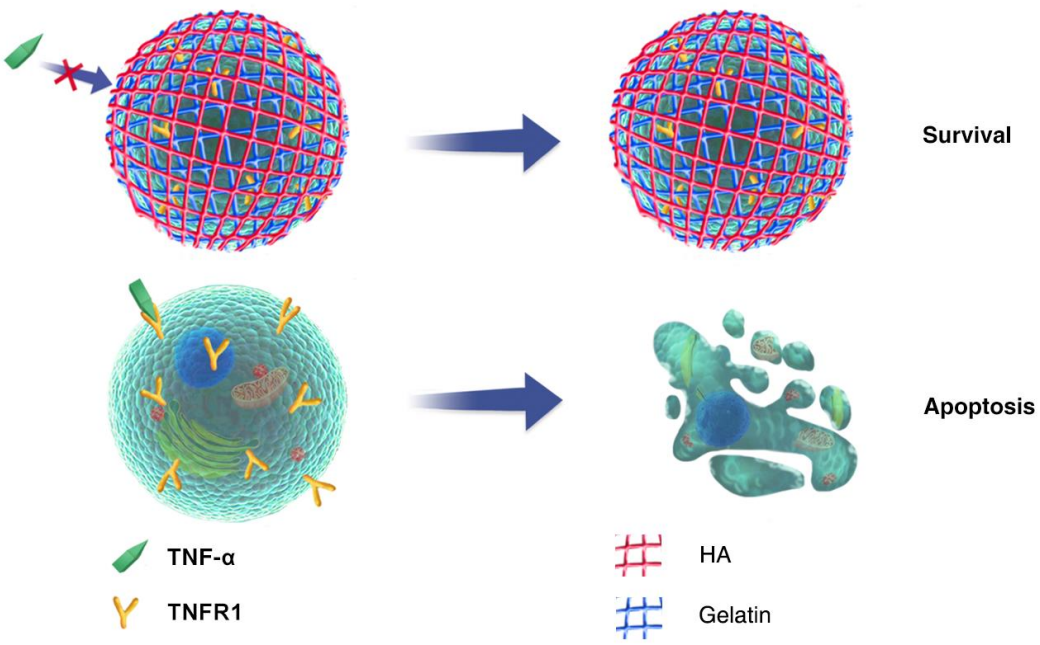

Scheme 3. The inhibition of binding between TNF-α and TNF-R1 by applying LbL encapsulation. In upper panel, the encapsulation is impermeable to TNF-α and blocks its binding with its receptor TNF-R1. In lower panel, TNF-α binds with TNF-R1 in untreated cells to induce apoptosis.

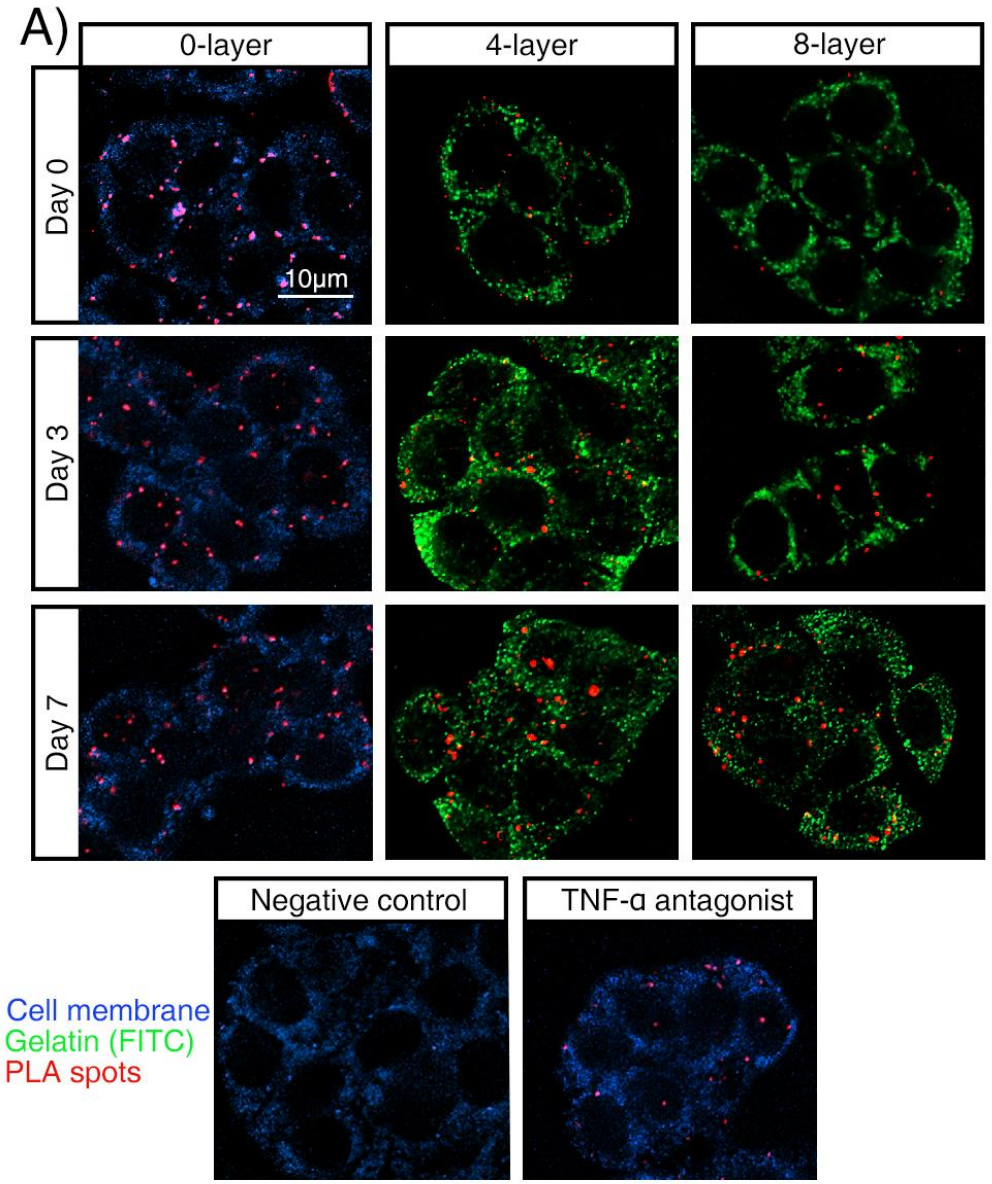
A)
0-layer
4-layer
8-layer
Day 0
Day 3
Day 7
10μm
Negative control
TNF-α antagonist
Cell membrane
Gelatin (FITC)
PLA spots

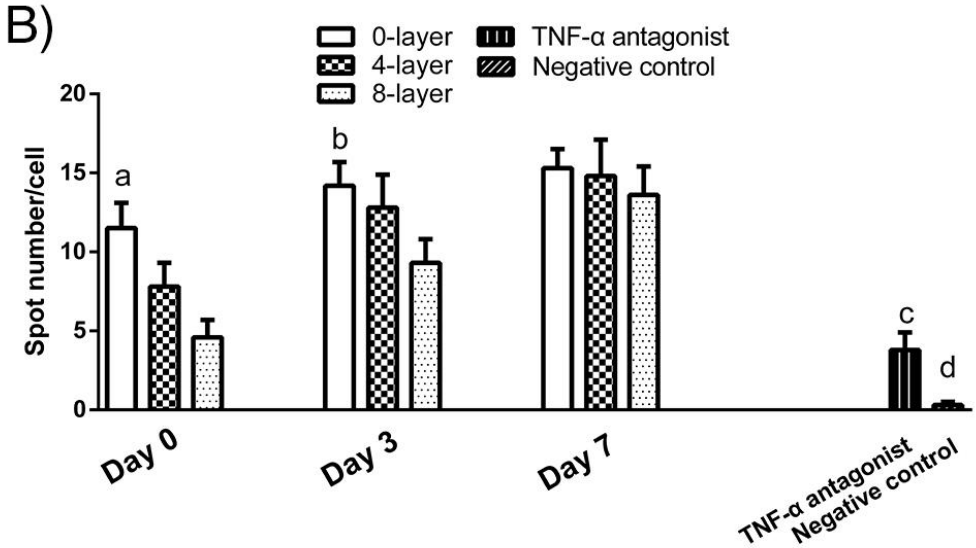
B)
0-layer
4-layer
8-layer
TNF-α antagonist
Negative control
Spot number/cell
20
15
10
5
0
a
b
c
d
Day 0
Day 3
Day 7
TNF-α antagonist
Negative control

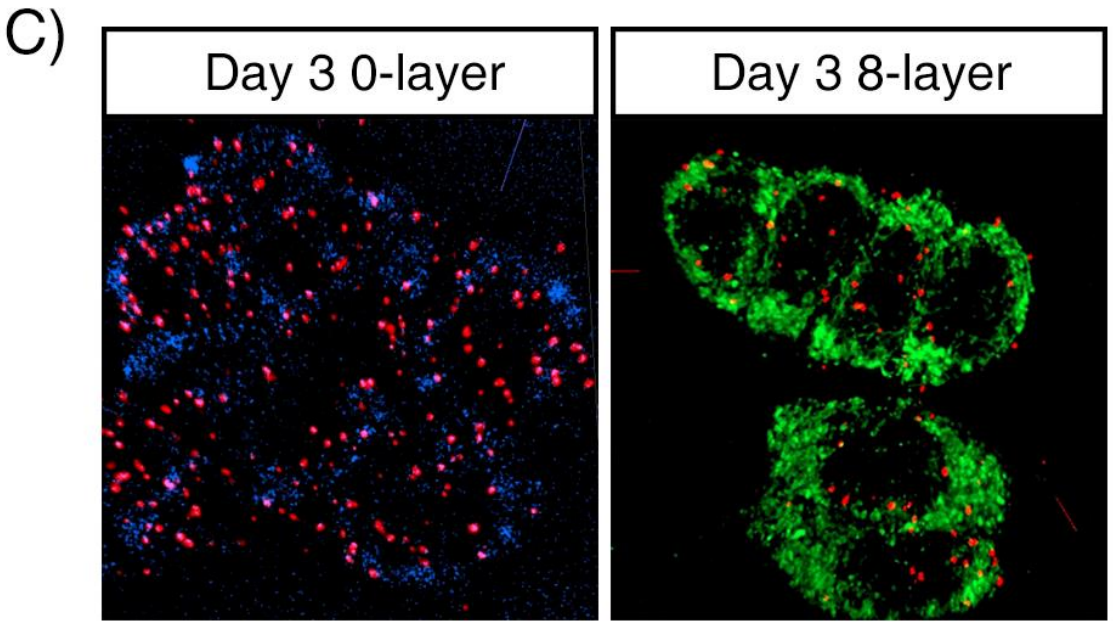
C)
Day 3 0-layer
Day 3 8-layer

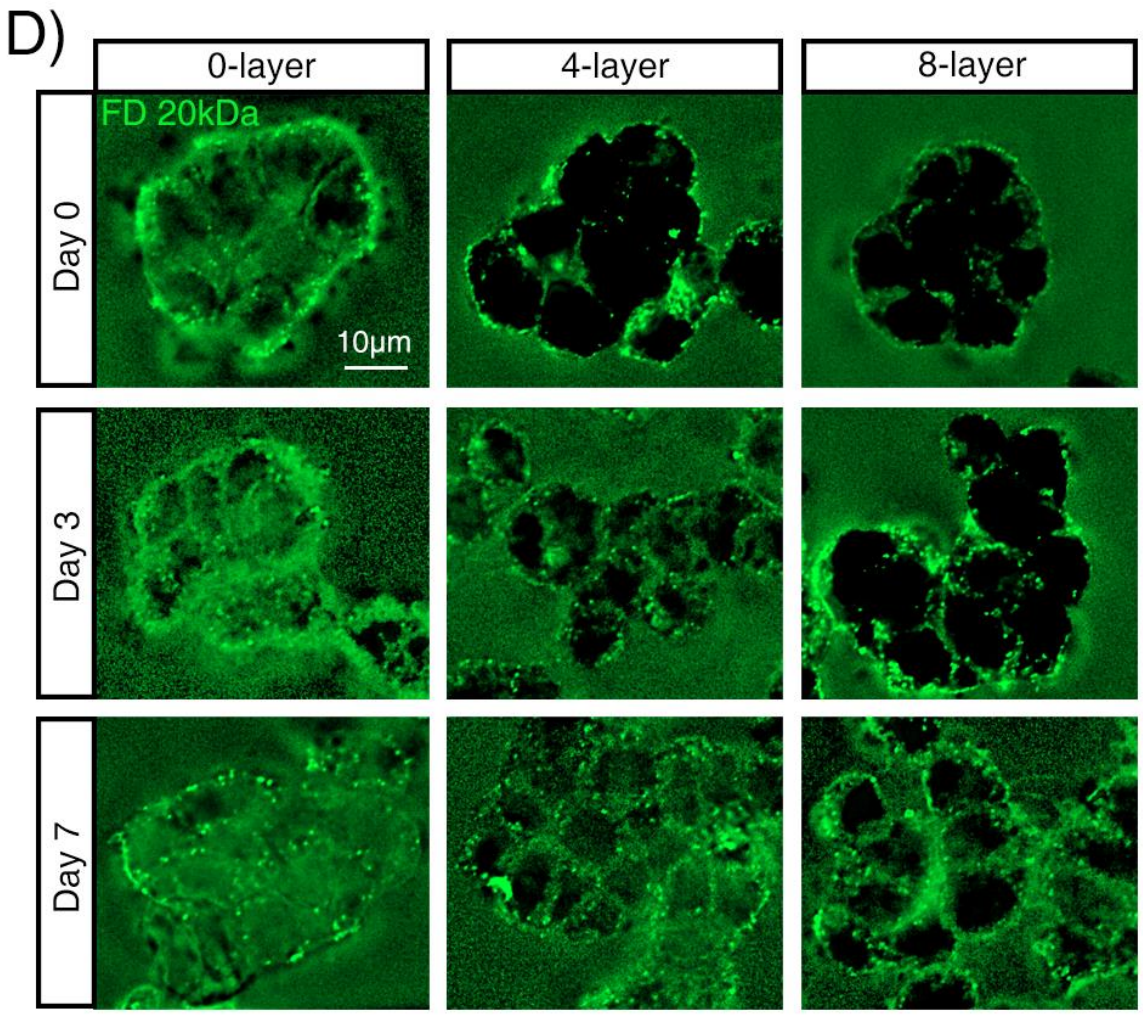
D)
0-layer
4-layer
8-layer
Day 0
Day 3
Day 7
FD 20kDa
10μm

Figure 25. Interaction between TNF-α and TNF-R1 by PLA. A) Uncoated PC12 cells were stained with CFP-membrane kit, and encapsulated cells were applied with FITC-labeled gelatin and HA. 20 ng/ml TNF-α was incubated with cells for 5 min at different time points. In negative control group on day 0, no primary antibody was used. In antagonist group, cells were added with 10 μM TNF-α antagonist prior to the addition of TNF-α on day 0. All the groups were processed with PLA and the positive signals were shown as red. B) Quantification of PLA dots in different groups. a: $p< 0.01$ when PLA dots in 0-layer group vs. that in encapsulation groups; b: $p< 0.01$ when PLA dots in 0-layer group vs. that in 8-layer encapsulation group; c: $p< 0.01$ when PLA dots in antagonist group vs. that in 0-layer and 4-layer encapsulation groups on day 0; d: $p< 0.01$ when PLA dots in negative control group vs. that in all groups on day 0; (n=5). C) Images captured from Movies 1 and Movie 3. D) Permeability of nanogel encapsulation to FD 20 kDa. Cells of 0-layer, 4-layer and 8-layer groups were grafted and incubated with FD 20 kDa at different time points. Fluorescence microscope was applied for imaging, showing the diffusion of FD molecules in each group.

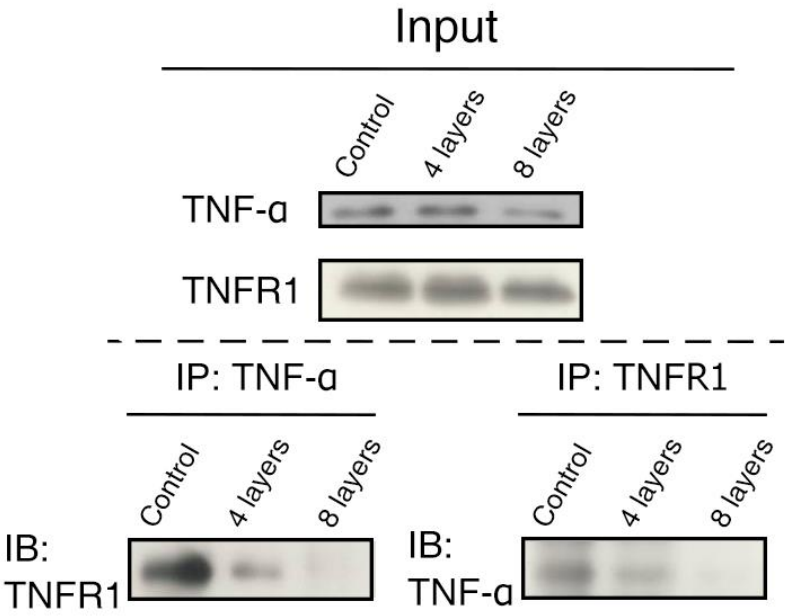

Figure 26. Co-IP of TNF-α and TNF-R1. Uncoated PC12 cells and encapsulated cells were treated with TNF-α for 5 min. The cell lysate was used as input. Cell lysate was also precipitated by anti-TNF-α and anti-TNF-R1 respectively and expression of TNF-R1 and TNF-α was detected.

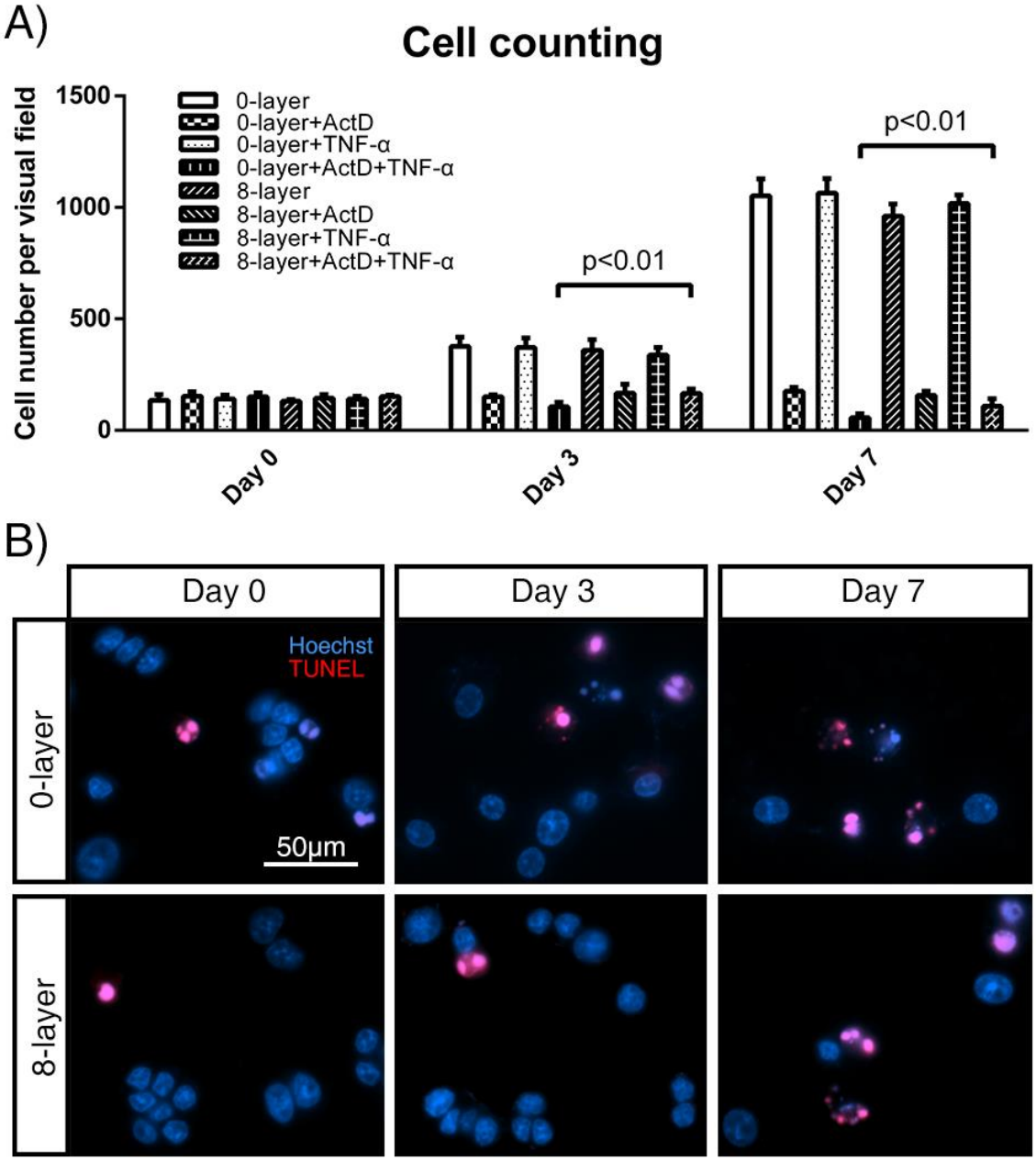
A)
Cell counting
Cell number per visual field
1500
1000
500
0
0-layer
0-layer+ActD
0-layer+TNF-α
0-layer+ActD+TNF-α
8-layer
8-layer+ActD
8-layer+TNF-α
8-layer+ActD+TNF-α
p<0.01
p<0.01
Day 0
Day 3
Day 7
B)
Day 0
Day 3
Day 7
Hoechst
TUNEL
0-layer
8-layer
50μm
C)
0-layer
8-layer
Apoptosis rate (%)
80
60
40
20
0
p<0.01
p<0.01
p<0.01
Day 0
Day 3
Day 7

Figure 27. Apoptosis of uncoated and encapsulated cells. A) Cell counting of each visual field in 0-layer and 8-layer encapsulation groups at different time points. a: $p < 0.01$ when cell amount in 8-layer+ActD+TNF-α group vs. that in 0-layer+ActD+TNF-α group; (n=5). B) TUNEL staining of cells in 0-layer and 8-layer encapsulation groups at different time points. C) Quantification of positive rate of TUNEL staining indicating apoptosis. (n=5).

Chapter 6. Discussion

6.1 Encapsulation of NSCs and its application in drug delivery

In this study, we have achieved the single-cell encapsulation with LbL self-assembly technique. Type A gelatin and alginate are proved to be suitable polycation and polyanion with reasonable biocompatibility and biodegradability, compared to synthetic materials such as PEI and PLL. TEM and SEM provide us convincing evidence of the LbL encapsulation, with a thickness of 6 ± 2.3 nanometers. Additionally, fluorescence labeling, fluorescence intensity test and zeta-potential assay have further verified the encapsulation. On the basis of successful coating with biocompatible materials, I have determined whether the technique and materials influence the normal functions of NSCs. By means of immunofluorescence staining, proliferation and differentiation of encapsulated NSCs are not impacted. However, the encapsulated cells show somewhat a shrunk appearance, indicating the cytoskeleton of the cells may be affected. To test its drug delivery capability, IGF-1 was loaded on alginate. When NSCs were encapsulated with gelatin and the IGF-1-loaded alginate, IGF-1 was released in a time-dependent pattern, and the release was more consistent under pH 6.5. As a result, the encapsulated NSCs exhibited better proliferation rate and higher survival rate under acidic condition. This feature is potentially applicable in the cell therapy for nervous system diseases in the future. As such, the study illustrated that LbL single-cell encapsulation as a novel tissue engineering technique, showing robust potentials in treating nervous system diseases and stem cell research

in the future.

6.2 LbL self-assembly technique for cell encapsulation

LbL self-assembly is a technique developed on the basis of electrostatic adsorption between oppositely charged polyelectrolytes[12]. The simple fabricating process which involves immersing substrate into polyelectrolyte solutions with opposite charges enables the expansion of the scope from polymers to nanoparticles[405], graphene[406], colloids[407] and biological molecules[408-410]. Besides the electrostatic adsorption, interactive mechanisms such as hydrogen bonding[411], stereo-complex formation[412], charge transfer[413] and covalent bonding[414] have been addressed to be available for construction of multilayers. It has already been applied in the fields such as chemistry, pharmacy and biology. In cell biology, novel applications such as bioreactors and biosensors have been achieved by means of LbL technique[415, 416]. For example, glucose oxidase was encapsulated with PAH and PSS to establish the bioreactor which has a homogeneous size, high enzymatic activity and high permeability to small substances. A significant shift of glucose concentration was detected, suggesting the enzymatic reaction within the nano-bioreactor system[415].

Inspired by the encapsulation study on the cores from chemical compounds, cells have been encapsulated to form the single-cell model. Cell membrane exhibits negative charges since there are abundant negatively charged groups such as phosphatidylserine and proteoglycans on the cell membrane[417, 418]. This feature facilitates the coating on cell surface by positively charged materials. With the simple

dip-coating of excessive gelatin and alginate, NSCs can be encapsulated in our study. This approach combines cell biology and material science together and opens up a new avenue for basic and translational studies in these fields.

6.3 Cell encapsulation in mammalian cells

Most of the cell encapsulation studies have been performed on bacteria and fungi initially, since lots of the polyelectrolytes are cytotoxic. For example, Park *et al*. designed a catalyzing peptide ($R_4C_{12}R_4$ (R: arginine; C: cysteine)) which mimics the activity of silicateins, for hydrolyzing tetraethyl orthosilicate to produce silica. The peptide was applied in the yeast cell encapsulation and helped to form an encapsulating shell of silica, which was demonstrated to effectively resist the enzymatic activity of lyticase[25].These cells have a cell wall, thereby they can tolerate the stimulation by foreign substances and the encapsulating process[419, 420]. Nevertheless, the conditions will lead to severe damage to mammalian cells so that they cannot be applied directly in mammalian cell studies. However, only the non-mammalian cells with a cell wall such as yeast cells can sustain the procedure. Contrarily, mammalian cells lack cell wall, so they are more sensitive when exposed to the toxic materials and irritating manipulating. This is prominent in synthetic polycations which form pores on cell membrane of mammalian cells to impair its integrity, causing cell death[29]. As such, the selection of materials on mammalian cells is restricted. For the fragile mammalian cells, especially the cells from nervous system, natural polymers such as gelatin, alginate and HA are more appropriate due to their biocompatibility without the need of modification[421]. Synthetic

polyelectrolytes are advantageous in batch consistency which is favorable for functional modifications. The potent positive electricity of synthetic polycations also exceeds that of natural polymers[81]. To reduce their cytotoxicity, chemical modification is verified to be effective. For example, PEG was conjugated on PLL branches prior to the cell encapsulation on mouse MSCs[422]. PEG conjugation is known to block the lysine residuals on PLL backbone, attenuating the pore formation on cell membrane caused by the strong positive charges[423]. In this context, the selection of appropriate polyelectrolytes needs solid screening from literature and practical work.

6.4 Encapsulation with gelatin and alginate

General processes of NSCs encapsulation is demonstrated in Scheme 1. The establishment of artificial microenvironment is an approach of functional regulation for NSCs. NSCs are acknowledged to be located in SVZ and SGZ, surrounded by endothelial cells, ependymal cells, astrocytes, ECM and regulators which compose the microenvironment. NSCs can only survive and function normally when homeostasis of the microenvironment is maintained[424]. Under the conditions of the nervous system insults, complements, radical oxygen species and excitatory amino acids will be aggregated in the focal areas, leading to the death of NSCs[355]. With the help of LbL technique, single-cell encapsulation manages to fabricate individual microenvironment by coating multiple material films on surface of each cell. Therefore, the functional regulation is exerted at single-cell scale instead of at cell mass to make the regulation more precise and homogeneous[425]. It will be

especially suitable to apply ECM-derived macromolecules such as gelatin, alginate and HA for providing affinitive and biocompatible environment for NSCs. In this study, gelatin and alginate are applied as the coating materials on NSCs. Gelatin which is highly biocompatible is derived from collagen, so that it has similar characteristics to the constituents of natural ECM. It also exhibits positive charges under certain conditions[357]. Alginate is a biocompatible polyanion being applied extensively in tissue engineering, especially the studies in nervous system[358]. These natural polymers are able to form protective layers on cells by electrostatic interaction under neutral condition for 7-10 days. As time passes by, it was observed with TEM and fluorescence labeling that NSCs divided and the attaching materials gradually became discontinuous or broken. One reason is that the materials are degraded by endocytosis[426]. The second possibility is that the materials disassembled following the changing of surface charge on NSCs caused by cellular behaviors such as pseudopodial protrusions[427]. The third possible reason is that cell dividing results in the impaired integrity of the coated materials[428].

6.5 Encapsulation for drug delivery

Chemically-reactive groups such as amine groups, carboxyl groups and hydroxyl groups exist in the structure of materials, therefore the materials can be functionally modified via chemical modification or bioactive molecules loading to further modulate the functions of encapsulated NSCs. For example, carboxyl groups on side chains of gelatin were crosslinked with amine groups to obtain cationic gelatin. The modification provides gelatin with more positive charges with higher affinity to

polyanions, without significant increasing of cytotoxicity[51]. In our study, LbL single-cell encapsulation endowed NSCs with an artificial microenvironment for regulation through IGF-1 delivery. IGF-1 belongs to the insulin-like hormone family, mainly synthesized in hepatocytes. It is also present in diverse types of cells, especially important in regulating development and plasticity of cells in nervous system[429]. IGF-1 binds to receptor IGF1R which is a glycoprotein located on cell membrane to implement the functions[430]. The β subunits of IGF1R serve as a tyrosine kinase to induce the downstream cascades such as PI3K/AKT1 and MAPK/ERK after the interaction with IGF-1[431, 432]. These signaling pathways are closely associated with promotion of cell survival, cytoskeleton kinetics, proliferation and differentiation[433-435]. In CNS, IGF-1 is demonstrated to be critical for brain formation and synapse integrity[436-438]. It is also shown to enhance the proliferation of NSCs and differentiation of neurons *in vitro*[378, 439]. In addition, the 4 reactive amino groups in IGF-1 and the IEP of 8.5 endow IGF-1 with the capacity of material-loading. The subsequent IGF-1 release is exhibited to exert trophic effects for target cells[440, 441].

As we addressed, IGF-1 was loaded on alginate and it could then be released after encapsulation to enhance viability and proliferation of NSCs. Since IGF-1 has a more sustained releasing pattern under pH 6.5, this approach is supposed to be ideal for improving NSCs therapy in nervous system diseases. In diseases such as spinal cord injury and stroke, pH in the lesion areas will be lowered to 6.5 due to the aggregation of acidic metabolites[355]. The value of 6.5 is in the middle between IEP of gelatin

and alginate, so that these polymers will ionize to a large extent to adsorb firmly[357]. In this way, the LbL encapsulation structure becomes stable to prevent IGF-1 in the inner layer from leaking out fast, therefore there will be less microenvironment intervention due to the burst release which also prevents sustained nourishing[389]. At the same time, these nonimmunogenic materials can stay in sites for about 7 to 10 days, which will be sufficient for drug releasing to improve the cell survival and other activities. From the above results, it can be drawn that the interaction between IGF-1 and the receptors are not significantly influenced. It is hypothesized that the combination of IGF-1 with its receptors will not be interfered by the interaction between receptors and the covered materials. Another explanation is that the materials do not block the binding sites for ligands, so that the IGF-1 which has a small molecular weight of 7.6 kDa can pass through the multilayers to activate the receptors. In the future study of cell transplantation, LbL encapsulation is expected to not only provide protection for NSCs, but also make each NSC an IGF-1 reservoir for modulating the microenvironment of grafting sites. Except for the promising aspects, the details of drug release from LbL structure needs clarifications in the future, such as the kinetics, concentration equilibrium and the functional status alteration.

6.6 Permeability of encapsulation structure and inhibition against apoptosis

In this part, we have investigated the permeability of LbL single-cell encapsulation on PC12 cells which serve as the neuronal model. Low cytotoxicity was observed after the encapsulation by gelatin and HA with varied parameters, but concentration of 1% often caused impaired proliferation. Characterization by TEM and fluorescence

labeling demonstrated the evidence of single-cell encapsulation. Surface distribution of the polymers was clearly exhibited by means of the AFM scanning which indicated the increased roughness coefficient after encapsulation. From the permeability study on the other parameters, it is found that molecular weight of FD is inversely proportional to the permeability. For a certain FD molecule, its permeability is inversely proportional to the material concentration and layer thickness. Moreover, with the use of materials with the concentration of 0.5%, interaction between TNF-α and TNF-R1 was effectively hindered on day 0 and day 3. The fact indicates decreased permeability of material layers to TNF-α molecules and improved survival of cells due to the protection by LbL encapsulation. The study has great potential in the transplantation research at next stage for providing cells a shell that is not only physically protective, but also selectively permeable. In this context, it is potentially a powerful approach for research in both cell biology and translational studies.

6.7 Permeability of LbL encapsulation structure

Permeability is an inherent feature of LbL multilayers. Since the LbL encapsulation forms a protective shell outside the cell, the permeability of the shell will undoubtedly influence the cellular functions. However, studies on this feature in cell encapsulation are rare. The number of layers is found to distinctly affect permeability to substances. The permeability decreases tremendously with the increasing of layer numbers before the 8th coating, and the trend will slow down in the subsequent coating. It can be explained that the inner eight layers of materials adsorb to each other compactly, endowing significant influence on permeability. Afterwards, the layers become loose

when more materials are applied, so that the influence is getting subtle. It is also explained that the blocked pores on the encapsulating materials reach saturation[442]. As another factor, pH value also affects the permeability of multilayers by influencing the ionization of polyelectrolytes. When the pH deviation from IEP values of the two polymers shifts to extreme value such as pH 11.0, the ion strength in the solution increases due to the foreign ions. As a result, these polymers will fail to attach firmly because of their deprotonation[443]. Another study points that strong ion concentration will probably break the electrostatic interaction among the layers, collapsing the LbL structure[444]. Material concentration is either important. Interfaces will adsorb more materials averagely and there will be denser pore distribution. Therefore, the increase of concentration is always inversely proportional to the permeability before the saturation of bound materials[137]. The influences of material concentration, layer thickness and pH have already been verified to be similar on permeability of cell encapsulation in our studies.

At present, permeability to the necessary ingredients for cells have not been investigated. Based on the existing documents of the medium formula for cell culture, most of the substances have the molecular weight of less than 1 kDa. Depending on facts that the encapsulation in our studies possesses no significant interference on cellular functions and the FD results exhibit a remarkable permeability of LbL structure to small molecules, it is implied that the encapsulation structure will not distinctly block the nutrients less than 1 kDa. Although a couple of proteins such as albumin and hemoglobin have the molecular weight of 60 kDa which will be partly

blocked, the overall metabolism can still be maintained normally. As shown in our IGF-1 delivery study, functions of IGF-1 are not interfered by cell encapsulation. Although it can be explained by the use of low material concentration and less coating layers, details in the IGF-1 permeability through the encapsulation structure is elusive. In the future, it is necessary to conduct comprehensive investigations on the multilayer permeability to these substances, which also include regulators such as IGF-1 (7 kDa) and bFGF (25 kDa), for obtaining a complete understanding of the influences on cellular functions. Simultaneously, cell-cell interaction is important for maintaining the normal functions of cells. Cells communicate and regulate functions by transporting messenger molecules through tight junctions and gap junctions which are constituted by occludins and connexins. One of the reasons why cell viability still remains generally intact is that junctions will regain the functions promptly after the coating materials are degraded or disassembled. Another possibility is that these natural polyelectrolytes will not disrupt the cellular junctions essentially, so that cells are barely influenced.

6.8 Permeability manipulation of cell encapsulation in cell therapy for central nervous system diseases

Exploration into the permeability of LbL single-cell encapsulation matters to the treatment of nervous system diseases. In nervous system trauma and disorders, homeostasis of the microenvironment in focal sites is disrupted. Survival and other functions of the cells in site and the fragile grafted stem cells in these areas will be harmed by different mechanisms. Various inflammatory factors such as TNF-α, C5a

and MMPs are involved[368, 445, 446]. Amongst blood components, thrombin inhibits migration of NSCs through the binding of protease-activated receptor (PAR)1, PAR3 and PAR4 located on the cell surface[447]; aggregation of ferric ions in the hemorrhagic cerebral injury also disrupts the microenvironment, deteriorating patients' prognosis[448]. Most of these cytotoxic factors exert biological effects by interaction with their receptors on cell membrane. In our study, LbL single-cell encapsulation with natural polyelectrolytes is used for cell protection. The materials are biocompatible and the encapsulation strategy is optimized to be gentle. Encapsulation with 0.1% of materials and 0.5% of materials for 4 and 8 layers is exhibited to be favorable for cellular functions. By adjusting the coating parameters, permeability to certain substances can be managed. For example, concentration of materials was adjusted to regulate the permeability to TNF-α for reducing the interaction with its receptor, alleviating the apoptosis of cells. It should be noted that these parameters are applied with the prerequisite of not influencing the cellular functions. Under the condition of cell therapy in the future, it may require higher concentration or more layers in encapsulation to inhibit adverse factors such as TNF-α to a larger extent. Theoretically, the survival of transplanted cells can be preserved in the acute phase with a temporary inhibition of proliferation. Afterwards, cells will regain the capacities of proliferation and differentiation when the coating materials are degraded.

In addition to the innate immune factors such as complements and inflammatory factors described above, adaptive immune response on allogenic cells should not be

neglected during the cell therapy. The most important proteins participating in the immunorecognition are the major histocompatibility complexes (MHC) I and II. They are synthesized in endoplasmic reticulum and translocated to cell membrane, mediated by the Golgi apparatus. During the immunology, MHC I which is expressed by all sorts of cells recognizes T cell receptors on $CD8^+$ cells and gets activated. On the contrary, MHC II complex binds to $CD4^+$ T cells to enhance them to differentiate into effector T cells. These effector T cells will then form memory T cells or stimulate B cells to produce antibodies[449]. In this context, following the cell transplantation, the allogenic cells expressing foreign proteins are recognized by recipients' antigen presenting cells and thus the cytotoxic T cells or helper T cells will be activated. Alternatively in a direct way, T cell receptors in hosts can also interact with MHC molecules located on the grafted cell surface to trigger the downstream incidents[450]. In nervous system, these principles also apply, although the CNS is previously regarded as immune-privileged[451]. In the clinical trials of cell therapies for nervous system disorders, for example PD, immunosuppressor was used simultaneously to maintain the long-term survival of the grafts[452]. However, it is acknowledged that application of immunosuppressor will bring about further concerns such as infections[453].

Immunoisolation is an alternative potential mechanism for cell protection by encapsulation permeability. As it is acknowledged, MSCs and NSCs which are commonly used cell grafts express MHC complexes and will be recognized by $CD4^+$/ $CD8^+$ T cells in the host in direct and indirect ways[454, 455]. In fact, some studies

have addressed that encapsulation of grafted stem cells effectively protect cells from immune attacks and enable them to function sustainably in treating neurodegenerative diseases[188, 456, 457]. For example, encapsulation of islets with poly (acrylonitrile-co-vinyl chloride) has already been verified for not provoking distinct immune activation following the transplantation[191]. Veiseh *et al*. addressed that alginate-based encapsulation could be tuned to elicit less immune responses by adjusting the size of the encapsulation capsule, and the effects could last up to 6 months[458]. Although these studies suggest good biocompatibility and immunoisolation with these encapsulating techniques, problems such as non-degradability and incapacity of homogeneous regulation exist. Contrarily, LbL single-cell encapsulation with natural materials will endow homogeneous regulation on individual cells and the materials can be degraded quickly. MHC molecules are supposed to be prevented from binding to T cell receptors since they cannot permeate the encapsulating materials with optimized parameters. Thus the downstream activation of immune responses is blocked so that the encapsulated grafts will be exempted from immune attack. Another possibility is that the antibody produced by B cells cannot permeate the encapsulation structure to interact with the antigens of the cells. In design of cell encapsulation for transplantation therapy, materials should be biocompatible for the grafted stem cells and also sustainable on the cell surface for a period, since it is acknowledged that the immune attack against these adult stem cell grafts in nervous system takes place 7 days after the transplantation[459]. To achieve satisfactory results in translational studies in the future, the mechanism of the

immune-privilege by encapsulation needs to be further clarified and the encapsulating technique needs to be optimized. As such, it is critical to design materials which not only prevent the recognition of adverse factors with receptors but also preserve the normal functions of cells, for stem cell therapy applying LbL encapsulation.

Chapter 7. Conclusions and Future Directions

LbL single-cell encapsulation is a combination of material science and cell biology. In the first part of the study (Specific Objective #1), we have verified the feasibility of this technique on NSCs and the application for drug delivery. Gelatin and alginate are used as the polyelectrolyte pair to encapsulate NSCs. Material layers of approximately 2 nm are observed on the cell surface with the aid of TEM. The survival, proliferation and differentiation of NSCs are proved to be not affected distinctly by the encapsulation. Movement of cytoskeleton is exhibited to be inhibited; however, it will gradually recover with time going on. IGF-1 which is an important growth factor in nervous system is loaded on alginate and then the obtained material is applied in NSCs encapsulation. IGF-1 is found to be released in a time-dependent and pH-dependent pattern. As a result, survival and proliferation of the encapsulated NSCs are greatly enhanced. These data suggest that LbL single-cell encapsulation can be safely performed on NSCs and applied in drug delivery.

In the second part of this study (Specific Objective #2), we have explored the permeability of the encapsulation structure and its application in inhibition of apoptosis. PC12 cells are encapsulated by gelatin and HA with the parameters which endow only slight influences on cellular functions such as survival and proliferation. FD permeability assay is processed to investigate the permeability of LbL structure to FD with different molecular weight and different coating parameters. Permeability is shown to be inversely proportional to molecular weight of FD, material concentration,

and number of layers. Extreme environmental pH facilitates the permeability while neutral pH does not. TNF-α/TNF-R1 interaction is applied as a ligand/receptor binding model for demonstrating the blocking effect on permeability of TNF-α through the multilayers. Encapsulation with 0.5% of materials for 8 layers interrupts the binding of TNF-α with TNF-R1, therefore the activation of downstream apoptotic cascades is interfered and thus the cell apoptosis rate is reduced.

In the future studies, cell therapy in nervous system diseases and trauma incorporated with single-cell encapsulation should be focused. Till now, the effects of cell therapies are still unsatisfactory, since the survival and differentiation of transplanted cells are usually interfered after the cells are grafted in the lesion sites. As supposed, LbL encapsulation will provide cells a refined microenvironment with loaded trophic factors. Meanwhile, the selective permeability of encapsulation structure can be manipulated to block adverse substances. In short, with the introduction of LbL encapsulation technique into cell therapy, microenvironment of transplanted cells will be tremendously improved and the therapeutic effects for nervous system disorders enhanced.

On the other hand, basic events involved in the cell encapsulation should be clarified. For example, the pattern and driving force of the drug release from materials are elusive. They may be disassembled from materials directly or released following the material degradation. Additionally, intervention of cell dividing and pseudopodia extension is presumably the result of the interruption of cell-cell interaction and kinetics alteration. Multilayer permeability for other regulators and nutrients also

requires more attentions. The clarification of the basis of cell encapsulation will boost the application in translational studies and provide a research tool for cell biology studies.

References

[1] Dove A. Cell-based therapies go live. Nat Biotechnol 2002;20:339-43.
[2] Orive G, Hernández RM, Gascón AR, Calafiore R, Chang TM, De Vos P, et al. Cell encapsulation: promise and progress. Nat Med 2003;9:104-7.
[3] Mazutis L, Gilbert J, Ung WL, Weitz DA, Griffiths AD, Heyman JA. Single-cell analysis and sorting using droplet-based microfluidics. Nat Protoc 2013;8:870-91.
[4] Lu Y-C, Song W, An D, Kim BJ, Schwartz R, Wu M, et al. Designing compartmentalized hydrogel microparticles for cell encapsulation and scalable 3D cell culture. J Mater Chem B 2015;3:353-60.
[5] Vasdekis AE, Stephanopoulos G. Review of methods to probe single cell metabolism and bioenergetics. Metab Eng 2015;27:115-35.
[6] Neu B, Voigt A, Mitlohner R, Leporatti S, Gao CY, Donath E, et al. Biological cells as templates for hollow microcapsules. J Microencapsul 2001;18:385-95.
[7] Nguyen TD, Guyot S, Lherminier J, Wache Y, Saurel R, Husson F. Protection of living yeast cells by micro-organized shells of natural polyelectrolytes. Process Biochem 2015;50:1528-36.
[8] Li M, Ai H, Mills DK, Lvov YM, McShane MJ, Gale BK. Using microfabrication and electrostatic layer-by-layer (LbL) sel -assembly technologies to improve the growth and alignment of smooth muscle cells. 2002.
[9] Mutlu BR, Yeom S, Wackett LP, Aksan A. Modelling and optimization of a bioremediation system utilizing silica gel encapsulated whole-cell biocatalyst. Chem Eng J 2015;259:574-80.
[10] Chen Z, Ji H, Zhao C, Ju E, Ren J, Qu X. Individual Surface-Engineered Microorganisms as Robust Pickering Interfacial Biocatalysts for Resistance-Minimized Phase-Transfer Bioconversion. Angew Chem Int Ed 2015;54:4904-8.
[11] Jing T, Ramji R, Warkiani ME, Han J, Lim CT, Chen C-H. Jetting microfluidics with size-sorting capability for single-cell protease detection. Biosens Bioelectron 2015;66:19-23.
[12] Decher G, Hong J, Schmitt J. Buildup of ultrathin multilayer films by a self-assembly process: III. Consecutively alternating adsorption of anionic and cationic polyelectrolytes on charged surfaces. Thin Solid Films 1992;210:831-5.
[13] Ariga K, Yamauchi Y, Rydzek G, Ji Q, Yonamine Y, Wu KC-W, et al. Layer-by-layer nanoarchitectonics: invention, innovation, and evolution. Chem Lett 2014;43:36-68.
[14] Sušec M, Ligon SC, Stampfl J, Liska R, Krajnc P. Hierarchically Porous Materials from Layer-by-Layer Photopolymerization of High Internal Phase Emulsions. Macromol Rapid Commun 2013;34:938-43.
[15] Wang D, Yang J, Li X, Geng D, Li R, Cai M, et al. Layer by layer assembly of

sandwiched graphene/SnO 2 nanorod/carbon nanostructures with ultrahigh lithium ion storage properties. Energy & Environmental Science 2013;6:2900-6.
[16] Yan Y, Björnmalm M, Caruso F. Assembly of layer-by-layer particles and their interactions with biological systems. Chem Mater 2013;26:452-60.
[17] Leporatti S, Voigt A, Mitlöhner R, Sukhorukov G, Donath E, Möhwald H. Scanning force microscopy investigation of polyelectrolyte nano-and microcapsule wall texture. Langmuir 2000;16:4059-63.
[18] Sugunan A, Melin P, Schnürer J, Hilborn JG, Dutta J. Nutrition-Driven Assembly of Colloidal Nanoparticles: Growing Fungi Assemble Gold Nanoparticles as Microwires. Adv Mater 2007;19:77-81.
[19] Zhang B, Yang S, Zhang Y, Wang Q, Ren T. Biotemplate-directed fabrication of size-controlled monodisperse magnetic silica microspheres. Colloids Surf, B 2015;131:129-35.
[20] Monge C, Almodóvar J, Boudou T, Picart C. Spatio-Temporal Control of LbL Films for Biomedical Applications: From 2D to 3D. Advanced healthcare materials 2015;4:811-30.
[21] Hiraoka R, Funasaki Y, Ishii J, Maruyama T. Rational design of a degradable polyanion for layer-by-layer assembly for encapsulation and release of cationic functional biomolecules. Chem Commun 2015;51:17447-50.
[22] Diaspro A, Silvano D, Krol S, Cavalleri O, Gliozzi A. Single living cell encapsulation in nano-organized polyelectrolyte shells. Langmuir 2002;18:5047-50.
[23] Mansouri S, Fatisson J, Miao Z, Merhi Y, Winnik FoM, Tabrizian M. Silencing Red Blood Cell Recognition toward Anti-A Antibody by Means of Polyelectrolyte Layer-by-Layer Assembly in a Two-Dimensional Model System†. Langmuir 2009;25:14071-8.
[24] Balkundi SS, Veerabadran NG, Eby DM, Johnson GR, Lvov YM. Encapsulation of Bacterial Spores in Nanoorganized Polyelectrolyte Shells†. Langmuir 2009;25:14011-6.
[25] Park JH, Choi IS, Yang SH. Peptide-catalyzed, bioinspired silicification for single-cell encapsulation in the imidazole-buffered system. Chem Commun 2015;51:5523-5.
[26] Li W, Guan T, Zhang X, Wang Z, Wang M, Zhong W, et al. The effect of layer-by-layer assembly coating on the proliferation and differentiation of neural stem cells. ACS applied materials & interfaces 2014.
[27] Lin B-j, Wang J, Miao Y, Liu Y-q, Jiang W, Fan Z-x, et al. Cytokine loaded layer-by-layer ultrathin matrices to deliver single dermal papilla cells for spot-by-spot hair follicle regeneration. J Mater Chem B 2016;4:489-504.
[28] Kearney CJ, Skaat H, Kennedy SM, Hu J, Darnell M, Raimondo TM, et al. Switchable release of entrapped nanoparticles from alginate hydrogels. Advanced healthcare materials 2015;4:1634-9.
[29] Kleinberger RM, Burke NA, Zhou C, Stöver HD. Synthetic polycations with controlled charge density and molecular weight as building blocks for biomaterials. J Biomater Sci Polym Ed 2016:1-19.
[30] Kryger MB, Pedersen SL, Wohl BM, Zelikin AN. Tools of gene transfer applied

to the intracellular delivery of non-nucleic acid polyanionic drugs. Chem Commun 2016;52:889-91.
[31] Xu H, Yao Q, Cai C, Gou J, Zhang Y, Zhong H, et al. Amphiphilic poly (amino acid) based micelles applied to drug delivery: The in vitro and in vivo challenges and the corresponding potential strategies. J Control Release 2015;199:84-97.
[32] Ivashkov OV, Sybachin AV, Efimova AA, Pergushov DV, Orlov VN, Schmalz H, et al. The Influence of the Chain Length of Polycations on their Complexation with Anionic Liposomes. Chemphyschem 2015;16:2849-53.
[33] Kulikov S, Khairullin R, Varlamov V. Influence of polycations on antibacterial activity of lysostaphin. Appl Biochem Microbiol 2015;51:683-7.
[34] Delaittre G, Greiner AM, Pauloehrl T, Bastmeyer M, Barner-Kowollik C. Chemical approaches to synthetic polymer surface biofunctionalization for targeted cell adhesion using small binding motifs. Soft Matter 2012;8:7323-47.
[35] Wang X, Niu D, Hu C, Li P. Polyethyleneimine-based nanocarriers for gene delivery. Curr Pharm Des 2015;21:6140-56.
[36] Peng Q, Zhong Z, Zhuo R. Disulfide cross-linked polyethylenimines (PEI) prepared via thiolation of low molecular weight PEI as highly efficient gene vectors. Bioconjug Chem 2008;19:499-506.
[37] Forrest ML, Meister GE, Koerber JT, Pack DW. Partial acetylation of polyethylenimine enhances in vitro gene delivery. Pharm Res 2004;21:365-71.
[38] Yang C, Cheng W, Teo PY, Engler AC, Coady DJ, Hedrick JL, et al. Mitigated Cytotoxicity and Tremendously Enhanced Gene Transfection Efficiency of PEI through Facile One-Step Carbamate Modification. Advanced healthcare materials 2013;2:1304-8.
[39] Bahadur KR, Uludağ H. PEI and its derivatives for gene therapy. Polymers and Nanomaterials for Gene Therapy 2016:29.
[40] Kozlovskaya V, Harbaugh S, Drachuk I, Shchepelina O, Kelley-Loughnane N, Stone M, et al. Hydrogen-bonded LbL shells for living cell surface engineering. Soft Matter 2011;7:2364-72.
[41] Elosua C, Lopez-Torres D, Hernaez M, Matias IR, Arregui FJ. Comparative study of layer-by-layer deposition techniques for poly (sodium phosphate) and poly (allylamine hydrochloride). Nanoscale research letters 2013;8:539.
[42] Krol S, Nolte M, Diaspro A, Mazza D, Magrassi R, Gliozzi A, et al. Encapsulated living cells on microstructured surfaces. Langmuir 2005;21:705-9.
[43] Konnova SA, Sharipova IR, Demina TA, Osin YN, Yarullina DR, Ilinskaya ON, et al. Biomimetic cell-mediated three-dimensional assembly of halloysite nanotubes. Chem Commun 2013;49:4208-10.
[44] Wandrey C, Hernandez-Barajas J, Hunkeler D. Diallyldimethylammonium chloride and its polymers. Radical polymerisation polyelectrolytes: Springer; 1999. p. 123-83.
[45] Franz B, Balkundi SS, Dahl C, Lvov YM, Prange A. Layer-by-Layer Nano-Encapsulation of Microbes: Controlled Cell Surface Modification and Investigation of Substrate Uptake in Bacteria. Macromol Biosci 2010;10:164-72.
[46] Zhang Z, Li Q, Han L, Zhong Y. Layer-by-layer films assembled from natural

polymers for sustained release of neurotrophin. Biomedical materials 2015;10:055006.
[47] Liao R, Yi S, Liu M, Jin W, Yang B. Folic-Acid-Targeted Self-Assembling Supramolecular Carrier for Gene Delivery. ChemBioChem 2015;16:1622-8.
[48] Junkers T. [2+ 2] Photo-cycloadditions for polymer modification and surface decoration. Eur Polym J 2015;62:273-80.
[49] Hoque ME, Nuge T, Yeow TK, Nordin N, Prasad R. GELATIN BASED SCAFFOLDS FOR TISSUE ENGINEERING-A REVIEW. Polymers Research Journal 2015;9:15.
[50] Liu D, Nikoo M, Boran G, Zhou P, Regenstein JM. Collagen and gelatin. Annual review of food science and technology 2015;6:527-57.
[51] Komatsu K, Shibata T, Shimada A, Ideno H, Nakashima K, Tabata Y, et al. Cationized gelatin hydrogels mixed with plasmid DNA induce stronger and more sustained gene expression than atelocollagen at calvarial bone defects in vivo. J Biomater Sci Polym Ed 2016;27:419-30.
[52] Klemm D, Heublein B, Fink HP, Bohn A. Cellulose: fascinating biopolymer and sustainable raw material. Angew Chem Int Ed 2005;44:3358-93.
[53] Dautzenberg H, Schuldt U, Grasnick G, Karle P, MÜller P, LÖhr M, et al. Development of Cellulose Sulfate-based Polyelectrolyte Complex Microcapsules for Medical Applications. Ann N Y Acad Sci 1999;875:46-63.
[54] Hon DN-S. Cellulose and its derivatives: structures, reactions, and medical uses. Polysaccharides in medicinal applications New York, USA: Marcel Dekker 1996:87-105.
[55] Carlsson L, Fall A, Chaduc I, Wågberg L, Charleux B, Malmström E, et al. Modification of cellulose model surfaces by cationic polymer latexes prepared by RAFT-mediated surfactant-free emulsion polymerization. Polymer Chemistry 2014;5:6076-86.
[56] Song Y, Zhang L, Gan W, Zhou J, Zhang L. Self-assembled micelles based on hydrophobically modified quaternized cellulose for drug delivery. Colloids Surf, B 2011;83:313-20.
[57] Karle P, Müller P, Renz R, Jesnowski R, Saller R, von Rombs K, et al. Intratumoral injection of encapsulated cells producing an oxazaphosphorine activating cytochrome P450 for targeted chemotherapy. Gene Therapy of Cancer: Springer; 1998. p. 97-106.
[58] Lacik I, Briššová M, Anilkumar A, Powers A, Wang T. New capsule with tailored properties for the encapsulation of living cells. Journal of Biomedical Materials Research Part A 1998;39:52-60.
[59] Prochorov A, Tretjak S, Goranov V, Glinnik A, Goltsev M. Treatment of insulin dependent diabetes mellitus with intravascular transplantation of pancreatic islet cells without immunosuppressive therapy. Adv Med Sci 2008;53:240.
[60] Hujaya SD, Engbersen JF, Paulusse JM. Multilayered thin films from boronic acid-functional Poly (amido amine) s. Pharm Res 2015;32:3066-86.
[61] Qi X, Qin J, Fan Y, Qin X, Jiang Y, Wu Z. Carboxymethyl Chitosan-Modified Polyamidoamine Dendrimer Enables Progressive Drug Targeting of Tumors via

pH-Sensitive Charge Inversion. Journal of biomedical nanotechnology 2016;12:667-78.
[62] Cortez MA, Godbey WT, Fang Y, Payne ME, Cafferty BJ, Kosakowska KA, et al. The Synthesis of Cyclic Poly (ethylene imine) and Exact Linear Analogues: An Evaluation of Gene Delivery Comparing Polymer Architectures. J Am Chem Soc 2015;137:6541-9.
[63] Urbán P, Ranucci E, Fernàndez-Busquets X. Polyamidoamine nanoparticles as nanocarriers for the drug delivery to malaria parasite stages in the mosquito vector. Nanomedicine 2015;10:3401-14.
[64] Frost R, CouétG, Engbersen JF, Zäch M, Kasemo B, Svedhem S. Bioreducible insulin-loaded nanoparticles and their interaction with model lipid membranes. J Colloid Interface Sci 2011;362:575-83.
[65] Gattás-Asfura KM, Stabler CL. Bioorthogonal layer-by-layer encapsulation of pancreatic islets via hyperbranched polymers. ACS applied materials & interfaces 2013;5:9964-74.
[66] El-Sherbiny IM, El-Baz NM. A Review on Bionanocomposites Based on Chitosan and Its Derivatives for Biomedical Applications. Eco-friendly Polymer Nanocomposites: Springer; 2015. p. 173-208.
[67] Lin WJ, Hsu WY. Pegylation effect of chitosan based polyplex on DNA transfection. Carbohydr Polym 2015;120:7-14.
[68] Patrulea V, Hirt-Burri N, Jeannerat A, Applegate L, Ostafe V, Jordan O, et al. Peptide-decorated chitosan derivatives enhance fibroblast adhesion and proliferation in wound healing. Carbohydr Polym 2016.
[69] Li L, Zhao F, Zhao B, Zhang J, Li C, Qiao R. Chitosan Grafted with Phosphorylcholine and Macrocyclic Polyamine as an Effective Gene Delivery Vector: Preparation, Characterization and In Vitro Transfection. Macromol Biosci 2015;15:912-26.
[70] Pei L, Cai Z, Shang S, Song Z. Synthesis and antibacterial activity of alkylated chitosan under basic ionic liquid conditions. J Appl Polym Sci 2014;131.
[71] Facchi SP, Scariot DB, Bueno PV, Souza PR, Figueiredo LC, Follmann HD, et al. Preparation and cytotoxicity of N-modified chitosan nanoparticles applied in curcumin delivery. Int J Biol Macromol 2016;87:237-45.
[72] Torabi S, Mahdavian AR, Sanei M, Abdollahi A. Chitosan and functionalized acrylic nanoparticles as the precursor of new generation of bio-based antibacterial films. Materials Science and Engineering: C 2016;59:1-9.
[73] Beidokhti HRN, Ghaffarzadegan R, Mirzakhanlouei S, Ghazizadeh L, Dorkoosh FA. Preparation, Characterization, and Optimization of Folic Acid-Chitosan-Methotrexate Core-Shell Nanoparticles by Box-Behnken Design for Tumor-Targeted Drug Delivery. AAPS PharmSciTech 2016:1-15.
[74] Liang H, Li J, He Y, Xu W, Liu S, Li Y, et al. Engineering multifunctional films based on metal-phenolic networks for rational pH-responsive delivery and cell imaging. ACS Biomaterials Science & Engineering 2016.
[75] Mekhail M, Jahan K, Tabrizian M. Genipin-crosslinked chitosan/poly-L-lysine gels promote fibroblast adhesion and proliferation. Carbohydr Polym 2014;108:91-8.

[76] Kanczler JM, Sura HS, Magnay J, Green D, Oreffo RO, Dobson JP, et al. Controlled differentiation of human bone marrow stromal cells using magnetic nanoparticle technology. Tissue engineering Part A 2010;16:3241-50.
[77] Emerich DF, Hammang JP, Baetge EE, Winn SR. Implantation of polymer-encapsulated human nerve growth factor-secreting fibroblasts attenuates the behavioral and neuropathological consequences of quinolinic acid injections into rodent striatum. Exp Neurol 1994;130:141-50.
[78] Skaugrud Ø, Hagen A, Borgersen B, Dornish M. Biomedical and pharmaceutical applications of alginate and chitosan. Biotechnol Genet Eng Rev 1999;16:23-40.
[79] Zhu J-H, Wang X-W, Ng S, Quek C-H, Ho H-T, Lao X-J, et al. Encapsulating live cells with water-soluble chitosan in physiological conditions. J Biotechnol 2005;117:355-65.
[80] Orive G, Tam SK, Pedraz JL, Hallé J-P. Biocompatibility of alginate–poly-l-lysine microcapsules for cell therapy. Biomaterials 2006;27:3691-700.
[81] Samal SK, Dash M, Van Vlierberghe S, Kaplan DL, Chiellini E, van Blitterswijk C, et al. Cationic polymers and their therapeutic potential. Chem Soc Rev 2012;41:7147-94.
[82] Yanagishima T, Di Michele L, Kotar J, Eiser E. Diffusive behaviour of PLL–PEG coated colloids on λ-DNA brushes–tuning hydrophobicity. Soft Matter 2012;8:6792-8.
[83] Nah J-W, Yu L, Han S-o, Ahn C-H, Kim SW. Artery wall binding peptide-poly (ethylene glycol)-grafted-poly (L-lysine)-based gene delivery to artery wall cells. J Control Release 2002;78:273-84.
[84] Jing H, Cheng W, Zhang J-W, Han X, Shao H, Sun Y-X. Galactosylated poly-L-lysine targeted microbubbles for ultrasound mediated antisense c-myc gene transfection in hepatocellular carcinoma cells. Archives of medical science: AMS 2015;11:292.
[85] Zhou Z, Tang J, Sun Q, Murdoch WJ, Shen Y. A multifunctional PEG–PLL drug conjugate forming redox-responsive nanoparticles for intracellular drug delivery. J Mater Chem B 2015;3:7594-603.
[86] Franiak-Pietryga I, Maciejewski H, Ostrowska K, Appelhans D, Voit B, Misiewicz M, et al. Dendrimer-based nanoparticles for potential personalized therapy in chronic lymphocytic leukemia: targeting the BCR-Signaling Pathway. Int J Biol Macromol 2016.
[87] Denkewalter R, Kolc J, Lukasavage W. US Pat. 4289872, 1981. Chem Abstr1985. p. P79324q.
[88] Biswas S, Torchilin VP. DENDRIMERS FOR CHEMOTHERAPEUTIC DRUG DELIVERY. Materials Science Research Journal 2014;8:433.
[89] Lam J, Clark EC, Fong EL, Lee EJ, Lu S, Tabata Y, et al. Evaluation of cell-laden polyelectrolyte hydrogels incorporating poly (l-Lysine) for applications in cartilage tissue engineering. Biomaterials 2016;83:332-46.
[90] Veerabadran NG, Goli PL, Stewart-Clark SS, Lvov YM, Mills DK. Nanoencapsulation of stem cells within polyelectrolyte multilayer shells. Macromol Biosci 2007;7:877-82.
[91] Wilson JT, Cui W, Chaikof EL. Layer-by-layer assembly of a conformal nanothin

PEG coating for intraportal islet transplantation. Nano Lett 2008;8:1940-8.
[92] Gombotz WR, Wee SF. Protein release from alginate matrices. Adv Drug Delivery Rev 2012;64:194-205.
[93] Uludag H, De Vos P, Tresco PA. Technology of mammalian cell encapsulation. Adv Drug Delivery Rev 2000;42:29-64.
[94] Stokke BT, Smidsroed O, Bruheim P, Skjaak-Braek G. Distribution of uronate residues in alginate chains in relation to alginate gelling properties. Macromolecules 1991;24:4637-45.
[95] Teramura Y, Oommen OP, Olerud J, Hilborn J, Nilsson B. Microencapsulation of cells, including islets, within stable ultra-thin membranes of maleimide-conjugated PEG-lipid with multifunctional crosslinkers. Biomaterials 2013;34:2683-93.
[96] Lanza RP, Ecker D, Kühtreiber WM, Staruk JE, Marsh J, Chick WL. A simple method for transplanting discordant islets into rats using alginate gel spheres. Transplantation 1995;59:1485-7.
[97] Vos Pd, Andersson A, Tam S, Faas M, Halle J. Advances and barriers in mammalian cell encapsulation for treatment of diabetes. Immunology, Endocrine & Metabolic Agents in Medicinal Chemistry (Formerly Current Medicinal Chemistry-Immunology, Endocrine and Metabolic Agents) 2006;6:139-53.
[98] De Vos P, De Haan B, Van Schilfgaarde R. Effect of the alginate composition on the biocompatibility of alginate-polylysine microcapsules. Biomaterials 1997;18:273-8.
[99] Basta G, Sarchielli P, Luca G, Racanicchi L, Nastruzzi C, Guido L, et al. Optimized parameters for microencapsulation of pancreatic islet cells: an in vitro study clueing on islet graft immunoprotection in type 1 diabetes mellitus. Transpl Immunol 2004;13:289-96.
[100] Spasojevic M, Bhujbal S, Paredes G, Haan BJ, Schouten AJ, Vos P. Considerations in binding diblock copolymers on hydrophilic alginate beads for providing an immunoprotective membrane. Journal of Biomedical Materials Research Part A 2014;102:1887-96.
[101] Chandy T, Mooradian DL, Rao GH. Evaluation of modified alginate-chitosan-polyethylene glycol microcapsules for cell encapsulation. Artif Organs 1999;23:894-903.
[102] Lacik I, Anilkumar A, Wang T. A two-step process for controlling the surface smoothness of polyelectrolyte-based microcapsules. J Microencapsul 2001;18:479-90.
[103] de Haan BJ, Faas MM, de Vos P. Factors influencing insulin secretion from encapsulated islets. Cell Transplant 2003;12:617-25.
[104] Chen J-P, Chu I-M, Shiao M-Y, Hsu BR-S, Fu S-H. Microencapsulation of islets in PEG-amine modified alginate-poly (L-lysine)-alginate microcapsules for constructing bioartificial pancreas. J Ferment Bioeng 1998;86:185-90.
[105] Dusseault J, Leblond FA, Robitaille R, Jourdan G, Tessier J, Ménard M, et al. Microencapsulation of living cells in semi-permeable membranes with covalently cross-linked layers. Biomaterials 2005;26:1515-22.
[106] Cross-Linking C. Functionalization of Alginate via Staudinger Ligation Gattas-Asfura, Kerim M.; Stabler, Cherie L. Biomacromolecules 2009;10:3122-9.

[107] Sakai S, Hashimoto I, Ogushi Y, Kawakami K. Peroxidase-catalyzed cell encapsulation in subsieve-size capsules of alginate with phenol moieties in water-immiscible fluid dissolving H2O2. Biomacromolecules 2007;8:2622-6.
[108] Sakai S, Kawakami K. Synthesis and characterization of both ionically and enzymatically cross-linkable alginate. Acta Biomater 2007;3:495-501.
[109] Klöck G, Frank H, Houben R, Zekorn T, Horcher A, Siebers U, et al. Production of purified alginates suitable for use in immunoisolated transplantation. Appl Microbiol Biotechnol 1994;40:638-43.
[110] Kumar S, Ingle H, Prasad DVR, Kumar H. Recognition of bacterial infection by innate immune sensors. Crit Rev Microbiol 2013;39:229-46.
[111] Rokstad AM, Brekke O-L, Steinkjer B, Ryan L, Kolláriková G, Strand BL, et al. The induction of cytokines by polycation containing microspheres by a complement dependent mechanism. Biomaterials 2013;34:621-30.
[112] Rokstad AM, Brekke O-L, Steinkjer B, Ryan L, Kolláriková G, Strand BL, et al. Alginate microbeads are complement compatible, in contrast to polycation containing microcapsules, as revealed in a human whole blood model. Acta Biomater 2011;7:2566-78.
[113] Collins MN, Birkinshaw C. Hyaluronic acid based scaffolds for tissue engineering—A review. Carbohydr Polym 2013;92:1262-79.
[114] Lam J, Truong NF, Segura T. Design of cell–matrix interactions in hyaluronic acid hydrogel scaffolds. Acta Biomater 2014;10:1571-80.
[115] Schanté CE, Zuber G, Herlin C, Vandamme TF. Chemical modifications of hyaluronic acid for the synthesis of derivatives for a broad range of biomedical applications. Carbohydr Polym 2011;85:469-89.
[116] Chung C, Burdick JA. Influence of three-dimensional hyaluronic acid microenvironments on mesenchymal stem cell chondrogenesis. Tissue Engineering Part A 2008;15:243-54.
[117] Seidlits SK, Khaing ZZ, Petersen RR, Nickels JD, Vanscoy JE, Shear JB, et al. The effects of hyaluronic acid hydrogels with tunable mechanical properties on neural progenitor cell differentiation. Biomaterials 2010;31:3930-40.
[118] Kim IL, Khetan S, Baker BM, Chen CS, Burdick JA. Fibrous hyaluronic acid hydrogels that direct MSC chondrogenesis through mechanical and adhesive cues. Biomaterials 2013;34:5571-80.
[119] Harel Z, Harel S, Shah PS, Wald R, Perl J, Bell CM. Gastrointestinal adverse events with sodium polystyrene sulfonate (Kayexalate) use: a systematic review. The American journal of medicine 2013;126:264. e9-. e24.
[120] Choi WS, Choi IS, Lee JK, Yoon KR. Preparation of fluorescein-functionalized electrospun fibers coated with TiO 2 and gold nanoparticles for visible-light-induced photocatalysis. Mater Chem Phys 2015;163:213-8.
[121] Åkerfeldt M, Nilsson E, Gillgard P, Walkenström P. Textile piezoelectric sensors–melt spun bi-component poly (vinylidene fluoride) fibres with conductive cores and poly (3, 4-ethylene dioxythiophene)-poly (styrene sulfonate) coating as the outer electrode. Fashion and Textiles 2014;1:1-17.
[122] Wan S, Egri G, Oddo L, Cerroni B, Dähne L, Paradossi G, et al. Biological in

situ characterization of polymeric microbubble contrast agents. The International Journal of Biochemistry & Cell Biology 2016.
[123] Fakhrullin RF, Zamaleeva AI, Morozov MV, Tazetdinova DI, Alimova FK, Hilmutdinov AK, et al. Living fungi cells encapsulated in polyelectrolyte shells doped with metal nanoparticles. Langmuir 2009;25:4628-34.
[124] Pandey A, Chouhan RS, Gurbuz Y, Niazi JH, Qureshi A. S. cerevisiae whole-cell based capacitive biochip for the detection of toxicity of different forms of carbon nanotubes. Sensors Actuators B: Chem 2015;218:253-60.
[125] Yang X-N, Xue D-D, Li J-Y, Liu M, Jia S-R, Chu L-Q, et al. Improvement of antimicrobial activity of graphene oxide/bacterial cellulose nanocomposites through the electrostatic modification. Carbohydr Polym 2016;136:1152-60.
[126] Safarik I, Safarikova M. Magnetically modified microbial cells: A new type of magnetic adsorbents. China Particuology 2007;5:19-25.
[127] Gorobets S, Gorobets OY, Demianenko I, Nikolaenko R. Self-organization of magnetite nanoparticles in providing Saccharomyces cerevisiae Yeasts with magnetic properties. J Magn Magn Mater 2013;337:53-7.
[128] Fakhrullin RF, Garc á-Alonso J, Paunov VN. A direct technique for preparation of magnetically functionalised living yeast cells. Soft Matter 2010;6:391-7.
[129] Dzamukova MR, Naumenko EA, Rozhina EV, Trifonov AA, Fakhrullin RF. Cell surface engineering with polyelectrolyte-stabilized magnetic nanoparticles: A facile approach for fabrication of artificial multicellular tissue-mimicking clusters. Nano Research 2015;8:2515-32.
[130] Dzamukova MR, Zamaleeva AI, Ishmuchametova DG, Osin YN, Kiyasov AP, Nurgaliev DK, et al. A direct technique for magnetic functionalization of living human cells. Langmuir 2011;27:14386-93.
[131] Qureshi SS, Zheng Z, Sarwar MI, F édix O, Decher G. Nanoprotective layer-by-layer coatings with epoxy components for enhancing abrasion resistance: toward robust multimaterial nanoscale films. ACS nano 2013;7:9336-44.
[132] Cook MT, Tzortzis G, Khutoryanskiy VV, Charalampopoulos D. Layer-by-layer coating of alginate matrices with chitosan–alginate for the improved survival and targeted delivery of probiotic bacteria after oral administration. J Mater Chem B 2013;1:52-60.
[133] K ékicheff P, Schneider GF, Decher G. Size-controlled polyelectrolyte complexes: Direct measurement of the balance of forces involved in the triggered collapse of layer-by-layer assembled nanocapsules. Langmuir 2013;29:10713-26.
[134] Zhang Z, Maji S, Antunes ABdF, De Rycke R, Zhang Q, Hoogenboom R, et al. Salt plays a pivotal role in the temperature-responsive aggregation and layer-by-layer assembly of polymer-decorated gold nanoparticles. Chem Mater 2013;25:4297-303.
[135] Frank C, Novak J, Banerjee R, Gerlach A, Schreiber F, Vorobiev A, et al. Island size evolution and molecular diffusion during growth of organic thin films followed by time-resolved specular and off-specular scattering. Physical Review B 2014;90:045410.
[136] Kim B, Kwon S, Lee M, Kim Q, An S, Jhe W. Probing nonlinear rheology layer-by-layer in interfacial hydration water. Proceedings of the National Academy of

Sciences 2015;112:15619-23.
[137] Szilagyi I, Trefalt G, Tiraferri A, Maroni P, Borkovec M. Polyelectrolyte adsorption, interparticle forces, and colloidal aggregation. Soft Matter 2014;10:2479-502.
[138] Li Y, Wang X, Sun J. Layer-by-layer assembly for rapid fabrication of thick polymeric films. Chem Soc Rev 2012;41:5998-6009.
[139] Kargl R, Mohan T, Bračič M, Kulterer M, Doliška A, Stana-Kleinschek K, et al. Adsorption of carboxymethyl cellulose on polymer surfaces: evidence of a specific interaction with cellulose. Langmuir 2012;28:11440-7.
[140] Xiao F-X, Miao J, Liu B. Layer-by-layer self-assembly of CdS quantum dots/graphene nanosheets hybrid films for photoelectrochemical and photocatalytic applications. J Am Chem Soc 2014;136:1559-69.
[141] Mazilu D, Mazilu I, Seredinski A, Kim V, Simpson B, Banks W. Cooperative sequential adsorption models on a Cayley tree: analytical results and applications. Journal of Statistical Mechanics: Theory and Experiment 2012;2012:P09002.
[142] Wang X, Choi S-I, Roling LT, Luo M, Ma C, Zhang L, et al. Palladium-platinum core-shell icosahedra with substantially enhanced activity and durability towards oxygen reduction. Nature communications 2015;6.
[143] Kuroda Y, Kuroda K. Layer-by-layer assembly of imogolite nanotubes and polyelectrolytes into core-shell particles and their conversion to hierarchically porous spheres. Science and Technology of Advanced Materials 2016.
[144] Feng L, Kobayashi M, Adachi Y. Initial stage dynamics of bridging flocculation of polystyrene latex particles with low charge density polycation in a mixing flow near the isoelectric point. Colloid Polym Sci 2015;293:3585-93.
[145] Vidotti M. Electrostatic Layer-By-Layer and Electrophoretic Deposition As Alternative Methods for Electrochromic Nanoparticles Immobilization. 227th ECS Meeting (May 24-28, 2015): Ecs; 2015.
[146] Katagiri K, Yamazaki S-i, Inumaru K, Koumoto K. Anti-reflective coatings prepared via layer-by-layer assembly of mesoporous silica nanoparticles and polyelectrolytes. Polym J 2015;47:190-4.
[147] Sergeeva YN, Huang T, Felix O, Jung L, Tropel P, Viville S, et al. What is really driving cell–surface interactions? Layer-by-layer assembled films may help to answer questions concerning cell attachment and response to biomaterials. Biointerphases 2016;11:019009.
[148] Godman NP, DeLuca JL, Mccollum SR, Schmidtke DW, Glatzhofer DT. Electrochemical Characterization of Layer-by-Layer Assembled Ferrocene-Modified Linear Poly (ethylenimine)/Enzyme Bioanodes for Glucose Sensor and Biofuel Cell Applications. Langmuir 2016.
[149] Vaterrodt A, Thallinger B, Daumann K, Koch D, Guebitz GM, Ulbricht M. Antifouling and antibacterial multi-functional polyzwitterion/enzyme coating on silicone catheter material prepared by electrostatic layer-by-layer assembly. Langmuir 2016.
[150] Xu J, Wang Z, Wen L, Zhou X, Xu J, Yang S. Dynamics of the layer-by-layer assembly of a poly (acrylic acid)–lanthanide complex colloid and poly

(diallyldimethyl ammonium). Soft matter 2016;12:867-75.
[151] Selin V, Ankner JF, Sukhishvili SA. Diffusional Response of Layer-by-Layer Assembled Polyelectrolyte Chains to Salt Annealing. Macromolecules 2015;48:3983-90.
[152] Varga I, Mezei A, Mészáros R, Claesson PM. Controlling the interaction of poly (ethylene imine) adsorption layers with oppositely charged surfactant by tuning the structure of the preadsorbed polyelectrolyte layer. Soft Matter 2011;7:10701-12.
[153] Popa I, Gillies G, Papastavrou G, Borkovec M. Attractive and repulsive electrostatic forces between positively charged latex particles in the presence of anionic linear polyelectrolytes. The Journal of Physical Chemistry B 2010;114:3170-7.
[154] Pericet-Camara R, Papastavrou G, Borkovec M. Atomic force microscopy study of the adsorption and electrostatic self-organization of poly (amidoamine) dendrimers on mica. Langmuir 2004;20:3264-70.
[155] Kirwan LJ, Papastavrou G, Borkovec M, Behrens SH. Imaging the coil-to-globule conformational transition of a weak polyelectrolyte by tuning the polyelectrolyte charge density. Nano Lett 2004;4:149-52.
[156] Valle F, Favre M, De Los Rios P, Rosa A, Dietler G. Scaling exponents and probability distributions of DNA end-to-end distance. Phys Rev Lett 2005;95:158105.
[157] Popa I, Papastavrou G, Borkovec M. Charge regulation effects on electrostatic patch-charge attraction induced by adsorbed dendrimers. Phys Chem Chem Phys 2010;12:4863-71.
[158] Gromer A, Rawiso M, Maaloum M. Visualization of hydrophobic polyelectrolytes using atomic force microscopy in solution. Langmuir 2008;24:8950-3.
[159] Jalali N, Briscoe J, Tan YZ, Woolliams P, Stewart M, Weaver PM, et al. ZnO nanorod surface modification with PDDA/PSS Bi-layer assembly for performance improvement of ZnO piezoelectric energy harvesting devices. J Sol-Gel Sci Technol 2015;73:544-9.
[160] Padilha J, Fazzio A, da Silva AJ. Van der waals heterostructure of phosphorene and graphene: Tuning the schottky barrier and doping by electrostatic gating. Phys Rev Lett 2015;114:066803.
[161] Potisatityuenyong A, Dubas S, Sukwattanasinitt M. Layer-by-Layer Deposition of Chitosan/Polydiacetylene Vesicles for Convenient Preparation of Colorimetric Sensing Film. une 2016;13:15.
[162] Min L, GAO Y, Hornicek FJ, Amiji MM, Duan Z. Abstract LB-102: Layer-by-layer engineering of upconversion nanoparticle based siRNA and miRNA delivery system for cancer therapy. Cancer Res 2015;75:LB-102-LB-.
[163] Batys P, Nosek M, Weroński P. Structure analysis of layer-by-layer multilayer films of colloidal particles. Appl Surf Sci 2015;332:318-27.
[164] Liu C, Shi L, Wang R. Enhanced hollow fiber membrane performance via semi-dynamic layer-by-layer polyelectrolyte inner surface deposition for nanofiltration and forward osmosis applications. React Funct Polym 2015;86:154-60.
[165] Bucur CB, Lita A, Osada N, Muldoon J. A soft, multilayered lithium–electrolyte

interface. Energy & Environmental Science 2016;9:112-6.
[166] Kleimann J, Gehin-Delval C, Auweter H, Borkovec M. Super-stoichiometric charge neutralization in particle− polyelectrolyte systems. Langmuir 2005;21:3688-98.
[167] Szilágyi I, Rosická D, Hierrezuelo J, Borkovec M. Charging and stability of anionic latex particles in the presence of linear poly (ethylene imine). J Colloid Interface Sci 2011;360:580-5.
[168] Yu W, Bouyer F, Borkovec M. Polystyrene sulfate latex particles in the presence of poly (vinylamine): absolute aggregation rate constants and charging behavior. J Colloid Interface Sci 2001;241:392-9.
[169] Cai C, Mao S, Kissel T. O-013-Layer-by-layer nanostructured protein loaded nanoparticles: a feasibility study using lysozyme as model protein and chitosan as coating material. Asian Journal of Pharmaceutical Sciences 2015;13.
[170] Richardson JJ, Tardy BL, Ejima H, Guo J, Cui J, Liang K, et al. Thermally Induced Charge Reversal of Layer-by-Layer Assembled Single-Component Polymer Films. ACS applied materials & interfaces 2016.
[171] Zhang X, Shen J, Ma H, Jiang Y, Huang C, Han E, et al. Optimized dendrimer-encapsulated gold nanoparticles and enhanced carbon nanotube nanoprobes for amplified electrochemical immunoassay of E. coli in dairy product based on enzymatically induced deposition of polyaniline. Biosens Bioelectron 2016;80:666-73.
[172] Felber M, Bauwens M, Mateos JM, Imstepf S, Mottaghy FM, Alberto R. 99mTc Radiolabeling and Biological Evaluation of Nanoparticles Functionalized with a Versatile Coating Ligand. Chemistry–A European Journal 2015;21:6090-9.
[173] Fakhrullin RF, Minullina RT. Hybrid cellular− inorganic core− shell microparticles: Encapsulation of individual living cells in calcium carbonate microshells. Langmuir 2009;25:6617-21.
[174] Wang B, Liu P, Jiang W, Pan H, Xu X, Tang R. Yeast cells with an artificial mineral shell: Protection and modification of living cells by biomimetic mineralization. Angew Chem Int Ed 2008;47:3560-4.
[175] Wang B, Liu P, Tang Y, Pan H, Xu X, Tang R. Guarding embryo development of zebrafish by shell engineering: a strategy to shield life from ozone depletion. PLoS One 2010;5:e9963.
[176] Kessler VG, Seisenbaeva GA, Unell M, Håkansson S. Chemically triggered biodelivery using metal–organic sol–gel synthesis. Angew Chem Int Ed 2008;47:8506-9.
[177] Maier GP, Rapp MV, Waite JH, Israelachvili JN, Butler A. Adaptive synergy between catechol and lysine promotes wet adhesion by surface salt displacement. Science 2015;349:628-32.
[178] Cho WK, Yang SH. Bio-Inspired Formation of Silica Thin Films: From Solid Substrates to Cellular Interfaces. Eur J Inorg Chem 2015;2015:4481-94.
[179] Yang SH, Lee KB, Kong B, Kim JH, Kim HS, Choi IS. Biomimetic encapsulation of individual cells with silica. Angew Chem Int Ed 2009;48:9160-3.
[180] Yang SH, Kang SM, Lee K-B, Chung TD, Lee H, Choi IS. Mussel-inspired

encapsulation and functionalization of individual yeast cells. J Am Chem Soc 2011;133:2795-7.
[181] Chan SC, Tekari A, Benneker LM, Heini PF, Gantenbein B. Osteogenic differentiation of bone marrow stromal cells is hindered by the presence of intervertebral disc cells. Arthritis Res Ther 2015;18:1.
[182] Aikawa T, Konno T, Ishihara K. Phospholipid polymer hydrogel microsphere modulates the cell cycle profile of encapsulated cells. Soft Matter 2013;9:4628-34.
[183] Kempaiah R, Salgado S, Chung WL, Maheshwari V. Graphene as membrane for encapsulation of yeast cells: protective and electrically conducting. Chem Commun 2011;47:11480-2.
[184] Kang Y, Georgiou AI, MacFarlane RJ, Klontzas ME, Heliotis M, Tsiridis E, et al. Fibronectin stimulates the osteogenic differentiation of murine embryonic stem cells. J Tissue Eng Regen Med 2015.
[185] Stojkovic D, Torzillo G, Faraloni C, Valant M. Hydrogen production by sulfur-deprived TiO 2-encapsulated Chlamydomonas reinhardtii cells. Int J Hydrogen Energy 2015;40:3201-6.
[186] Luo D, Gould DJ, Sukhorukov GB. Local and sustained activity of doxycycline delivered with layer-by-layer microcapsules. Biomacromolecules 2016.
[187] Zhang Z, Zhang R, Chen L, McClements DJ. Encapsulation of lactase (β-galactosidase) into κ-carrageenan-based hydrogel beads: Impact of environmental conditions on enzyme activity. Food Chem 2016;200:69-75.
[188] Eriksdotter-Jönhagen M, Linderoth B, Lind G, Aladellie L, Almkvist O, Andreasen N, et al. Encapsulated cell biodelivery of nerve growth factor to the basal forebrain in patients with Alzheimer's disease. Dement Geriatr Cogn Disord 2012;33:18-28.
[189] Ferreira D, Westman E, Eyjolfsdottir H, Almqvist P, Lind G, Linderoth B, et al. Brain changes in Alzheimer's disease patients with implanted encapsulated cells releasing nerve growth factor. J Alzheimers Dis 2015;43:1059-72.
[190] Soon-Shiong P, Heintz RE, Merideth N, Yao QX, Yao Z, Zheng T, et al. Insulin independence in a type 1 diabetic patient after encapsulated islet transplantation. The Lancet 1994;343:950-1.
[191] Scharp DW, Swanson CJ, Olack BJ, Latta PP, Hegre OD, Doherty EJ, et al. Protection of encapsulated human islets implanted without immunosuppression in patients with type I or type II diabetes and in nondiabetic control subjects. Diabetes 1994;43:1167-70.
[192] Calafiore R, Basta G, Luca G, Lemmi A, Montanucci MP, Calabrese G, et al. Microencapsulated pancreatic islet allografts into nonimmunosuppressed patients with type 1 diabetes. Diabetes Care 2006;29:137-8.
[193] Jacobs-Tulleneers-Thevissen D, Chintinne M, Ling Z, Gillard P, Schoonjans L, Delvaux G, et al. Sustained function of alginate-encapsulated human islet cell implants in the peritoneal cavity of mice leading to a pilot study in a type 1 diabetic patient. Diabetologia 2013;56:1605-14.
[194] De Vos P, De Haan B, Pater J, Van Schilfgaarde R. Association between capsule diameter, adequacy of encapsulation, and survival of microencapsulated rat islet

allografts1. Transplantation 1996;62:893-9.
[195] Bhujbal SV, Paredes-Juarez GA, Niclou SP, de Vos P. Factors influencing the mechanical stability of alginate beads applicable for immunoisolation of mammalian cells. Journal of the mechanical behavior of biomedical materials 2014;37:196-208.
[196] de Haan BJ, Rossi A, Faas MM, Smelt MJ, Sonvico F, Colombo P, et al. Structural surface changes and inflammatory responses against alginate-based microcapsules after exposure to human peritoneal fluid. Journal of Biomedical Materials Research Part A 2011;98:394-403.
[197] Tan S, Deglon N, Zurn A, Baetge E, Bamber B, Kato A, et al. Rescue of motoneurons from axotomy-induced cell death by polymer encapsulated cells genetically engineered to release CNTF. Cell Transplant 1996;5:577-87.
[198] Borlongan CV, Thanos CG, Skinner SJ, Geaney M, Emerich DF. Transplants of encapsulated rat choroid plexus cells exert neuroprotection in a rodent model of Huntington's disease. Cell Transplant 2007;16:987-92.
[199] Emerich DF, Orive G, Thanos C, Tornoe J, Wahlberg LU. Encapsulated cell therapy for neurodegenerative diseases: from promise to product. Adv Drug Delivery Rev 2014;67:131-41.
[200] Kauper K, McGovern C, Sherman S, Heatherton P, Rapoza R, Stabila P, et al. Two-Year Intraocular Delivery of Ciliary Neurotrophic Factor by Encapsulated Cell Technology Implants in Patients with Chronic Retinal Degenerative DiseasesIntraocular Delivery of CNTF via ECT. Invest Ophthalmol Vis Sci 2012;53:7484-91.
[201] Lindvall O, Wahlberg LU. Encapsulated cell biodelivery of GDNF: a novel clinical strategy for neuroprotection and neuroregeneration in Parkinson's disease? Exp Neurol 2008;209:82-8.
[202] Dove A. Drug screening? beyond the bottleneck. Nat Biotechnol 1999;17.
[203] Guo MT, Rotem A, Heyman JA, Weitz DA. Droplet microfluidics for high-throughput biological assays. Lab on a chip 2012;12:2146-55.
[204] Tawfik DS, Griffiths AD. Man-made cell-like compartments for molecular evolution. Nat Biotechnol 1998;16:652-6.
[205] Baret J-C, Miller OJ, Taly V, Ryckelynck M, El-Harrak A, Frenz L, et al. Fluorescence-activated droplet sorting (FADS): efficient microfluidic cell sorting based on enzymatic activity. Lab on a chip 2009;9:1850-8.
[206] Kintses B, Hein C, Mohamed MF, Fischlechner M, Courtois F, Lainé C, et al. Picoliter cell lysate assays in microfluidic droplet compartments for directed enzyme evolution. Chem Biol 2012;19:1001-9.
[207] Brouzes E, Medkova M, Savenelli N, Marran D, Twardowski M, Hutchison JB, et al. Droplet microfluidic technology for single-cell high-throughput screening. Proceedings of the National Academy of Sciences 2009;106:14195-200.
[208] Hatch AC, Fisher JS, Tovar AR, Hsieh AT, Lin R, Pentoney SL, et al. 1-Million droplet array with wide-field fluorescence imaging for digital PCR. Lab on a chip 2011;11:3838-45.
[209] Beer NR, Wheeler EK, Lee-Houghton L, Watkins N, Nasarabadi S, Hebert N, et al. On-chip single-copy real-time reverse-transcription PCR in isolated picoliter

droplets. Anal Chem 2008;80:1854-8.
[210] Olsen MJ, Stephens D, Griffiths D, Daugherty P, Georgiou G, Iverson BL. Function-based isolation of novel enzymes from a large library. Nat Biotechnol 2000;18:1071.
[211] Aharoni A, Thieme K, Chiu CP, Buchini S, Lairson LL, Chen H, et al. High-throughput screening methodology for the directed evolution of glycosyltransferases. Nat Methods 2006;3:609.
[212] Lecault V, VanInsberghe M, Sekulovic S, Knapp DJ, Wohrer S, Bowden W, et al. High-throughput analysis of single hematopoietic stem cell proliferation in microfluidic cell culture arrays. Nat Methods 2011;8:581-6.
[213] Love JC, Ronan JL, Grotenbreg GM, van der Veen AG, Ploegh HL. A microengraving method for rapid selection of single cells producing antigen-specific antibodies. Nat Biotechnol 2006;24:703.
[214] Agresti JJ, Antipov E, Abate AR, Ahn K, Rowat AC, Baret J-C, et al. Ultrahigh-throughput screening in drop-based microfluidics for directed evolution. Proceedings of the National Academy of Sciences 2010;107:4004-9.
[215] El Debs B, Utharala R, Balyasnikova IV, Griffiths AD, Merten CA. Functional single-cell hybridoma screening using droplet-based microfluidics. Proceedings of the National Academy of Sciences 2012;109:11570-5.
[216] Mazutis L, Griffiths AD. Selective droplet coalescence using microfluidic systems. Lab on a chip 2012;12:1800-6.
[217] Abate AR, Hung T, Mary P, Agresti JJ, Weitz DA. High-throughput injection with microfluidics using picoinjectors. Proceedings of the National Academy of Sciences 2010;107:19163-6.
[218] Huebner A, Olguin LF, Bratton D, Whyte G, Huck WT, De Mello AJ, et al. Development of quantitative cell-based enzyme assays in microdroplets. Anal Chem 2008;80:3890-6.
[219] Köster S, Angile FE, Duan H, Agresti JJ, Wintner A, Schmitz C, et al. Drop-based microfluidic devices for encapsulation of single cells. Lab on a chip 2008;8:1110-5.
[220] Lutolf MP, Gilbert PM, Blau HM. Designing materials to direct stem-cell fate. Nature 2009;462:433.
[221] Discher DE, Mooney DJ, Zandstra PW. Growth factors, matrices, and forces combine and control stem cells. Science 2009;324:1673-7.
[222] Gobaa S, Hoehnel S, Roccio M, Negro A, Kobel S, Lutolf MP. Artificial niche microarrays for probing single stem cell fate in high throughput. Nat Methods 2011;8:949-55.
[223] Khetan S, Burdick JA. Patterning network structure to spatially control cellular remodeling and stem cell fate within 3-dimensional hydrogels. Biomaterials 2010;31:8228-34.
[224] Lutolf MP. Integration column: artificial ECM: expanding the cell biology toolbox in 3D. Integrative Biology 2009;1:235-41.
[225] Flynn L. The use of decellularized adipose tissue to provide an inductive microenvironment for the adipogenic differentiation of human adipose-derived stem

cells. Biomaterials 2010;31:4715-24.
[226] Benoit DS, Schwartz MP, Durney AR, Anseth KS. Small functional groups for controlled differentiation of hydrogel-encapsulated human mesenchymal stem cells. Nature materials 2008;7:816-23.
[227] Choi NW, Cabodi M, Held B, Gleghorn JP, Bonassar LJ, Stroock AD. Microfluidic scaffolds for tissue engineering. Nature materials 2007;6:908.
[228] Sylvester KG, Longaker MT. Stem cells: review and update. Arch Surg 2004;139:93-9.
[229] Palmer TD, Takahashi J, Gage FH. The adult rat hippocampus contains primordial neural stem cells. Mol Cell Neurosci 1997;8:389-404.
[230] Reynolds BA, Weiss S. Generation of neurons and astrocytes from isolated cells of the adult mammalian central nervous system. Science 1992;255:1707.
[231] Van Praag H, Kempermann G, Gage FH. Running increases cell proliferation and neurogenesis in the adult mouse dentate gyrus. Nat Neurosci 1999;2:266-70.
[232] Kempermann G, Kuhn HG, Gage FH. More hippocampal neurons in adult mice living in an enriched environment. Nature 1997;386:493-5.
[233] Gould E, Cameron HA, Daniels DC, Woolley CS, McEwen BS. Adrenal hormones suppress cell division in the adult rat dentate gyrus. J Neurosci 1992;12:3642-50.
[234] Lois C, Alvarez-Buylla A. Long-distance neuronal migration in the adult mammalian brain. Science 1994;264:1145-8.
[235] Doetsch F, Caille I, Lim DA, Garc á-Verdugo JM, Alvarez-Buylla A. Subventricular zone astrocytes are neural stem cells in the adult mammalian brain. Cell 1999;97:703-16.
[236] Eriksson PS, Perfilieva E, Bj örk-Eriksson T, Alborn A-M, Nordborg C, Peterson DA, et al. Neurogenesis in the adult human hippocampus. Nat Med 1998;4:1313-7.
[237] Ma DK, Ming G-l, Song H. Glial influences on neural stem cell development: cellular niches for adult neurogenesis. Curr Opin Neurobiol 2005;15:514-20.
[238] Palmer TD, Markakis EA, Willhoite AR, Safar F, Gage FH. Fibroblast growth factor-2 activates a latent neurogenic program in neural stem cells from diverse regions of the adult CNS. J Neurosci 1999;19:8487-97.
[239] Seidenfaden R, Desoeuvre A, Bosio A, Virard I, Cremer H. Glial conversion of SVZ-derived committed neuronal precursors after ectopic grafting into the adult brain. Mol Cell Neurosci 2006;32:187-98.
[240] Shihabuddin LS, Horner PJ, Ray J, Gage FH. Adult spinal cord stem cells generate neurons after transplantation in the adult dentate gyrus. J Neurosci 2000;20:8727-35.
[241] Quiñones-Hinojosa A, Sanai N, Soriano-Navarro M, Gonzalez-Perez O, Mirzadeh Z, Gil-Perotin S, et al. Cellular composition and cytoarchitecture of the adult human subventricular zone: a niche of neural stem cells. J Comp Neurol 2006;494:415-34.
[242] Capela A, Temple S. LeX/ssea-1 is expressed by adult mouse CNS stem cells, identifying them as nonependymal. Neuron 2002;35:865-75.
[243] Rietze RL, Valcanis H, Brooker GF, Thomas T, Voss AK, Bartlett PF.

Purification of a pluripotent neural stem cell from the adult mouse brain. Nature 2001;412:736-9.
[244] Seri B, García-Verdugo JM, Collado-Morente L, McEwen BS, Alvarez-Buylla A. Cell types, lineage, and architecture of the germinal zone in the adult dentate gyrus. J Comp Neurol 2004;478:359-78.
[245] Kuhn HG, Eisch AJ. Neural Stem Cells in Development, Adulthood and Disease: Springer; 2014.
[246] Weiss S, Dunne C, Hewson J, Wohl C, Wheatley M, Peterson AC, et al. Multipotent CNS stem cells are present in the adult mammalian spinal cord and ventricular neuroaxis. J Neurosci 1996;16:7599-609.
[247] Martens DJ, Seaberg RM, Van Der Kooy D. In vivo infusions of exogenous growth factors into the fourth ventricle of the adult mouse brain increase the proliferation of neural progenitors around the fourth ventricle and the central canal of the spinal cord. Eur J Neurosci 2002;16:1045-57.
[248] Sabourin JC, Ackema KB, Ohayon D, Guichet PO, Perrin FE, Garces A, et al. A Mesenchymal-Like ZEB1+ Niche Harbors Dorsal Radial Glial Fibrillary Acidic Protein-Positive Stem Cells in the Spinal Cord. Stem Cells 2009;27:2722-33.
[249] Louis SA, Rietze RL, Deleyrolle L, Wagey RE, Thomas TE, Eaves AC, et al. Enumeration of neural stem and progenitor cells in the neural colony-forming cell assay. Stem Cells 2008;26:988-96.
[250] Meletis K, Barnabé-Heider F, Carlén M, Evergren E, Tomilin N, Shupliakov O, et al. Spinal cord injury reveals multilineage differentiation of ependymal cells. PLoS Biol 2008;6:e182.
[251] Gould E, Reeves AJ, Graziano MS, Gross CG. Neurogenesis in the neocortex of adult primates. Science 1999;286:548-52.
[252] Lie DC, Dziewczapolski G, Willhoite AR, Kaspar BK, Shults CW, Gage FH. The adult substantia nigra contains progenitor cells with neurogenic potential. J Neurosci 2002;22:6639-49.
[253] Pencea V, Bingaman KD, Wiegand SJ, Luskin MB. Infusion of brain-derived neurotrophic factor into the lateral ventricle of the adult rat leads to new neurons in the parenchyma of the striatum, septum, thalamus, and hypothalamus. J Neurosci 2001;21:6706-17.
[254] Shapiro LA, Ng KL, Kinyamu R, Whitaker-Azmitia P, Geisert EE, Blurton-Jones M, et al. Origin, migration and fate of newly generated neurons in the adult rodent piriform cortex. Brain structure and Function 2007;212:133-48.
[255] Shapiro LA, Ng K, Zhou Q-Y, Ribak CE. Subventricular zone-derived, newly generated neurons populate several olfactory and limbic forebrain regions. Epilepsy Behav 2009;14:74-80.
[256] Dworkin S, Mantamadiotis T. Targeting CREB signalling in neurogenesis. Expert Opin Ther Targets 2010;14:869-79.
[257] Hack M, Sugimori M, Lundberg C, Nakafuku M, Götz M. Regionalization and fate specification in neurospheres: the role of Olig2 and Pax6. Mol Cell Neurosci 2004;25:664-78.
[258] Kim EJ, Leung CT, Reed RR, Johnson JE. In vivo analysis of Ascl1 defined

progenitors reveals distinct developmental dynamics during adult neurogenesis and gliogenesis. J Neurosci 2007;27:12764-74.
[259] Wu H, Coskun V, Tao J, Xie W, Ge W, Yoshikawa K, et al. Dnmt3a-dependent nonpromoter DNA methylation facilitates transcription of neurogenic genes. Science 2010;329:444-8.
[260] Cheng L-C, Pastrana E, Tavazoie M, Doetsch F. miR-124 regulates adult neurogenesis in the subventricular zone stem cell niche. Nat Neurosci 2009;12:399-408.
[261] Candelario KM, Shuttleworth CW, Cunningham LA. Neural stem/progenitor cells display a low requirement for oxidative metabolism independent of hypoxia inducible factor-1alpha expression. J Neurochem 2013;125:420-9.
[262] Chiaramello S, Dalmasso G, Bezin L, Marcel D, Jourdan F, Peretto P, et al. BDNF/TrkB interaction regulates migration of SVZ precursor cells via PI3-K and MAP-K signalling pathways. Eur J Neurosci 2007;26:1780-90.
[263] Lie D-C, Colamarino SA, Song H-J, Désir éL, Mira H, Consiglio A, et al. Wnt signalling regulates adult hippocampal neurogenesis. Nature 2005;437:1370-5.
[264] Cartier L, Hartley O, Dubois-Dauphin M, Krause K-H. Chemokine receptors in the central nervous system: role in brain inflammation and neurodegenerative diseases. Brain Res Rev 2005;48:16-42.
[265] Baker SA, Baker KA, Hagg T. Dopaminergic nigrostriatal projections regulate neural precursor proliferation in the adult mouse subventricular zone. Eur J Neurosci 2004;20:575-9.
[266] Tong CK, Chen J, Cebri án-Silla A, Mirzadeh Z, Obernier K, Guinto CD, et al. Axonal control of the adult neural stem cell niche. Cell stem cell 2014;14:500-11.
[267] Paez-Gonzalez P, Asrican B, Rodriguez E, Kuo CT. Identification of distinct ChAT+ neurons and activity-dependent control of postnatal SVZ neurogenesis. Nat Neurosci 2014;17:934-42.
[268] Karpowicz P, Willaime-Morawek S, Balenci L, DeVeale B, Inoue T, van der Kooy D. E-Cadherin regulates neural stem cell self-renewal. J Neurosci 2009;29:3885-96.
[269] Lacar B, Young SZ, Platel JC, Bordey A. Gap junction-mediated calcium waves define communication networks among murine postnatal neural progenitor cells. Eur J Neurosci 2011;34:1895-905.
[270] Kokovay E, Wang Y, Kusek G, Wurster R, Lederman P, Lowry N, et al. VCAM1 is essential to maintain the structure of the SVZ niche and acts as an environmental sensor to regulate SVZ lineage progression. Cell stem cell 2012;11:220-30.
[271] Takahashi K, Yamanaka S. Induction of pluripotent stem cells from mouse embryonic and adult fibroblast cultures by defined factors. Cell 2006;126:663-76.
[272] Liu J. Induced pluripotent stem cell-derived neural stem cells: new hope for stroke? Stem Cell Res Ther 2013;4:1.
[273] Brambrink T, Foreman R, Welstead GG, Lengner CJ, Wernig M, Suh H, et al. Sequential expression of pluripotency markers during direct reprogramming of mouse somatic cells. Cell stem cell 2008;2:151-9.
[274] Stadtfeld M, Maherali N, Breault DT, Hochedlinger K. Defining molecular

cornerstones during fibroblast to iPS cell reprogramming in mouse. Cell stem cell 2008;2:230-40.
[275] Laurent LC, Ulitsky I, Slavin I, Tran H, Schork A, Morey R, et al. Dynamic changes in the copy number of pluripotency and cell proliferation genes in human ESCs and iPSCs during reprogramming and time in culture. Cell stem cell 2011;8:106-18.
[276] Gore A, Li Z, Fung H-L, Young JE, Agarwal S, Antosiewicz-Bourget J, et al. Somatic coding mutations in human induced pluripotent stem cells. Nature 2011;471:63-7.
[277] Lister R, Pelizzola M, Kida YS, Hawkins RD, Nery JR, Hon G, et al. Hotspots of aberrant epigenomic reprogramming in human induced pluripotent stem cells. Nature 2011;471:68-73.
[278] Ben-David U, Benvenisty N. The tumorigenicity of human embryonic and induced pluripotent stem cells. Nature Reviews Cancer 2011;11:268-77.
[279] Stadtfeld M, Nagaya M, Utikal J, Weir G, Hochedlinger K. Induced pluripotent stem cells generated without viral integration. Science 2008;322:945-9.
[280] Albihn A, Johnsen JI, Henriksson MA. MYC in oncogenesis and as a target for cancer therapies. Adv Cancer Res 2010;107:163-224.
[281] Harrison NJ, Baker D, Andrews PW. Culture adaptation of embryonic stem cells echoes germ cell malignancy. Int J Androl 2007;30:275-81.
[282] Onorati M, Camnasio S, Binetti M, Jung CB, Moretti A, Cattaneo E. Neuropotent self-renewing neural stem (NS) cells derived from mouse induced pluripotent stem (iPS) cells. Mol Cell Neurosci 2010;43:287-95.
[283] Chambers SM, Fasano CA, Papapetrou EP, Tomishima M, Sadelain M, Studer L. Highly efficient neural conversion of human ES and iPS cells by dual inhibition of SMAD signaling. Nat Biotechnol 2009;27:275-80.
[284] Douvaras P, Wang J, Zimmer M, Hanchuk S, O'Bara MA, Sadiq S, et al. Efficient generation of myelinating oligodendrocytes from primary progressive multiple sclerosis patients by induced pluripotent stem cells. Stem cell reports 2014;3:250-9.
[285] Goldman SA. Stem and progenitor cell-based therapy of the central nervous system: hopes, hype, and wishful thinking. Cell stem cell 2016;18:174-88.
[286] Sauka-Spengler T, Bronner-Fraser M. A gene regulatory network orchestrates neural crest formation. Nature reviews Molecular cell biology 2008;9:557-68.
[287] Eroglu C, Barres BA. Regulation of synaptic connectivity by glia. Nature 2010;468:223-31.
[288] Poss KD. Advances in understanding tissue regenerative capacity and mechanisms in animals. Nature Reviews Genetics 2010;11:710-22.
[289] Wictorin K, Brundin P, Sauer H, Lindvall O, Björklund A. Long distance directed axonal growth from human dopaminergic mesencephalic neuroblasts implanted along the nigrostriatal pathway in 6-hydroxydopamine lesioned adult rats. J Comp Neurol 1992;323:475-94.
[290] Cummings BJ, Uchida N, Tamaki SJ, Salazar DL, Hooshmand M, Summers R, et al. Human neural stem cells differentiate and promote locomotor recovery in spinal

cord-injured mice. Proc Natl Acad Sci U S A 2005;102:14069-74.
[291] Daadi MM, Li Z, Arac A, Grueter BA, Sofilos M, Malenka RC, et al. Molecular and magnetic resonance imaging of human embryonic stem cell–derived neural stem cell grafts in ischemic rat brain. Mol Ther 2009;17:1282-91.
[292] Pluchino S, Quattrini A, Brambilla E, Gritti A, Salani G, Dina G, et al. Injection of adult neurospheres induces recovery in a chronic model of multiple sclerosis. Nature 2003;422:688-94.
[293] Shihabuddin L, Holets V, Whittemore S. Selective hippocampal lesions differentially affect the phenotypic fate of transplanted neuronal precursor cells. Exp Neurol 1996;139:61-72.
[294] Goldman S. Stem and progenitor cell–based therapy of the human central nervous system. Nat Biotechnol 2005;23:862-71.
[295] Redmond DE, Bjugstad KB, Teng YD, Ourednik V, Ourednik J, Wakeman DR, et al. Behavioral improvement in a primate Parkinson's model is associated with multiple homeostatic effects of human neural stem cells. Proceedings of the National Academy of Sciences 2007;104:12175-80.
[296] Aharonowiz M, Einstein O, Fainstein N, Lassmann H, Reubinoff B, Ben-Hur T. Neuroprotective effect of transplanted human embryonic stem cell-derived neural precursors in an animal model of multiple sclerosis. PLoS One 2008;3:e3145.
[297] Ryu JK, Kim J, Cho SJ, Hatori K, Nagai A, Choi HB, et al. Proactive transplantation of human neural stem cells prevents degeneration of striatal neurons in a rat model of Huntington disease. Neurobiol Dis 2004;16:68-77.
[298] Kokaia Z, Martino G, Schwartz M, Lindvall O. Cross-talk between neural stem cells and immune cells: the key to better brain repair [quest]. Nat Neurosci 2012;15:1078-87.
[299] Kordower JH, Freeman TB, Snow BJ, Vingerhoets FJ, Mufson EJ, Sanberg PR, et al. Neuropathological evidence of graft survival and striatal reinnervation after the transplantation of fetal mesencephalic tissue in a patient with Parkinson's disease. N Engl J Med 1995;332:1118-24.
[300] Gomi M, Aoki T, Takagi Y, Nishimura M, Ohsugi Y, Mihara M, et al. Single and local blockade of interleukin-6 signaling promotes neuronal differentiation from transplanted embryonic stem cell-derived neural precursor cells. J Neurosci Res 2011;89:1388-99.
[301] Martino G, Pluchino S. The therapeutic potential of neural stem cells. Nat Rev Neurosci 2006;7:395-406.
[302] Pluchino S, Zanotti L, Rossi B, Brambilla E, Ottoboni L, Salani G, et al. Neurosphere-derived multipotent precursors promote neuroprotection by an immunomodulatory mechanism. Nature 2005;436:266-71.
[303] Lee S-T, Chu K, Jung K-H, Kim S-J, Kim D-H, Kang K-M, et al. Anti-inflammatory mechanism of intravascular neural stem cell transplantation in haemorrhagic stroke. Brain 2008;131:616-29.
[304] Cusimano M, Biziato D, Brambilla E, Donegà M, Alfaro-Cervello C, Snider S, et al. Transplanted neural stem/precursor cells instruct phagocytes and reduce secondary tissue damage in the injured spinal cord. Brain 2012;135:447-60.

[305] Cao W, Yang Y, Wang Z, Liu A, Fang L, Wu F, et al. Leukemia inhibitory factor inhibits T helper 17 cell differentiation and confers treatment effects of neural progenitor cell therapy in autoimmune disease. Immunity 2011;35:273-84.
[306] Ziv Y, Avidan H, Pluchino S, Martino G, Schwartz M. Synergy between immune cells and adult neural stem/progenitor cells promotes functional recovery from spinal cord injury. Proceedings of the National Academy of Sciences 2006;103:13174-9.
[307] Lu P, Jones L, Snyder E, Tuszynski M. Neural stem cells constitutively secrete neurotrophic factors and promote extensive host axonal growth after spinal cord injury. Exp Neurol 2003;181:115-29.
[308] Lindvall O, Kokaia Z. Stem cells in human neurodegenerative disorders—time for clinical translation? The Journal of clinical investigation 2010;120:29-40.
[309] Andres RH, Horie N, Slikker W, Keren-Gill H, Zhan K, Sun G, et al. Human neural stem cells enhance structural plasticity and axonal transport in the ischaemic brain. Brain 2011;134:1777-89.
[310] Jäderstad J, Jäderstad LM, Li J, Chintawar S, Salto C, Pandolfo M, et al. Communication via gap junctions underlies early functional and beneficial interactions between grafted neural stem cells and the host. Proceedings of the National Academy of Sciences 2010;107:5184-9.
[311] Lunn JS, Sakowski SA, Hur J, Feldman EL. Stem cell technology for neurodegenerative diseases. Ann Neurol 2011;70:353-61.
[312] Lindvall O, Kokaia Z. Stem cells for the treatment of neurological disorders. Nature 2006;441:1094-6.
[313] Kish SJ, Shannak K, Hornykiewicz O. Uneven pattern of dopamine loss in the striatum of patients with idiopathic Parkinson's disease. N Engl J Med 1988;318:876-80.
[314] Poewe W. Treatments for Parkinson disease—past achievements and current clinical needs. Neurology 2009;72:S65-S73.
[315] Benabid AL, Chabardes S, Mitrofanis J, Pollak P. Deep brain stimulation of the subthalamic nucleus for the treatment of Parkinson's disease. The Lancet Neurology 2009;8:67-81.
[316] Krack P, Batir A, Van Blercom N, Chabardes S, Fraix V, Ardouin C, et al. Five-year follow-up of bilateral stimulation of the subthalamic nucleus in advanced Parkinson's disease. N Engl J Med 2003;349:1925-34.
[317] Brundin P, Barker RA, Parmar M. Neural grafting in Parkinson’s disease: problems and possibilities. Prog Brain Res 2010;184:265-94.
[318] Cui Y-F, Xu J-C, Hargus G, Jakovcevski I, Schachner M, Bernreuther C. Embryonic stem cell-derived L1 overexpressing neural aggregates enhance recovery after spinal cord injury in mice. PLoS One 2011;6:e17126.
[319] Emborg ME, Ebert AD, Moirano J, Peng S, Suzuki M, Capowski E, et al. GDNF-secreting human neural progenitor cells increase tyrosine hydroxylase and VMAT2 expression in MPTP-treated cynomolgus monkeys. Cell Transplant 2008;17:383-95.
[320] Hargus G, Cooper O, Deleidi M, Levy A, Lee K, Marlow E, et al. Differentiated

Parkinson patient-derived induced pluripotent stem cells grow in the adult rodent brain and reduce motor asymmetry in Parkinsonian rats. Proceedings of the National Academy of Sciences 2010;107:15921-6.
[321] Ebert AD, Beres AJ, Barber AE, Svendsen CN. Human neural progenitor cells over-expressing IGF-1 protect dopamine neurons and restore function in a rat model of Parkinson's disease. Exp Neurol 2008;209:213-23.
[322] Xiong N, Zhang Z, Huang J, Chen C, Jia M, Xiong J, et al. VEGF-expressing human umbilical cord mesenchymal stem cells, an improved therapy strategy for Parkinson's disease. Gene Ther 2011;18:394.
[323] Whitehouse PJ, Price DL, Clark AW, Coyle JT, DeLong MR. Alzheimer disease: evidence for selective loss of cholinergic neurons in the nucleus basalis. Ann Neurol 1981;10:122-6.
[324] Bartus RT, Dean Rr, Beer B, Lippa AS. The cholinergic hypothesis of geriatric memory dysfunction. Science 1982;217:408-14.
[325] Blurton-Jones M, Kitazawa M, Martinez-Coria H, Castello NA, Müller F-J, Loring JF, et al. Neural stem cells improve cognition via BDNF in a transgenic model of Alzheimer disease. Proceedings of the National Academy of Sciences 2009;106:13594-9.
[326] Wu S, Sasaki A, Yoshimoto R, Kawahara Y, Manabe T, Kataoka K, et al. Neural stem cells improve learning and memory in rats with Alzheimer's disease. Pathobiology 2008;75:186-94.
[327] Rowland LP, Shneider NA. Amyotrophic lateral sclerosis. N Engl J Med 2001;344:1688-700.
[328] Goldblatt D. Amyotrophic Lateral Sclerosis. Concepts in Pathogenesis and Etiology. Arch Neurol 1991;48:465-.
[329] Klein SM, Behrstock S, McHugh J, Hoffmann K, Wallace K, Suzuki M, et al. GDNF delivery using human neural progenitor cells in a rat model of ALS. Hum Gene Ther 2005;16:509-21.
[330] Lunn JS, Hefferan MP, Marsala M, Feldman EL. Stem cells: comprehensive treatments for amyotrophic lateral sclerosis in conjunction with growth factor delivery. Growth Factors 2009;27:133-40.
[331] Xu L, Ryugo DK, Pongstaporn T, Johe K, Koliatsos VE. Human neural stem cell grafts in the spinal cord of SOD1 transgenic rats: differentiation and structural integration into the segmental motor circuitry. J Comp Neurol 2009;514:297-309.
[332] Raore B, Federici T, Taub J, Wu MC, Riley J, Franz CK, et al. Cervical multilevel intraspinal stem cell therapy: assessment of surgical risks in Gottingen minipigs. Spine 2011;36:E164-E71.
[333] MacDonald ME, Ambrose CM, Duyao MP, Myers RH, Lin C, Srinidhi L, et al. A novel gene containing a trinucleotide repeat that is expanded and unstable on Huntington's disease chromosomes. Cell 1993;72:971-83.
[334] Walker FO. Huntington's disease. The Lancet 2007;369:218-28.
[335] Kelly CM, Dunnett SB, Rosser AE. Medium spiny neurons for transplantation in Huntington's disease. Portland Press Limited; 2009.
[336] McBride JL, Behrstock SP, Chen EY, Jakel RJ, Siegel I, Svendsen CN, et al.

Human neural stem cell transplants improve motor function in a rat model of Huntington's disease. J Comp Neurol 2004;475:211-9.
[337] Ebert AD, Barber AE, Heins BM, Svendsen CN. Ex vivo delivery of GDNF maintains motor function and prevents neuronal loss in a transgenic mouse model of Huntington's disease. Exp Neurol 2010;224:155-62.
[338] De Feo D, Merlini A, Laterza C, Martino G. Neural stem cell transplantation in central nervous system disorders: from cell replacement to neuroprotection. Curr Opin Neurol 2012;25:322-33.
[339] Roy NS, Cleren C, Singh SK, Yang L, Beal MF, Goldman SA. Functional engraftment of human ES cell-derived dopaminergic neurons enriched by coculture with telomerase-immortalized midbrain astrocytes. Nat Med 2006;12:1259.
[340] Amariglio N, Hirshberg A, Scheithauer BW, Cohen Y, Loewenthal R, Trakhtenbrot L, et al. Donor-derived brain tumor following neural stem cell transplantation in an ataxia telangiectasia patient. PLoS Med 2009;6:e1000029.
[341] Guillemot F. Spatial and temporal specification of neural fates by transcription factor codes. Development 2007;134:3771-80.
[342] Trounson A, McDonald C. Stem cell therapies in clinical trials: progress and challenges. Cell stem cell 2015;17:11-22.
[343] Piantadosi S. Clinical trials: a methodologic perspective: John Wiley & Sons; 2017.
[344] Kishima H, Poyot T, Bloch J, Dauguet J, Condé F, Dollé F, et al. Encapsulated GDNF-producing C2C12 cells for Parkinson's disease: a pre-clinical study in chronic MPTP-treated baboons. Neurobiol Dis 2004;16:428-39.
[345] Lindner MD, Plone MA, Frydel B, Kaplan FA, Krueger PM, Bell WJ, et al. Intraventricular encapsulated calf adrenal chromaffin cells: viable for at least 500 days in vivo without detectable adverse effects on behavioral/cognitive function or host immune sensitization in rats. Restor Neurol Neurosci 1997;11:21-35.
[346] Barati D, Kader S, Pajoum Shariati SR, Moeinzadeh S, Sawyer RH, Jabbari E. Synthesis and Characterization of Photo-Cross-Linkable Keratin Hydrogels for Stem Cell Encapsulation. Biomacromolecules 2017;18:398-412.
[347] Madl CM, Katz LM, Heilshorn SC. Bio-Orthogonally Crosslinked, Engineered Protein Hydrogels with Tunable Mechanics and Biochemistry for Cell Encapsulation. Adv Funct Mater 2016;26:3612-20.
[348] Vega SL, Kwon M, Mauck RL, Burdick JA. Single Cell Imaging to Probe Mesenchymal Stem Cell N-Cadherin Mediated Signaling within Hydrogels. Ann Biomed Eng 2016;44:1921-30.
[349] Emanet M, Fakhrullin R, Çulha M. Boron Nitride Nanotubes and Layer-By-Layer Polyelectrolyte Coating for Yeast Cell Surface Engineering. ChemNanoMat 2016.
[350] Drachuk I, Calabrese R, Harbaugh S, Kelley-Loughnane N, Kaplan DL, Stone M, et al. Silk Macromolecules with Amino Acid–Poly (Ethylene Glycol) Grafts for Controlling Layer-by-Layer Encapsulation and Aggregation of Recombinant Bacterial Cells. ACS nano 2015;9:1219-35.
[351] Dooves S, van der Knaap MS, Heine VM. Stem cell therapy for white matter

disorders: don’t forget the microenvironment! J Inherit Metab Dis 2016:1-6.
[352] grosse Austing J, Kirchner CN, Komsiyska L, Wittstock G. Layer-by-layer modification of Nafion membranes for increased life-time and efficiency of vanadium/air redox flow batteries. J Membr Sci 2016;510:259-69.
[353] Jin Y, Bouyer J, Shumsky J, Haas C, Fischer I. Transplantation of neural progenitor cells in chronic spinal cord injury. Neuroscience 2016;320:69-82.
[354] Lu Y, Jiang L, He X, Yang G-Y, Wang Y. Optogenetic Inhibition of Striatal Neurons Improves the Survival of Implanted Neural Stem Cell and Neurological Outcomes After Ischemic Stroke. Stroke 2016;47:A129-A.
[355] Hu R, Duan B, Wang D, Yu Y, Li W, Luo H, et al. Role of acid-sensing ion channel 1a in the secondary damage of traumatic spinal cord injury. Ann Surg 2011;254:353-62.
[356] Hu R, Sun H, Zhang Q, Chen J, Wu N, Meng H, et al. G-protein coupled estrogen receptor 1 mediated estrogenic neuroprotection against spinal cord injury*. Crit Care Med 2012;40:3230-7.
[357] Bhowmick S, Scharnweber D, Koul V. Co-cultivation of keratinocyte-human mesenchymal stem cell (hMSC) on sericin loaded electrospun nanofibrous composite scaffold (cationic gelatin/hyaluronan/chondroitin sulfate) stimulates epithelial differentiation in hMSCs: In vitro study. Biomaterials 2016;88:83-96.
[358] Zhang C, Xu W, Jin W, Shah BR, Li Y, Li B. Influence of anionic alginate and cationic chitosan on physicochemical stability and carotenoids bioaccessibility of soy protein isolate-stabilized emulsions. Food Res Int 2015;77:419-25.
[359] Zhang X, Song G-J, Cao X-J, Liu J-T, Chen M-Y, Cao X-Q, et al. A new fluorescent pH probe for acidic conditions. RSC Advances 2015;5:89827-32.
[360] Wang L, Wang N, Li J, Li J, Bian W, Ji S. Layer-by-layer self-assembly of polycation/GO nanofiltration membrane with enhanced stability and fouling resistance. Sep Purif Technol 2016.
[361] Xiao F-X, Pagliaro M, Xu Y-J, Liu B. Layer-by-layer assembly of versatile nanoarchitectures with diverse dimensionality: a new perspective for rational construction of multilayer assemblies. Chem Soc Rev 2016.
[362] Jiang C, Luo C, Liu X, Shao L, Dong Y, Zhang Y, et al. Adjusting the ion permeability of polyelectrolyte multilayers through layer-by-layer assembly under a high gravity field. ACS applied materials & interfaces 2015;7:10920-7.
[363] Qin Z, Ren X, Shan L, Guo H, Geng C, Zhang G, et al. Nacrelike-structured multilayered polyelectrolyte/calcium carbonate nanocomposite membrane via Ca-incorporated layer-by-layer-assembly and CO 2-induced biomineralization. J Membr Sci 2016;498:180-91.
[364] Wu F, Ju X-J, He X-H, Jiang M-Y, Wang W, Liu Z, et al. A novel synthetic microfiber with controllable size for cell encapsulation and culture. J Mater Chem B 2016;4:2455-65.
[365] Duncan RN, Xie Y, McPherson AD, Taibi AV, Bonkowsky JL, Douglass AD, et al. Hypothalamic radial glia function as self-renewing neural progenitors in the absence of Wnt/β-catenin signaling. Development 2016;143:45-53.
[366] Sullivan JM, Havrda MC, Kettenbach AN, Paolella BR, Zhang Z, Gerber SA, et

al. Phosphorylation regulates Id2 degradation and mediates the proliferation of neural precursor cells. Stem Cells 2016.
[367] Cui W, Wang A, Zhao J, Yang X, Cai P, Li J. Layer by layer assembly of albumin nanoparticles with selective recognition of tumor necrosis factor-related apoptosis-inducing ligand (TRAIL). J Colloid Interface Sci 2016;465:11-7.
[368] Li L, Xiong ZY, Qian ZM, Zhao TZ, Feng H, Hu S, et al. Complement C5a is detrimental to histological and functional locomotor recovery after spinal cord injury in mice. Neurobiol Dis 2014;66:74-82.
[369] Elkind MS, McClure LA, Luna JM, Del Brutto OH, Pikula A, Benavente OR. Tumor Necrosis Factor Receptor 1 and Subclinical Cerebrovascular Disease: the Levels of Inflammatory Markers in Treatment of Stroke Study. Stroke 2016;47:A219-A.
[370] Wack KE, Ross MA, Zegarra V, Sysko LR, Watkins SC, Stolz DB. Sinusoidal ultrastructure evaluated during the revascularization of regenerating rat liver. Hepatology 2001;33:363-78.
[371] Wang H, Hansen MB, Lowik DW, van Hest JC, Li Y, Jansen JA, et al. Oppositely charged gelatin nanospheres as building blocks for injectable and biodegradable gels. Adv Mater 2011;23:H119-24.
[372] Purcell EK, Singh A, Kipke DR. Alginate Composition Effects on a Neural Stem Cell-Seeded Scaffold. Tissue Eng, Part C 2009;15:541-50.
[373] Park TG, Jeong JH, Kim SW. Current status of polymeric gene delivery systems. Adv Drug Delivery Rev 2006;58:467-86.
[374] Mansouri S, Merhi Y, Winnik FM, Tabrizian M. Investigation of layer-by-layer assembly of polyelectrolytes on fully functional human red blood cells in suspension for attenuated immune response. Biomacromolecules 2011;12:585-92.
[375] Lehner B, Sandner B, Marschallinger J, Lehner C, Furtner T, Couillard-Despres S, et al. The dark side of BrdU in neural stem cell biology: detrimental effects on cell cycle, differentiation and survival. Cell Tissue Res 2011;345:313-28.
[376] Carter JL, Drachuk I, Harbaugh S, Kelley-Loughnane N, Stone M, Tsukruk VV. Truly nonionic polymer shells for the encapsulation of living cells. Macromol Biosci 2011;11:1244-53.
[377] Krol S, Diaspro A, Magrassi R, Ballario P, Grimaldi B, Filetici P, et al. Nanocapsules: coating for living cells. IEEE Trans NanoBiosci 2004;3:32-8.
[378] Arsenijevic Y, Weiss S, Schneider B, Aebischer P. Insulin-like growth factor-I is necessary for neural stem cell proliferation and demonstrates distinct actions of epidermal growth factor and fibroblast growth factor-2. J Neurosci 2001;21:7194-202.
[379] Schneider A, Krüger C, Steigleder T, Weber D, Pitzer C, Laage R, et al. The hematopoietic factor G-CSF is a neuronal ligand that counteracts programmed cell death and drives neurogenesis. J Clin Invest 2005;115:2083-98.
[380] Manna U, Patil S. Dual drug delivery microcapsules via layer-by-layer self-assembly. Langmuir 2009;25:10515-22.
[381] Zelikin AN. Drug releasing polymer thin films: new era of surface-mediated drug delivery. ACS nano 2010;4:2494-509.
[382] Yoshida K, Hashide R, Ishii T, Takahashi S, Sato K, Anzai J-i. Layer-by-layer

films composed of poly (allylamine) and insulin for pH-triggered release of insulin. Colloids Surf, B 2012;91:274-9.
[383] Shen H, Shi H, Xie M, Ma K, Li B, Shen S, et al. Biodegradable chitosan/alginate BSA-gel-capsules for pH-controlled loading and release of doxorubicin and treatment of pulmonary melanoma. J Mater Chem B 2013;1:3906-17.
[384] Crouzier T, Ren K, Nicolas C, Roy C, Picart C. Layer-By-Layer Films as a Biomimetic Reservoir for rhBMP-2 Delivery: Controlled Differentiation of Myoblasts to Osteoblasts. Small 2009;5:598-608.
[385] Frederick TJ, Wood TL. IGF-I and FGF-2 coordinately enhance cyclin D1 and cyclin E–cdk2 association and activity to promote G1 progression in oligodendrocyte progenitor cells. Mol Cell Neurosci 2004;25:480-92.
[386] Kaku DA, Giffard RG, Choi DW. Neuroprotective effects of glutamate antagonists and extracellular acidity. Science 1993;260:1516-8.
[387] Sato K, Yoshida K, Takahashi S, Anzai J. pH- and sugar-sensitive layer-by-layer films and microcapsules for drug delivery. Adv Drug Delivery Rev 2011;63:809-21.
[388] Åberg MAI, Åberg ND, Palmer TD, Alborn A-M, Carlsson-Skwirut C, Bang P, et al. IGF-I has a direct proliferative effect in adult hippocampal progenitor cells. Mol Cell Neurosci 2003;24:23-40.
[389] Huang X, Brazel CS. On the importance and mechanisms of burst release in matrix-controlled drug delivery systems. J Control Release 2001;73:121-36.
[390] Darbinian N. Cultured Cell Line Models of Neuronal Differentiation: NT2, PC12. Neuronal Cell Culture: Methods and Protocols 2013:23-33.
[391] Mao J. Effects of hyaluronic acid-chitosan-gelatin complex on the apoptosis and cell cycle of L929 cells. Chin Sci Bull 2003;48:1807.
[392] Scholzen T, Gerdes J. The Ki-67 protein: from the known and the unknown. J Cell Physiol 2000;182:311-22.
[393] Eckel-Passow JE, Serie DJ, Cheville JC, Ho TH, Harrington SM, Hilton T, et al. Concordance of BAP1, PBRM1, Ki-67, and TOPOIIa protein expression in primary clear cell renal cell carcinoma tumors and patient-matched metastatic tumors. Clin Cancer Res 2016;22:10-.
[394] Francois JM, Formosa C, Schiavone M, Pillet F, Martin-Yken H, Dague E. Use of atomic force microscopy (AFM) to explore cell wall properties and response to stress in the yeast Saccharomyces cerevisiae. Curr Genet 2013;59:187-96.
[395] Hulström D, Svensjö E. Intravital and electron microscopic study of bradykinin-induced vascular permeability changes using FITC-dextran as a tracer. The Journal of pathology 1979;129:125-33.
[396] Chen F, Hou M, Ye F, Lv W, Xie X. Ovarian cancer cells induce peripheral mature dendritic cells to differentiate into macrophagelike cells in vitro. Int J Gynecol Cancer 2009;19:1487-93.
[397] Antipov AA, Sukhorukov GB, Leporatti S, Radtchenko IL, Donath E, Möhwald H. Polyelectrolyte multilayer capsule permeability control. Colloids Surf Physicochem Eng Aspects 2002;198:535-41.
[398] Lu Z, Prouty MD, Guo Z, Golub VO, Kumar CS, Lvov YM. Magnetic switch of permeability for polyelectrolyte microcapsules embedded with Co@ Au nanoparticles.

Langmuir 2005;21:2042-50.
[399] Yu Z, Zhang J, Coulston RJ, Parker RM, Biedermann F, Liu X, et al. Supramolecular hydrogel microcapsules via cucurbit [8] uril host–guest interactions with triggered and UV-controlled molecular permeability. Chemical Science 2015;6:4929-33.
[400] Taylor RA, Sansing LH. Microglial responses after ischemic stroke and intracerebral hemorrhage. Clin Dev Immunol 2013;2013:746068.
[401] Hausmann ON. Post-traumatic inflammation following spinal cord injury. Spinal Cord 2003;41:369-78.
[402] Shalini S, Dorstyn L, Dawar S, Kumar S. Old, new and emerging functions of caspases. Cell Death Differ 2015;22:526-39.
[403] Macmillan H, Strohman MJ, Ayyangar S, Jiang W, Rajasekaran N, Spura A, et al. The MHC Class II Cofactor HLA-DM Interacts with Ig in B Cells. The Journal of Immunology 2014;193:2641-50.
[404] Gozzelino R, Sole C, Llecha N, Segura MF, Moubarak RS, Iglesias-Guimarais V, et al. BCL-XL regulates TNF-alpha-mediated cell death independently of NF-kappaB, FLIP and IAPs. Cell Res 2008;18:1020-36.
[405] Andres CM, Kotov NA. Inkjet deposition of layer-by-layer assembled films. J Am Chem Soc 2010;132:14496-502.
[406] Wang Y, Tong SW, Xu XF, Özyilmaz B, Loh KP. Interface engineering of Layer-by-Layer stacked graphene anodes for High-Performance organic solar cells. Adv Mater 2011;23:1514-8.
[407] Lvov Y, Ariga K, Onda M, Ichinose I, Kunitake T. Alternate assembly of ordered multilayers of SiO2 and other nanoparticles and polyions. Langmuir 1997;13:6195-203.
[408] Lvov Y, Haas H, Decher G, Moehwald H, Mikhailov A, Mtchedlishvily B, et al. Successive deposition of alternate layers of polyelectrolytes and a charged virus. Langmuir 1994;10:4232-6.
[409] Ariga K, McShane M, Lvov YM, Ji Q, Hill JP. Layer-by-layer assembly for drug delivery and related applications. Expert opinion on drug delivery 2011;8:633-44.
[410] Komatsu T, Qu X, Ihara H, Fujihara M, Azuma H, Ikeda H. Virus trap in human serum albumin nanotube. J Am Chem Soc 2011;133:3246-8.
[411] Sukhishvili SA, Granick S. Layered, erasable, ultrathin polymer films. J Am Chem Soc 2000;122:9550-1.
[412] Serizawa T, Hamada K-i, Akashi M. Polymerization within a molecular-scale stereogular template. Nature 2004;429:52.
[413] Wang F, Ma N, Chen Q, Wang W, Wang L. Halogen bonding as a new driving force for layer-by-layer assembly. Langmuir 2007;23:9540-2.
[414] Li M, Ishihara S, Akada M, Liao M, Sang L, Hill JP, et al. Electrochemical-coupling layer-by-layer (ECC–LbL) assembly. J Am Chem Soc 2011;133:7348-51.
[415] Trau D, Renneberg R. Encapsulation of glucose oxidase microparticles within a nanoscale layer-by-layer film: immobilization and biosensor applications. Biosens

Bioelectron 2003;18:1491-9.
[416] Zhang Y, Arugula MA, Wales M, Wild J, Simonian AL. A novel layer-by-layer assembled multi-enzyme/CNT biosensor for discriminative detection between organophosphorus and non-organophosphrus pesticides. Biosens Bioelectron 2015;67:287-95.
[417] Cong X, Poyton MF, Baxter AJ, Pullanchery S, Cremer PS. Unquenchable surface potential dramatically enhances Cu2+ binding to phosphatidylserine lipids. J Am Chem Soc 2015;137:7785-92.
[418] Bernfield M, Götte M, Park PW, Reizes O, Fitzgerald ML, Lincecum J, et al. Functions of cell surface heparan sulfate proteoglycans. Annu Rev Biochem 1999;68:729-77.
[419] Parhamifar L, Larsen AK, Hunter AC, Andresen TL, Moghimi SM. Polycation cytotoxicity: a delicate matter for nucleic acid therapy—focus on polyethylenimine. Soft Matter 2010;6:4001.
[420] Lee H, Hong D, Choi JY, Kim JY, Lee SH, Kim HM, et al. Layer-by-Layer-Based Silica Encapsulation of Individual Yeast with Thickness Control. Chemistry–An Asian Journal 2015;10:129-32.
[421] Lu S, Yang Y, Yao J, Shao Z, Chen X. Exploration of the nature of a unique natural polymer-based thermosensitive hydrogel. Soft matter 2016;12:492-9.
[422] Pacelli S, Manoharan V, Desalvo A, Lomis N, Jodha KS, Prakash S, et al. Tailoring biomaterial surface properties to modulate host-implant interactions: implication in cardiovascular and bone therapy. J Mater Chem B 2016.
[423] Wilson JT, Krishnamurthy VR, Cui W, Qu Z, Chaikof EL. Noncovalent cell surface engineering with cationic graft copolymers. J Am Chem Soc 2009;131:18228-9.
[424] Santos T, Boto C, Saraiva CM, Bernardino L, Ferreira L. Nanomedicine Approaches to Modulate Neural Stem Cells in Brain Repair. Trends Biotechnol 2016.
[425] Haque MA, Nagaoka M, Hexig B, Akaike T. Artificial extracellular matrix for embryonic stem cell cultures: a new frontier of nanobiomaterials. Science and Technology of Advanced Materials 2016.
[426] Slowing I, Trewyn BG, Lin VS-Y. Effect of surface functionalization of MCM-41-type mesoporous silica nanoparticles on the endocytosis by human cancer cells. J Am Chem Soc 2006;128:14792-3.
[427] Blacklock J, Handa H, Manickam DS, Mao G, Mukhopadhyay A, Oupický D. Disassembly of layer-by-layer films of plasmid DNA and reducible TAT polypeptide. Biomaterials 2007;28:117-24.
[428] Priya AJ, Vijayalakshmi S, Raichur AM. Enhanced survival of probiotic Lactobacillus acidophilus by encapsulation with nanostructured polyelectrolyte layers through layer-by-layer approach. J Agric Food Chem 2011;59:11838-45.
[429] Yakar S, Liu J-L, Stannard B, Butler A, Accili D, Sauer B, et al. Normal growth and development in the absence of hepatic insulin-like growth factor I. Proceedings of the National Academy of Sciences 1999;96:7324-9.
[430] Prager D, Melmed S. Insulin and insulin-like growth factor I receptors: are there functional distinctions? Endocrinology 1993;132:1419-20.

[431] Escott GM, Jacobus AP, Loss ES. PI3K-dependent actions of insulin and IGF-I on seminiferous tubules from immature rats. Pflügers Archiv-European Journal of Physiology 2013;465:1497-505.
[432] Xu G-J, Cai S, Wu J-B. Effect of insulin-like growth factor-1 on bone morphogenetic protein-2 expression in hepatic carcinoma SMMC7721 cells through the p38 MAPK signaling pathway. Asian Pac J Cancer Prev 2012;13:1183-6.
[433] McIlroy J, Chen D, Wjasow C, Michaeli T, Backer JM. Specific activation of p85-p110 phosphatidylinositol 3'-kinase stimulates DNA synthesis by ras-and p70 S6 kinase-dependent pathways. Mol Cell Biol 1997;17:248-55.
[434] Kotani K, Yonezawa K, Hara K, Ueda H, Kitamura Y, Sakaue H, et al. Involvement of phosphoinositide 3-kinase in insulin-or IGF-1-induced membrane ruffling. The EMBO Journal 1994;13:2313.
[435] Clerk A, Aggeli I-KS, Stathopoulou K, Sugden PH. Peptide growth factors signal differentially through protein kinase C to extracellular signal-regulated kinases in neonatal cardiomyocytes. Cell Signal 2006;18:225-35.
[436] Ye P, Li L, Richards RG, DiAugustine RP, D'Ercole AJ. Myelination is altered in insulin-like growth factor-I null mutant mice. J Neurosci 2002;22:6041-51.
[437] Cheng CM, Mervis RF, Niu SL, Salem N, Witters LA, Tseng V, et al. Insulin-like growth factor 1 is essential for normal dendritic growth. J Neurosci Res 2003;73:1-9.
[438] Beck KD, Powell-Braxtont L, Widmer H-R, Valverde J, Hefti F. Igf1 gene disruption results in reduced brain size, CNS hypomyelination, and loss of hippocampal granule and striatal parvalbumin-containing neurons. Neuron 1995;14:717-30.
[439] Arsenijevic Y, Weiss S. Insulin-like growth factor-I is a differentiation factor for postmitotic CNS stem cell-derived neuronal precursors: distinct actions from those of brain-derived neurotrophic factor. J Neurosci 1998;18:2118-28.
[440] McTavish H, Griffin RJ, Terai K, Dudek AZ. Novel insulin-like growth factor-methotrexate covalent conjugate inhibits tumor growth in vivo at lower dosage than methotrexate alone. Transl Res 2009;153:275-82.
[441] Kim S, Kang Y, Krueger CA, Sen M, Holcomb JB, Chen D, et al. Sequential delivery of BMP-2 and IGF-1 using a chitosan gel with gelatin microspheres enhances early osteoblastic differentiation. Acta Biomater 2012;8:1768-77.
[442] Antipov AA, Sukhorukov GB. Polyelectrolyte multilayer capsules as vehicles with tunable permeability. Adv Colloid Interface Sci 2004;111:49-61.
[443] Osypova A, Magnin D, Sibret P, Aqil A, Jérôme C, Dupont-Gillain C, et al. Dual stimuli-responsive coating designed through layer-by-layer assembly of PAA-b-PNIPAM block copolymers for the control of protein adsorption. Soft matter 2015;11:8154-64.
[444] Zhang H, Deng L, Sun P, Que F, Weiss J. Solubilization of octane in cationic surfactant–anionic polymer complexes: Effect of ionic strength. J Colloid Interface Sci 2016;461:88-95.
[445] Li L, Tao Y, Tang J, Chen Q, Yang Y, Feng Z, et al. A Cannabinoid Receptor 2 Agonist Prevents Thrombin-Induced Blood–Brain Barrier Damage via the Inhibition

of Microglial Activation and Matrix Metalloproteinase Expression in Rats. Translational stroke research 2015;6:467-77.
[446] McLean NA, Verge VM. Dynamic impact of brief electrical nerve stimulation on the neural immune axis—polarization of macrophages toward a pro-repair phenotype in demyelinated peripheral nerve. Glia 2016;64:1546-61.
[447] Kolpakov MA, Rafiq K, Guo X, Hooshdaran B, Wang T, Vlasenko L, et al. Protease-activated receptor 4 deficiency offers cardioprotection after acute ischemia reperfusion injury. J Mol Cell Cardiol 2016;90:21-9.
[448] Yang G, Hu R, Zhang C, Qian C, Luo QQ, Yung WH, et al. A combination of serum iron, ferritin and transferrin predicts outcome in patients with intracerebral hemorrhage. Sci Rep 2016;6:21970.
[449] Tullis GE, Spears K, Kirk MD. Immunological barriers to stem cell therapy in the central nervous system. Stem cells international 2014;2014.
[450] Garnett C, Apperley JF, Pavlů J. Treatment and management of graft-versus-host disease: improving response and survival. Therapeutic advances in hematology 2013;4:366-78.
[451] Carson MJ, Doose JM, Melchior B, Schmid CD, Ploix CC. CNS immune privilege: hiding in plain sight. Immunol Rev 2006;213:48-65.
[452] Olanow CW, Goetz CG, Kordower JH, Stoessl AJ, Sossi V, Brin MF, et al. A double-blind controlled trial of bilateral fetal nigral transplantation in Parkinson's disease. Ann Neurol 2003;54:403-14.
[453] PB M. Immunity to homologous grafted skin; the fate of skin homografts transplanted to the brain, to subcutaneous tissue, and to the anterior chamber of the eye. Br J Exp Pathol 1948;29:58-69.
[454] Klassen H, Schwartz MR, Bailey AH, Young MJ. Surface markers expressed by multipotent human and mouse neural progenitor cells include tetraspanins and non-protein epitopes. Neurosci Lett 2001;312:180-2.
[455] Camp DM, Loeffler DA, Farrah DM, Borneman JN, LeWitt PA. Cellular immune response to intrastriatally implanted allogeneic bone marrow stromal cells in a rat model of Parkinson's disease. J Neuroinflammation 2009;6:17.
[456] Aebischer P, Schluep M, Déglon N, Joseph J-M, Hirt L, Heyd B, et al. Intrathecal delivery of CNTF using encapsulated genetically modifiedxenogeneic cells in amyotrophic lateral sclerosis patients. Nat Med 1996;2:696-9.
[457] Bachoud-Lévi A-C, Deglon N, Nguyen J-P, Bloch J, Bourdet C, Winkel L, et al. Neuroprotective gene therapy for Huntington's disease using a polymer encapsulated BHK cell line engineered to secrete human CNTF. Hum Gene Ther 2000;11:1723-9.
[458] Veiseh O, Doloff JC, Ma M, Vegas AJ, Tam HH, Bader AR, et al. Size-and shape-dependent foreign body immune response to materials implanted in rodents and non-human primates. Nature materials 2015;14:643.
[459] Spears K. Immunogenic Properties of Neuralized Embryonic Stem Cells in a Model of Allogenic Intracranial Transplantation: University of Missouri--Columbia; 2011.